Supporting Information

Comparative genomic and metabolic analysis of *Streptomyces* sp. RB110 morphotypes illuminates genomic rearrangements and formation of a new 46-membered antimicrobial macrolide

Soohyun Um,[a#] Huijuan Guo,[a#] Sirinthra Thiengmag,[b#] René Benndorf,[a] Robert Murphy,[c] Maja Rischer,[a] Daniel Braga,[b] Michael Poulsen,[c] Z. Wilhelm de Beer,[d] Gerald Lackner,[b*] and Christine Beemelmanns[a]*

a. Chemical Biology of Microbe-Host Interactions, Leibniz Institute for Natural Product Research and Infection Biology, Hans Knöll Institute (HKI), Beutenbergstraße 11a, 07745 Jena, Germany. E-mail: christine.beemelmanns@hki-jena.de

b. Synthetic Microbiology, Leibniz Institute for Natural Product Research and Infection Biology, Hans Knöll Institute (HKI), Beutenbergstraße 11a, 07745 Jena, Germany. E-mail: gerald.lackner@hki-jena.de

c. Section for Ecology and Evolution, Department of Biology, University of Copenhagen, Universitetsparken 15, 2100 Copenhagen East, Denmark.

d. Department of Biochemistry, Genetics, and Microbiology, Forestry and Agricultural Biotechnology Institute, University of Pretoria, Pretoria 0002, South Africa

‡ contributed equally.

Corresponding Authors

*E-mail: Christine.Beemelmanns@hki-jena.de.

*E-mail: Gerald.Lackner@hki-jena.de.

Contents

List of Figures

List of Tables

1. General Experimental Procedures

Optical rotation was recorded using a P-1020 polarimeter (JASCO). **IR spectrum** was obtained on an FT/IR-4100 ATR spectrometer (JASCO). **UV spectrum** was acquired on a Shimadzu HPLC system. **NMR experiments** were carried out on a Bruker AVANCE III 600 MHz spectrometer, equipped with a Bruker Cryoplatform. The chemical shifts are reported in parts per million (ppm) relative to the solvent residual peak of pyridine-d_5 (^{1}H: 7.19, 7.55, 8.71 ppm; ^{13}C: 123.5, 135.5, 149.5 ppm). **Semi-preparative HPLC** was performed on a Shimadzu HPLC system using a phenyl-hexyl column C18(2) 250 x 10 mm column (particle size 10 µm, pore diameter 100 Å). **Low resolution LCMS** measurements were performed on a Shimadzu LCMS-2020 system equipped with single quadrupole mass spectrometer using a Phenomenex Kinetex C18 column (50 x 2.1 mm, particle size 1.7 µm, pore diameter 100 Å). Column oven was set to 40 °C; scan range of MS was set to *m*/*z* 150 to 2,000 with a scan speed of 10,000 u/s and event time of 0.25s under positive and negative mode. **UHPLC-HESI-HRMS** measurement was performed on a Dionex Ultimate3000 system combined with a Q-Exactive Plus mass spectrometer (Thermo Scientific) with a heated electrospray ion source (HESI). *Streptomyces* extracts were chromatographed in a Luna Omega C18 column (100 x 2.1 mm, particle size 1.6 µm, pore diameter 100 Å, Phenomenex) assembled with a SecurityGuard™ ULTRA guard cartridge (2 x 2.1 mm, Phenomenex). The column was held at 40 °C and with a flow rate of 300 µl/min. **Chemicals**: Methanol (VWR, Germany); water for analytical and preparative HPLC (Millipore, Germany); formic acid (Carl Roth, Germany); acetonitrile (VWR as LC-MS grade); media ingredients (Carl Roth, Germany). All the experiments were performed at Leibniz Institute for Natural Product Research and Infection Biology – Hans Knöll Institute, Jena, Germany.

2. Fermentation

Media preparation: Media was prepared as shown in Table S1. All media were prepared with distilled water with the exception of MS, which was prepared with tap water. For solid medium, 2.0% agar was added (20 g/L). The media were sterilized by autoclaving for 20 min at 121 °C. The pH was adjusted with 1 M HCl or 1 M NaOH.

Table S1. Media compositions used for isolation and growth assay.

Medium	Content per L
ISP1	3.0 g yeast extract, 5.0 g tryptone, pH 7.0-7.2
ISP2	4.0 g yeast extract, 10.0 g malt extract, 4.0 g glucose, pH 7.0-7.2
ISP2*M	4 g yeast extract, 10 g malt extract, 4 g dextrose, 2 g mannitol, pH 7.2
ISP3	20.0 g oat meal, 0.1 mg $FeSO_4 \cdot 7H_2O$, 0.1 mg $MnCl_2 \cdot 4H_2O$, 0.1 mg $ZnSO_4 \cdot 7H_2O$, pH 7.2
ISP4	10.0 g soluble starch, 1.0 g K_2HPO_4, 1.0 $MgSO_4 \cdot 7H_2O$, 1.0 g NaCl, 2.0 g $(NH_4)_2SO_4$, 2.0 g $CaCO_3$, 0.1 mg $FeSO_4 \cdot 7H_2O$, 0.1 mg $MnCl_2 \cdot 4H_2O$, 0.1 mg $ZnSO_4 \cdot 7H_2O$, pH 7.0-7.4
ISP5	10.0 g glycerol, 1.0 g L-asparagine, 1.0 g K_2HPO_4, 0.1 mg $FeSO_4 \cdot 7H_2O$, 0.1 mg $MnCl_2 \cdot 4H_2O$, 0.1 mg $ZnSO_4 \cdot 7H_2O$, pH 7.2-7.6
PD	26.5 g potato extract glucose (6.5 g potato extract, 20 g glucose), pH 7.0
MS	20.0 g mannitol, 20.0 g soy flour, pH 6.5
TSB	17.0 g pancreatic digested casein, 5.0 g NaCl, 3.0 g enzymatic digest soya bean, 2.5 g K_2HPO_4, 2.0 g glucose, pH 7.1-7.5

Cultivation of parental strain: *Streptomyces* sp. RB110 was cultivated on solid medium (4 g of yeast extract, 10 g of malt extract, 4 g of glucose, and 18 g of agar per 1 L of sterilized water) at 25 °C. The bacterium was transferred to liquid 50 mL ISP2 broth in a 100-mL Erlenmeyer flask and cultivated at 30 °C at 180 rpm. After incubation for 7 days, 1 mL of the liquid culture was inoculated to each modified ISP medium 2 agar plate (150 x20 mm, 40 0ea). The culture was incubated at 30 °C under dark conditions to prevent compound degradation for 6 days. The entire culture was extracted twice with 20 L of EtOAc overnight at 4 °C and the organic phase was concentrated *in vacuo* to yield 33.9 g of dry extract.

Cultivation of morphotypes: *Streptomyces* sp. RB110-1 and RB110-2 were cultivated on TSB at 30 °C for seven days (preculture) and then incubated on ISP media (ISP1-ISP5 using a 6 well-plate assay) using 50 µl of preculture for 18 days. Time and media dependent analysis showed that there are indeed consistent differences between the two morphotypes, which differed in sporulation rate and colony morphology. For morphotype RB110-1 sporulation occurred after five days of incubation while no or only weak production of spores was observed for strain RB110-2 on ISP3, ISP4 and ISP5 even after five days (Figure S2). Colonies of RB110-1 had a violet-white color on ISP1, a light red color on ISP2 and a white color on ISP3-ISP5. Colonies of RB110-2 were of white color on ISP1 and revealed a red to violet pigment production on ISP2-ISP5.

3. Morphotype Analysis

Morphotype differentiation of *Streptomyces* sp. RB110: On MSA the "original isolate", referred to as *Streptomyces* sp. RB110-1, produced colonies of greenish-grey colour. A second colony type (*Streptomyces* sp. RB110-2), which seemed to originate from the young mycelium of the grey morphotype was of violet color and displayed delayed reduced sporulation (see Figure S25-Figure S27).

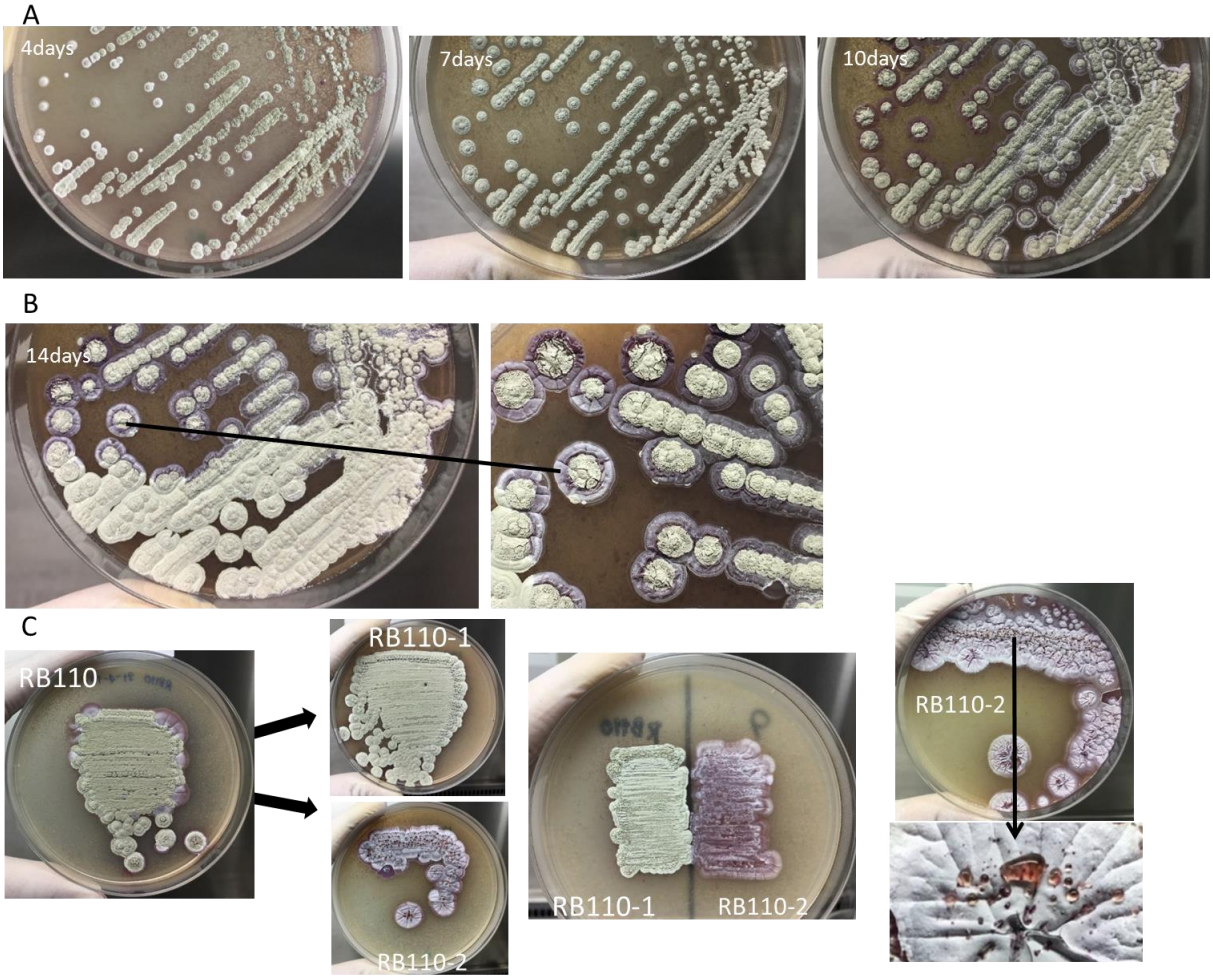

Figure S1. A) Cultivation of RB110 on MS-agar plates for up to 14 days at 28 °C. B) Zoom-in on colony showing violet-colored morphology at the edges of a large whitish-grey colony (middle). C) Cultuvation of whitish-grey morphotype RB110-1 and violet-colored morphotype RB110-2 on MS medium after 5 days of incubation at 28 °C.

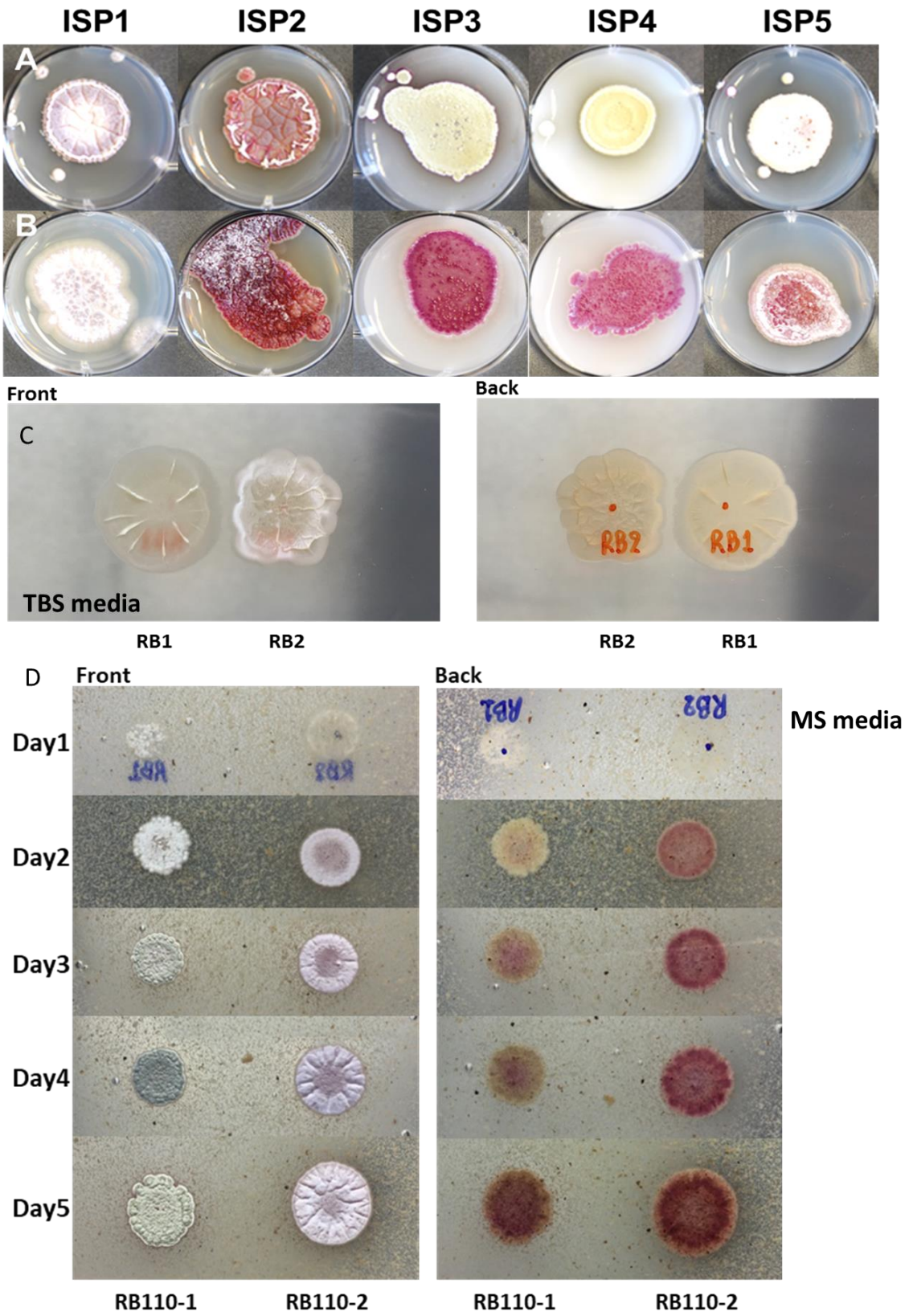

Figure S2. A) Cultivation of RB110-1 (whitish-grey morphotype) and B) RB110-2 purple morphotype on ISP media at 28 °C after 7 days, C) TBS medium at 28 °C, D) MS medium at 28 °C from 1-5 days (back and front side).

4. Genome Analysis and Phylogenetic Placement

DNA extraction: *Streptomyces* sp. RB110-1 and RB110-2 were grown in nutrient-rich ISP2 broth for 3 to 5 days at 30 °C (180 rpm) and cells were harvested after incubation by centrifugation for 10 min at 8000 x g. Genomic DNA was first extracted using the GenJet Genomic DNA Purification Kit (Thermo Scientific, #K0721) following the manufacture instructions with two slight changes (lysozym incubation time 40 min, protein kinase K treatment 40 min). DNA was quantified photometrically using a Nanodrop Lite Spectrometer (Thermo Scientific) photometer. High molecular weight DNA for PACBIO based whole genome sequencing was extracted using NucleoBond HMW DNA kit (Macherey-Nagel). Genome sequencing, assembly and annotation was performed as reported by Murphey *et al.*[1]and genomes were deposted at NCBI under the accession numbers RB110-1: JAEKDS000000000.1 and RB110-2: JAEKDR000000000.1.

DNA-DNA hybridization (DDH): DNA-DNA hybridization was performed *in silico* at the GGDC web server with closest neighbour *Streptomyces californicus* NBRC12750. [2] Genome sequence of *Streptomyces californicus* NBRC12750 was downloaded from NCBI database (JNXW00000000.1).

Synteny plot: All genome contigs resulting from sequencing of the RB110-1 and RB110-2 morphotypes were used for a computation of syntenic regions (regions of conserved gene order) using Mummer 3.23.[3] While RB110-1 contigs were used as reference sequence, the contigs originating from RB110-2 served as query sequence. Visualization of synteny was performed using Mummerplot and Gnuplot.

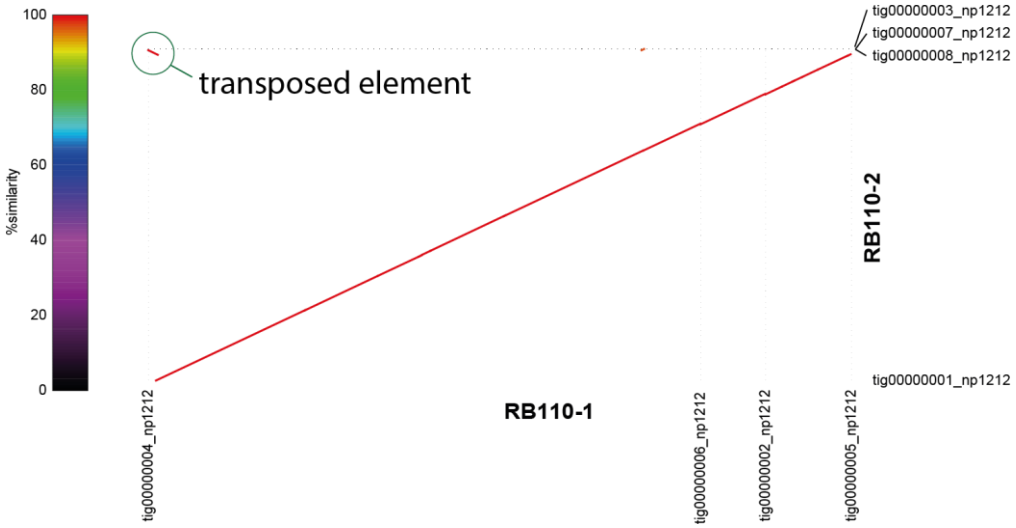

Figure S3. Synteny plot of the whole genomes of *Streptomyces* sp. RB110-1 versus RB110-2. Nucleotide coordinate (contig names are indicated) of the RB110-1 genome is plotted on the X-axis, nucleotides coordinate of the RB110-2 genome is plotted on the Y-axis. Maximum unique matches (MUMs) are plotted as colored dots, colors represent different levels of similarity (see legend). The genomes are nearly 100% identical and are syntenic over more than 99% of the genome as expected for two morphotypes of the same isolate. The transposition of a 106.8 kb region between the start of the RB110-1 genome and the end of the RB110-2, is marked in the plot. This is the only major rearrangement of the genome.

Phylogenetic placement of *Streptomyces* sp. RB110-1 and RB110-2: For phylogenetic studies, the 16S rRNA gene was amplified using the primer set 1492R/27F. Each amplification reaction was prepared in a 25 µL final reaction volume containing 7.25 µL of distilled water, 5 µL of HF buffer, 5 µL of each primer (2.5 µM), 0.5 µL of dNTPs (10 µM), 0.25 µL of Phusion High-Fidelity DNA polymerase (New England Biolabs), and 2 µL of extracted DNA (template). PCR was performed under the following conditions: 98 °C/38 s; 32 cycles of 98 °C/30 s, 52 °C/45 s, 72 °C/1 min 20 s; and a final extension of 72 °C/8 min. PCR products were visualized by agarose gel electrophoresis. PCR reactions were purified using a PCR purification kit (Thermo Scientific). DNA fragments were sequenced at GATC (Konstanz). Resulting sequences were used for a BLASTn search in GenBank using "refseq_rna" database. Closest relatives of BLASTn search were used to calculate sequence similarities between closest neighbours (Annexe) and isolated bacteria strains. Pairwise sequence similarities were calculated using the method recommended by Meier-Kolthoff *et al*. for the 16S rRNA gene available at the GGDC web server (http://ggdc.dsmz.de/).[4] SINA sequence alignment service was used to align 16S rRNA gene sequences.[5] Phylogenetic analysis was done with 16S rRNA sequences of both morphotypes (RB110-1 and RB110-2) and closest relatives according to BLASTn search using the "refseq_rna" database.[6] For phylogenetic placement two different phylogenetic trees were reconstructed with maximum likelihood and neighbour joining algorithms[7] using MEGA software version 7.0.26.[8] The evolutionary distances were computed using the Tamura 3-parameter method[9] with deletion of complete gaps and missing data. For both algorithms a gamma distribution was used to model rate variations among sites. For all constructed trees the confidence values of nodes were evaluated by bootstrap analysis based on 1000 re-samplings.[10]

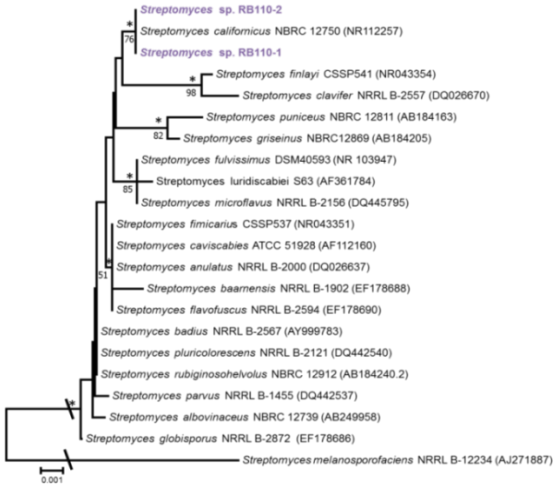

Figure S4. Neighbour-joining tree based on almost complete 16S rRNA gene sequences showing relationship between both morphotypes of *Streptomyces* sp. RB110 (RB110-1 and RB110-2) and species of the genus *Streptomyces*. *Streptomyces melanosporofaciens* NRRL B-12234 was used as outgroup. A star denotes branches that were recovered in the maximum-likelihood tree. Only bootstrap values above 50% (percentages of 1000 replications) are shown. Scale bar corresponds to 0.001 substitutions per nucleotide position.

5. Metabolomic Analysis of Morphotypes

Cultivation and extraction for GNPS-based analysis: Bacterial strains were cultured in 20 mL ISP2 medium. After incubation at 30 °C (180 rpm) for 7 days, the cultures were used to inoculate ISP2*M agar plates (1 mL culture was used for 150 x 20 mm plates, 3 agar plates) and ISP2*M liquid culture (100 mL, 150 rpm), which were incubated at 30 °C for 7 days. The liquid culture was extracted with of ethyl acetate (2 x 100 mL) using a separation funnel. The organic phase was concentrated *in vacuo* and analyzed by LC-MS^2. The agar culture was extracted with ethyl acetate (200 mL) overnight, filtered and ethyl acetate extract was dried under vacuum. The crude extract was dissolved with methanol and centrifuged for 10 min. The culture in methanol was analyzed with LC-MS^2.

General procedures for liquid-chromatography coupled to tandem mass spectrometry (LC-MS/MS): LC-MS/MS was performed on a Dionex Ultimate3000 system combined with a Q-Exactive Plus mass spectrometer (Thermo Scientific) with a heated electrospray ion source (HESI). Metabolite separation was carried out using a Luna Omega C18 column (100 x 2.1 mm, particle size 1.6 µm, pore diameter 100 Å, Phenomenex) at 40 °C. The gas flow rates were set to 35 and 10 for the sheath and auxiliary gases, respectively. The capillary and the probe heater temperatures were 340 °C and 200 °C, respectively. The spray voltages were 4 kV and 3.3 kV for the positive and negative ionization modes, respectively. Resolving power was 17,500 FWHM at m/z 200, AGC target was 1e5, injection time was 50 ms, and an isolation window of 1.0 m/z. Fragmentations were performed with stepped NCEs (normalized collision energy) values of 20, 30, and 40.

Mass spectral molecular networking analysis: LC-MS/MS raw files were converted to mzXML format using MSConvert (bundled with the Proteowizard software package) and uploaded to the GNPS webserver (https://gnps.ucsd.edu).[11] Molecular networking was performed using a minimum requirement of four matched fragments and a cosine distance of 0.8 to establish connections of nodes. Networks were visualized in Cytoscape[12] according to instruction provided on the GNPS website. Compounds were computationally derived from raw data by using Compound Discoverer 3.1.0.305 (Thermo Scientific) by a targeted search with indicated parent compounds.

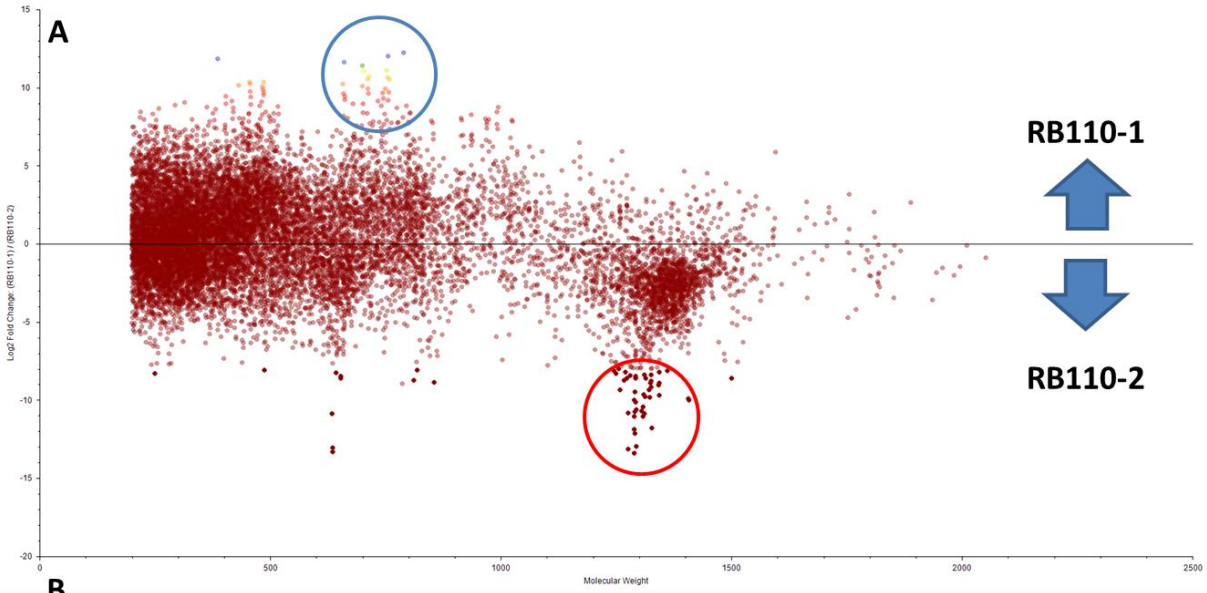

Top 20 ion features
RB110-1 culture

m/z	RT [min]
404.23986	4.755
381.08339	4.365
481.28784	4.359
477.12856	3.853
416.24083	6.034
458.21205	3.841
486.24324	4.361
516.1857	4.36
419.25137	5.804
386.21935	4.751
657.27719	4.767
789.48595	6.639
750.3112	4.362
745.28156	5.263
755.23534	5.246
743.28463	5.247
713.18916	4.763
758.24611	5.246
733.17618	4.762
661.28227	4.775

Top 20 ion features
RB110-2 culture

m/z	RT [min]
1293.83022	6.322
1267.8159	6.261
1296.83843	6.613
1343.85427	6.179
1321.85344	6.493
1289.8394	6.323
1343.83655	6.055
1326.82536	6.113
1338.8626	6.17
1281.83	6.395
635.91393	6.317
635.91039	6.308
653.41804	5.857
633.41003	6.502
855.56783	10.457
652.91673	5.842
811.51811	8.687
642.40972	5.987
635.91312	6.495
816.47234	8.68

Figure S5. A) Scatter plot of crude extracts of RB110-1 and RB110-2 using Compound Discoverer 3.1. B) Top 20 molecular ion features detected from RB110-1culture extracts (left) and RB110-2 (right).

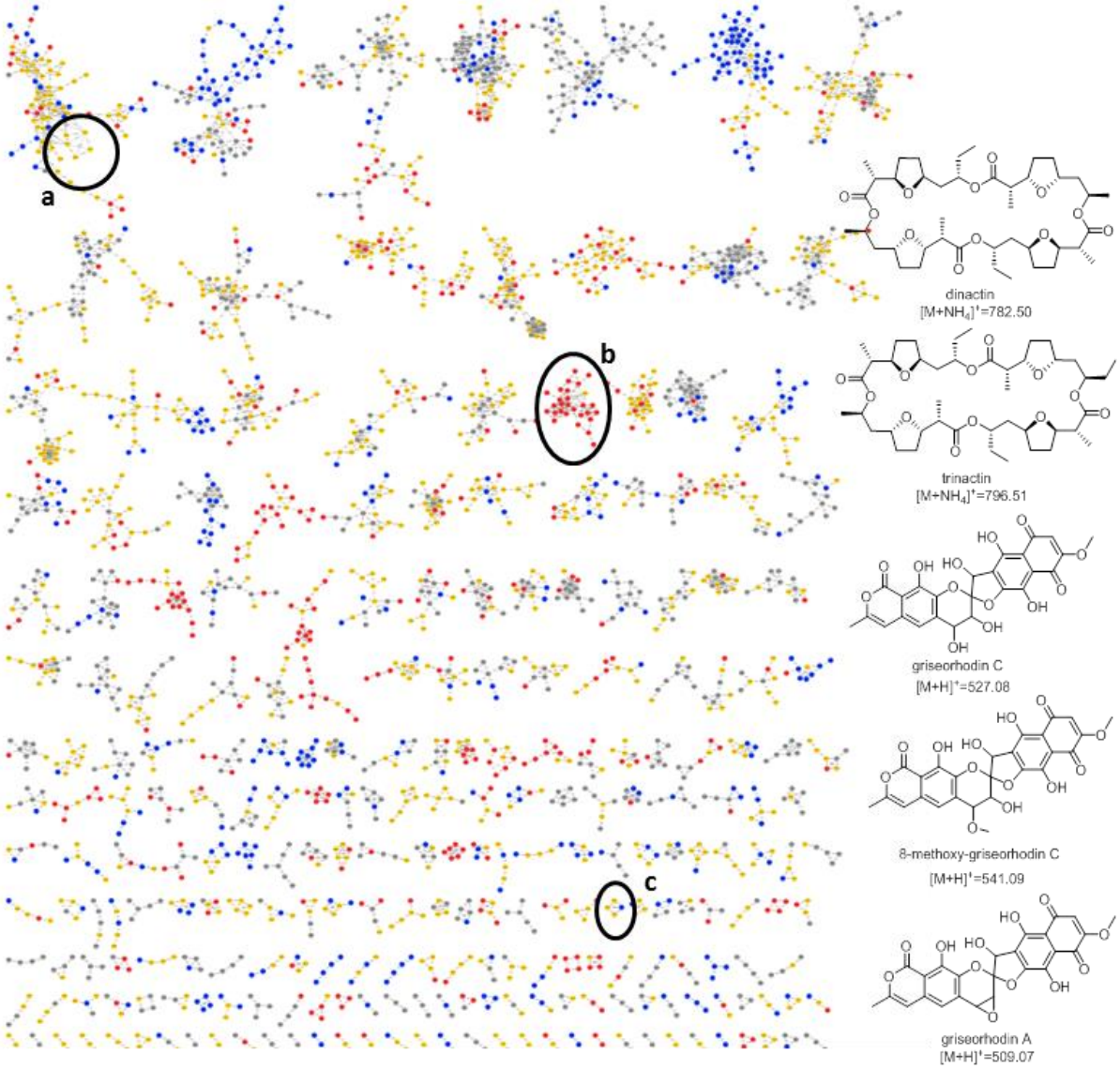

Figure S6. HMRS^2-based mass-spectral molecular network (GNPS) of culture extracts obtained from *Streptomyces* sp. RB110-1 and RB110-2 solid cultures after 7 days (gold: RB110-1 and RB-110-2; blue: RB110-1; red: RB110-2, black: ISP2 medium control). Putatively assigned clusters: a) nonactins, b) termidomycins and c) griseorhodins. Connections between nodes indicate relatedness based on similarities in MS^2 spectra. The network was generated using 6 minimum matched ion fragments, a minimum cluster size of 2 and a cosine score of 0.8.

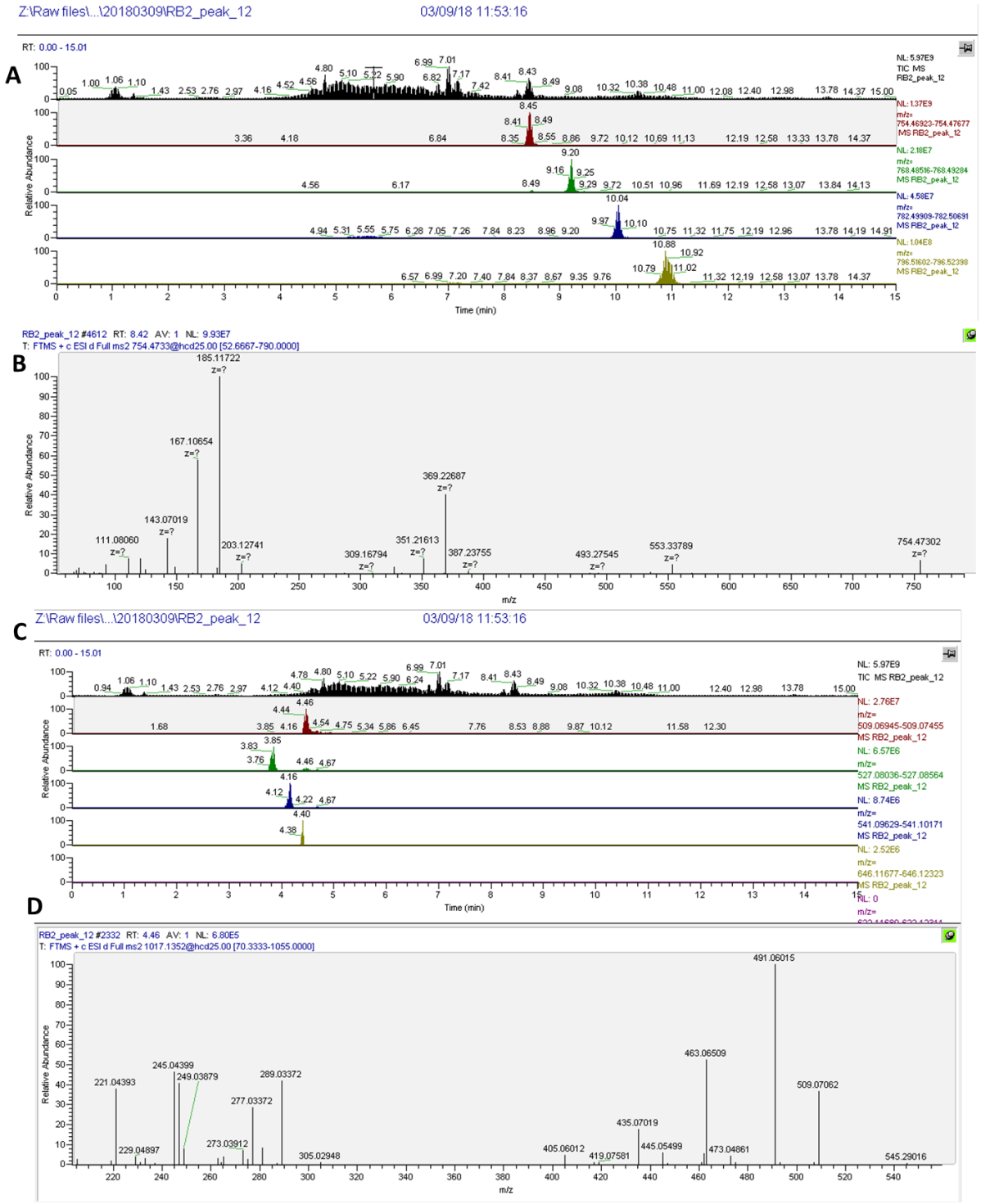

Figure S7. A) LC-MS analysis of crude culture extracts showing A) total ion chromatogram and extracted ion chromatogram (nonactin $[M+NH_4]^+$ = 754.4736, monactin $[M+NH_4]^+$ = 768.4676; dinactin $[M+NH_4]^+$ = 782.4779; trinactin $[M+ NH_4]^+$ = 796.5376); B) HR-MS^2 spectrum of nonactin $[M+H]^+$ = 754.4736; C) LC-MS analysis of crude culture extracts showing extracted ion chromatogram (griseorhodin C $[M+H]^+$ = 527.08, griseorhodin A $[M+H]^+$ = 509.07; 8-methoxy-griseorhodin C $[M+H]^+$ = 541.09); D) HR-MS^2 spectrum of molecular ion feature at 4.46 min (griseorhodin A $[M+H]^+$ = 509.0706).

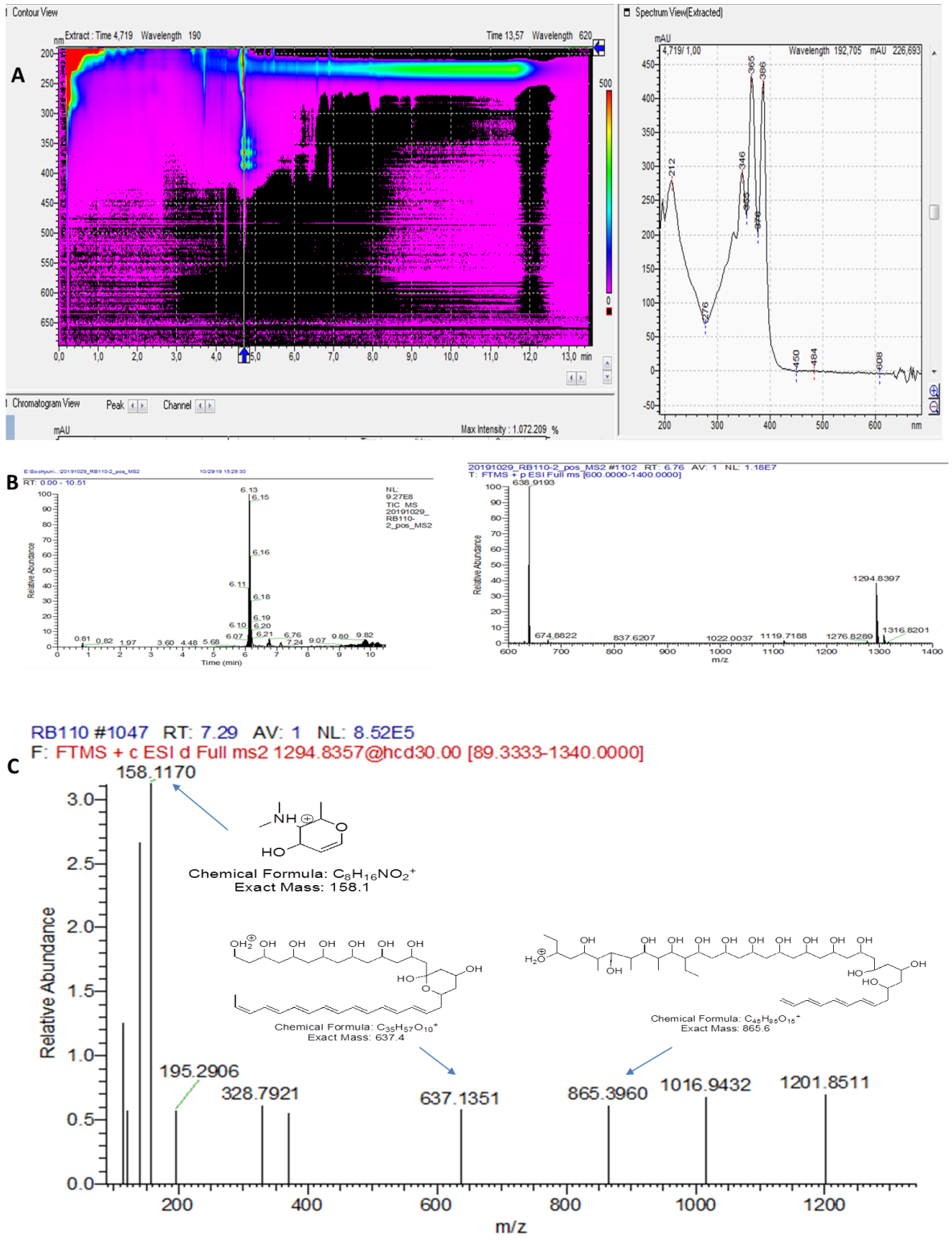

Figure S8. A) HPLC chromatogram and UV-Vis spectrum of RB110-2 culture extract showing termidomycins typical UV-Vis spectrum (λ = 383 nm, 26 min). B) ESI-HRMS spectra of termidomycin A (**1**) (calcd. for $C_{70}H_{120}NO_{20}$ 1294.8398 $[M + H]^+$, obsd. 1294.8397). C) MS^2 spectrum of termidomycin A (**1**) indicating the presence of the sugar moiety ($C_8H_{16}NO_2$, cacld. $[M + H]^+$ = 158.1176).

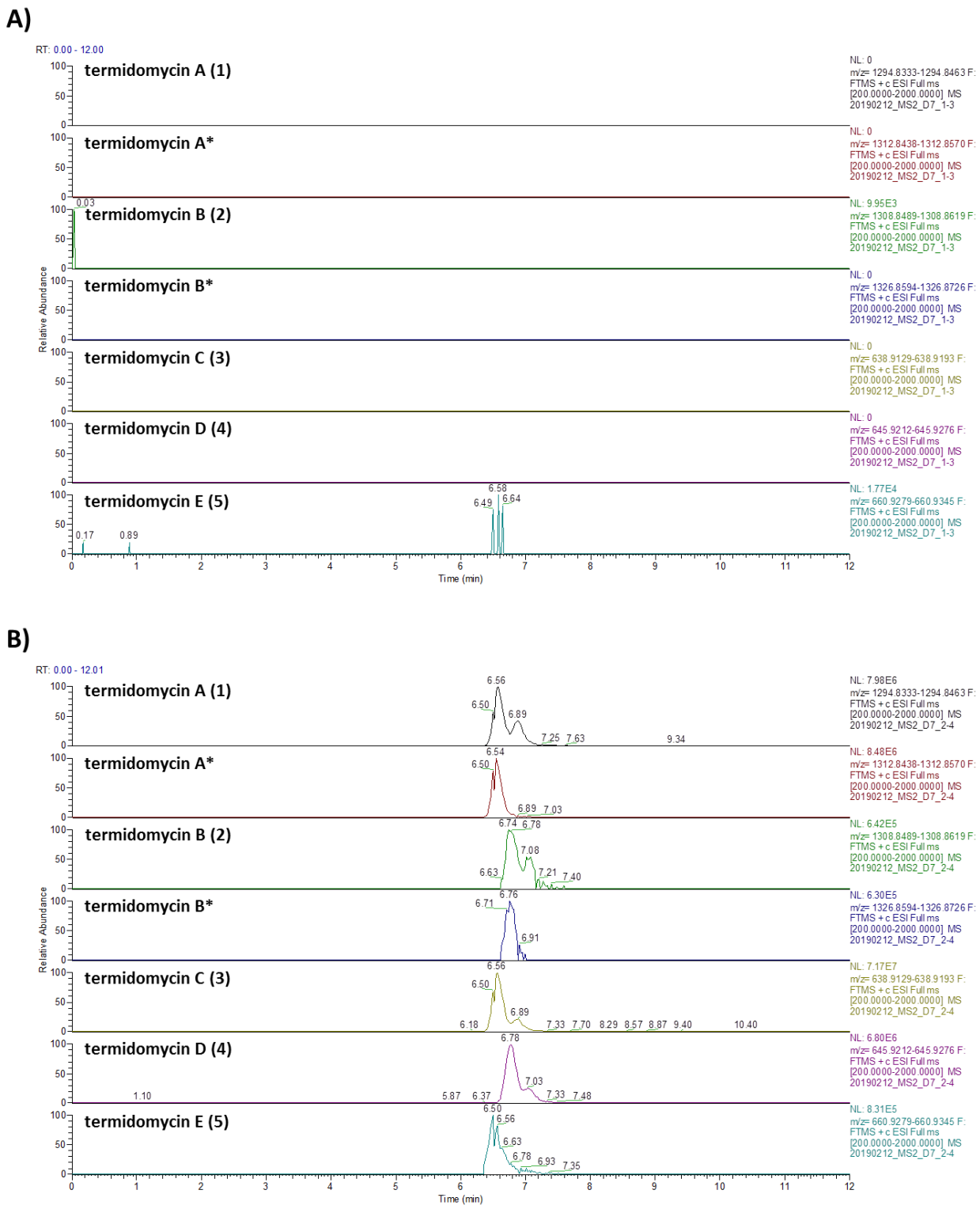

Figure S9. HPLC-MS chromatogram of RB110-1 (**A**) and RB110-2 (**B**) culture extract (7 days) showing termidomycin congeners under TIC mode. Termidomycin A (**1**) ($[M + H]^+$, 1294.8398); termidomycin A* ($[M + H]^+$, 1312.8504, putative linear form); termidomycin B (**2**) ($[M + H]^+$, 1308.8554); termidomycin B* ($[M + H]^+$, 1326.8660, putative linear form); termidomycin C (**3**) ($[M + 2H]^{2+}$, 638.9161); termidomycin D (**4**) ($[M + 2H]^{2+}$, 645.9244); termidomycin E (**5**) ($[M + 2H]^{2+}$, 660.9312).

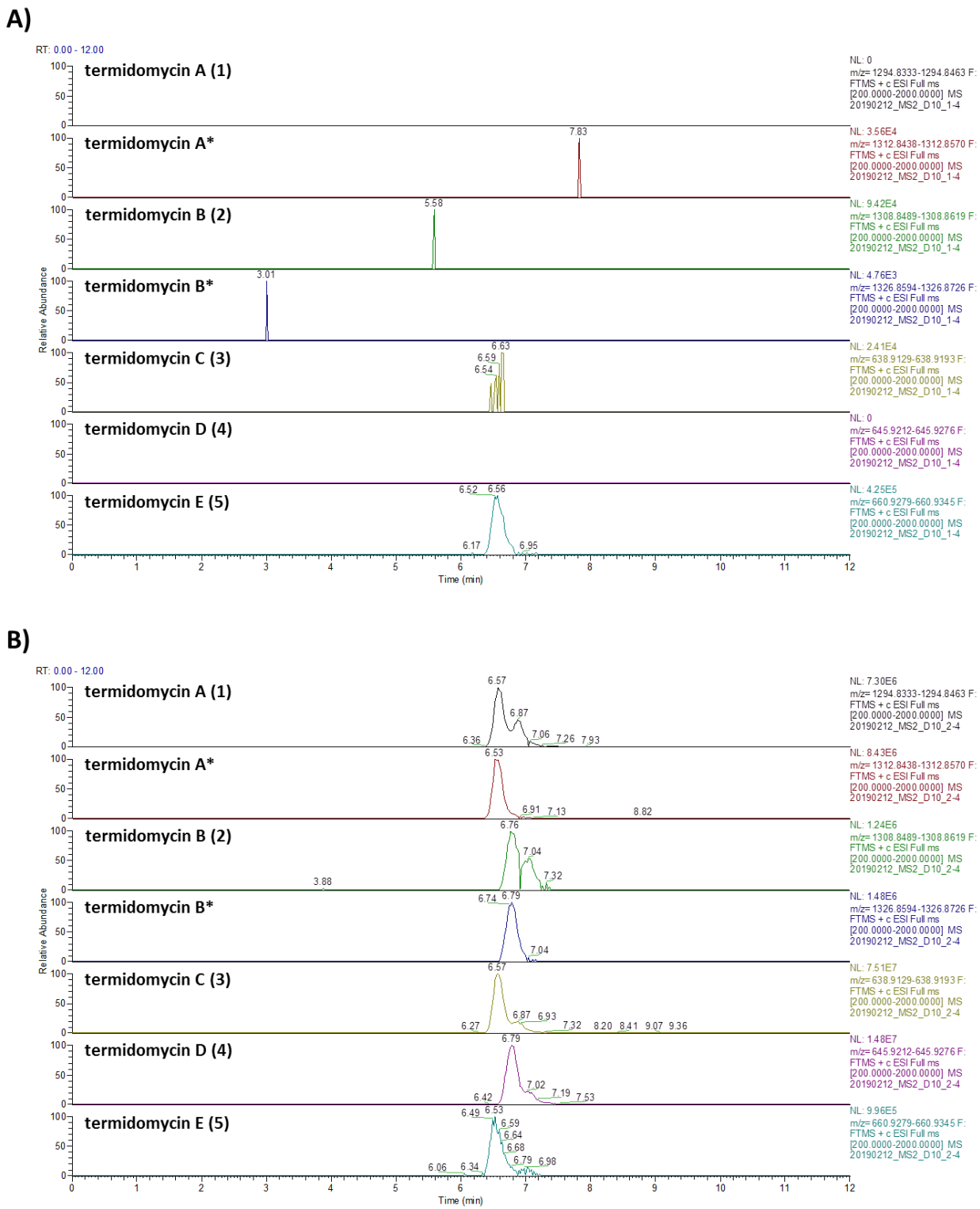

Figure S10. HPLC-MS chromatogram of RB110-1 (**A**) and RB110-2 (**B**) culture extract (10 days) showing termidomycin congeners under TIC mode. Termidomycin A (**1**) ($[M + H]^+$, 1294.8398); termidomycin A* ($[M + H]^+$, 1312.8504, putative linear form); termidomycin B (**2**) ($[M + H]^+$, 1308.8554); termidomycin B* ($[M + H]^+$, 1326.8660, putative linear form); termidomycin C (**3**) ($[M + 2H]^{2+}$, 638.9161); termidomycin D (**4**) ($[M + 2H]^{2+}$, 645.9244); termidomycin E (**5**) ($[M + 2H]^{2+}$, 660.9312).

6. Isolation and Structure Elucidation of Termidomycin A (1)

Large scale fermentation and purification

Strain RB110-2 was cultured on ISP2 medium at 28 °C and used to inoculate 200 mL ISP2*M liquid medium. After five days of incubation (30 °C at 180 rpm), 1 mL of the culture was used to inoculate ISP2 agar medium (500 plates, 150 x 20 mm) containing 0.2 mg of 1-^{13}C sodium acetate per liter to maximize the carbon chemical signals for ^{13}C NMR spectrum. After 7 days of cultivation at 30 °C in a dark incubator, plate cultures were cut into small pieces (50 x 50 mm) and extracted twice with 20 L of EtOAc overnight. The EtOAc layer was dried over Na_2SO_4 and concentrated *in vacuo* to yield 15.5 g of extract. To obtain pure termidomycin A (**1**), the dried substance was purified by semi-preparative reversed-phase HPLC on a phenyl-hexyl column (10 μm, 250 × 10 mm, a gradient solvent system; flow rate: 2 mL/min, detection: UV 383 nm, 20 to 50 % aqueous acetonitrile with 0.1 % F.A over 30 min) without an SPE fraction procedure to prevent from compound decomposition. Termidomycin A (**1**) eluted at 26 min. All the experiments were performed in the dark to avoid light-induced decomposition.

Physicochemical Data

Termidomycin A (**1**): yellow solid; $[\alpha]^{25}_{D}$ -42.0 (c 0.1 w/v%, MeOH); UV (MeOH) λ_{max} 348, 363, 387 nm; IR (ATR) ν_{max} 3399, 2610, 2360, 1741, 1581, 1460, 1425, 1387, 1263, 1194, 1099, 1023, 956, 913, 862, 774; NMR spectral data, see Table**1**; ESI-HRMS $[M + H]^+$ *m/z* 1294.8397 (calcd for $C_{70}H_{120}N_1O_{20}$, 1294.8398)

Structural Analysis

Termidomycin A (**1**) was purified as a yellow powder. The molecular formula of **1** was determined as $C_{70}H_{119}NO_{20}$ (*m/z* obsd. 1294.8397 $[M + H]^+$, calcd. 1294.8398; Δ–0.10 mmu) by ESI-HRMS and ^{1}H and ^{13}C NMR spectra indicating 12 degrees of unsaturation. Interpretation of the ^{1}H NMR spectrum of **1** revealed polyunsaturated proton signals and a UV-vis spectrophotometric band (λ_{max} 348, 363, and 387 nm) for a heptaene core moiety and polyhydroxylated proton signals were suggestive of a type I polyketide compound. Further combined analyses of 1D (^{1}H and ^{13}C) and 2D (HSQC, COSY, and HMBC) NMR data in pyridine-d_5 led to the planar structure elucidation for termidomycin A (**1**). The first connectivity was deduced by HMBC correlations from methyl protons [H_3-3, δ_H 1.35] attached to methine carbon [C-2, δ_C 48.6] supported by ^{1}H-^{1}H correlation of the methyl group protons [H_3-3, δ_H 1.35] and methine proton [H-2, δ_H 2.95]. The COSY NMR spectrum showed a correlation between methine proton signal [H-2, δ_H 2.95] and oxymethine proton [H-4, δ_H 4.53] and HMBC correlations also indicated the connections from H-4 [δ_H 4.53] to C-2 and C-3 [δ_C 48.6 and 15.2]. A COSY correlation allowed the oxymethine proton H-4 was determined to be connected to an olefinic proton [H-5, δ_H 5.74] as well as HMBC correlations supported the connectivity from the

olefinic proton H-5 to C-4 [δ_C 74.8]. Two unsaturated protons H-5 and H-6 [δ_H 5.61] showed COSY correlations and further extension from C-6 to C-7 was deduced by COSY and HMBC correlations from H-6 to C-7 and C-8 [δ_C 49.7 and 25.0]and from H-7 [δ_H 2.45] to C-6 [δ_C 133.9]. The ethyl group connected to the olefinic carbon C-6 was assigned from COSY correlations between H-7 [δ_H 2.45]/H_2-8 [δ_H 2.33 and 1.50] and H_2-8/H_3-9 [δ_H 0.99] and HMBC correlations from methyl protons H_3-9 to C-7 and C-8 [δ_C 49.7 and 25.0]. Methine proton H-7 at the ethyl group showed a COSY correlation with oxymethine proton H-10 [δ_H 4.15].

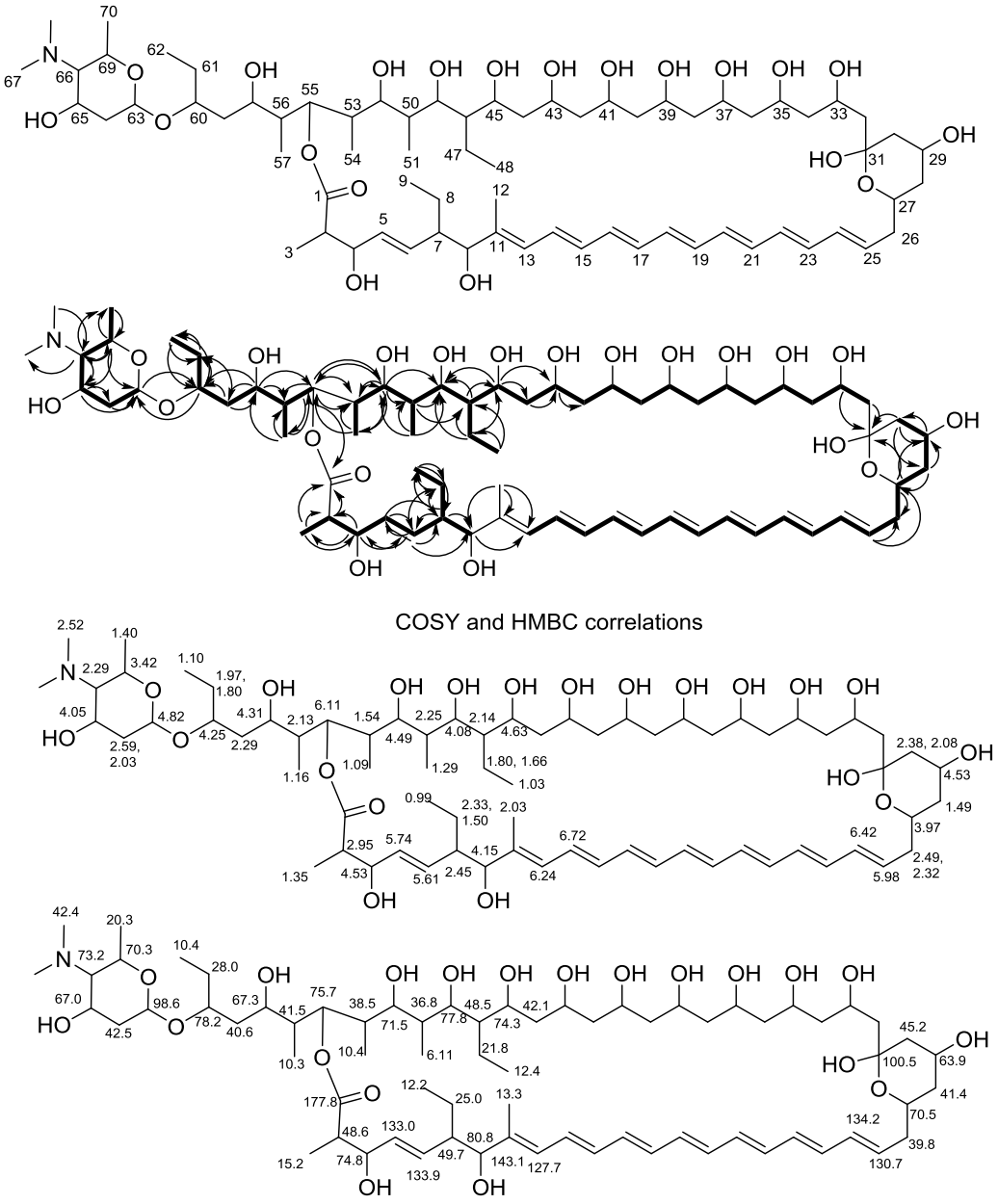

Figure S11. Proposed planar structure and key ^{1}H and ^{13}C chemical shifts of termidomycin in pyridine-d_5.

The connectivity from C-11 [δ_C 143.1] to C-25 [δ_C 130.7] was deduced by the array of COSY couplings among the 13 olefinic protons. Also, HMBC correlations from H-13 [δ_H 6.24] to C-11, 14, and 15 [δ_C 143.1, 130.0, and 134.2], from H-14 [δ_H 6.72] to C-11, 13, and 15 [δ_C 143.1, 127.7, and 134.2], from H-24 [δ_H 6.42] to C-23 and C-25 [δ_C 133.5 and 130.7], and from H-25 [δ_H 5.98] to C-23 and C-24 [δ_C 133.5 and 134.2] confirmed the connectivity in the polyunsaturated carbon sequence. The polyene characteristic UV-Vis spectrum of **1** (λ_{max} 348, 363, and 387 nm) and an integration of ^{1}H NMR spectrum supported the presence of a heptaene moiety despite of the overlapped carbons at C-18–22 and protons at H-18–22 [δ_C 133.0-134.5; δ_H 6.63-6.45]. Further HMBC correlations from H-7, H-10, and H_3-12 [δ_H 2.03] to C-11 [δ_C 143.1] assigned the placement of quaternary carbon C-11 at the heptaene moiety. COSY and HMBC correlations allowed us to construct further connectivity to a six membered hemiketal ring [C-27, 28, 29, 30, and 31; δ_C 70.5, 41.4, 63.9, 45.2, and 100.5] from the heptaene moiety via the methylene bridge carbon C-26 [δ_C 39.8]. The methylene protons H_2-26 [δ_H 2.49, 2.32] showed correlations to C-24, 25, 27, and 28. HMBC correlations from the oxymethine proton H-27 [δ_H 3.97] and methylene proton H_2-30 [δ_H 2.39] in the ring to a tertiary alcohol substituted quaternary carbon C-31 support the hemiketal ring formation. COSY and HMBC correlations of **1** indicated a polyhydroxylated carbon sequence from C-32 [δ_C 41.1] to C-60 [δ_C 78.2] containing 12 hydroxylated carbons [C-33, 35, 37, 39, 41, 43, 45, 49, 52, 55, 58, and 60; δ_C 77.4, 74.7, 70.8, 77.5, 72.3, 69.2, 74.3, 77.8, 71.5, 75.7, 67.3, and 78.2], 8 methylene linker carbons [C-32, 34, 36, 38, 40, 42, 44, and 59; 41.1, 45.4, 45.9, 40.4, 45.8, 48.9, 44.5, and 40.6], two ethyl substituted groups [C-46, 47, and 48; δ_C 48.5, 21.8, and 12.3, C-61 and 62; δ_C 28.0 and 10.4], and three methyl substituted groups [C-50 and 51; C-53 and 54; C56 and 57] showing a repeating 1,3-pattern, a typical feature of type I polyketide synthase.

Aminoglycoside (3-hydroxy-forosamine) was determined by COSY couplings from H_3-70 [δ_H 1.40] to H-63 [δ_H 4.82] supported by HMBC correlations from H_3-70 to C-66 and C-69 [δ_C 73.2 and 70.3], and from 2 N-methyl protons H_3-67, 68 [δ_H 2.52] to C-66, from H-66 [δ_H 2.29] to C-65, 69, and 70. Also HMBC correlations from H-65 [δ_H 4.05] to C-64, C-65 showed further extension. The ring formation was deduced by HMBC correlation from methine proton H-69 [δ_H 3.42] to oxymethine carbon C-63 [δ_C 98.6]. The aminoglycoside moiety was elucidated as 3-hydroxy-forosamin, rare aminoglycoside, and additional HMBC correlations from H-63 to C-60 [δ_C 78.2] and from H-60 [δ_H 4.25] to C-63 exhibited the connection between the aminoglycoside moiety and the polyhydroxylated chain. Lastly, HMBC correlation from a broad proton H-55 [δ_H 6.11] to C-1 [δ_C 177.8] allowed the assignment for the planar structure of **1** forming as a 46 membered-ring macrolide.

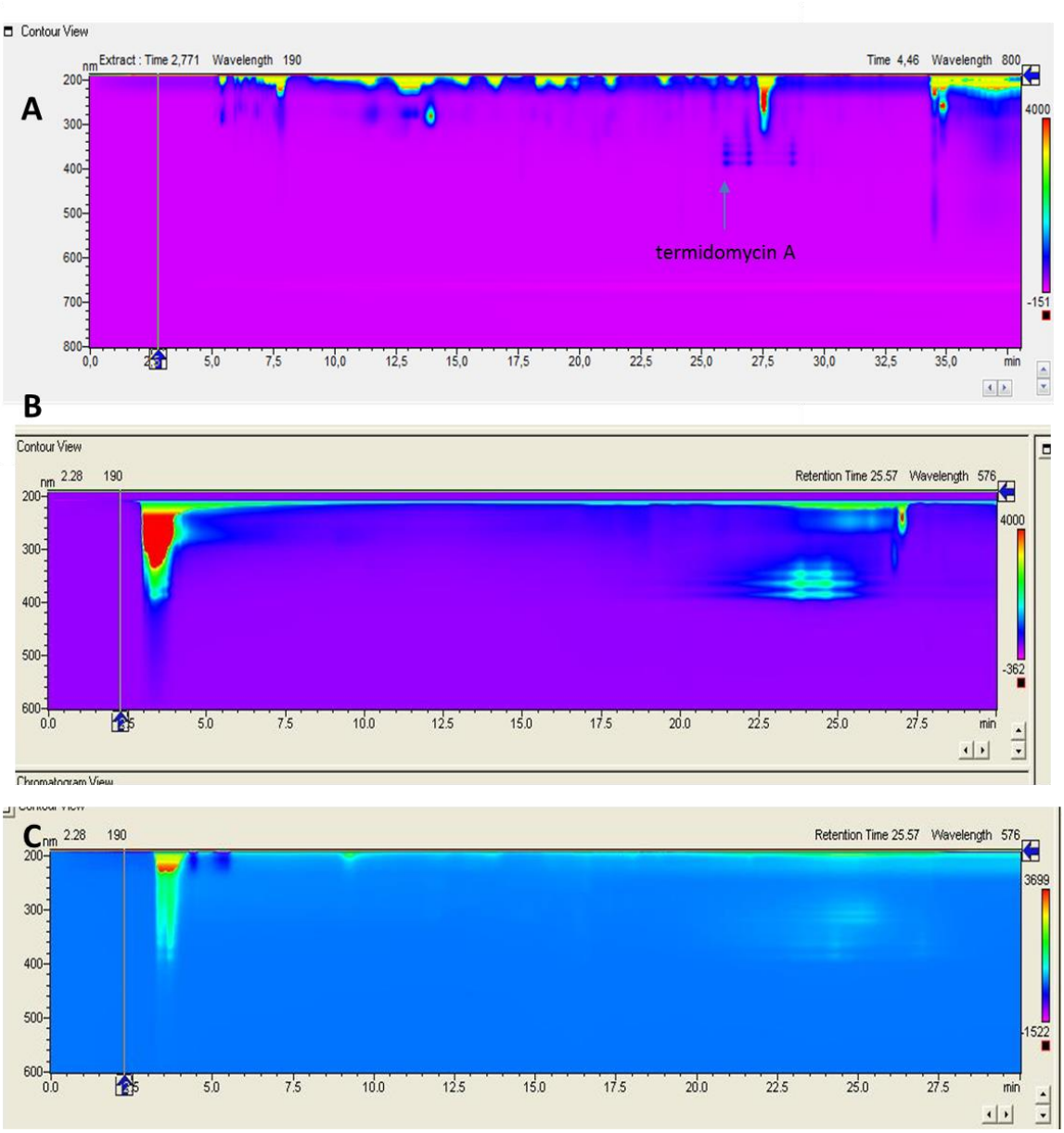

Figure S12. A) 2D UV-Vis spectrum of a LC-MS-UV-Vis measurement of crude culture extracts indicating a specific termidomycin UV-Vis signals; B) 2D UV-Vis spectrum (LC-MS-UV-Vis measurement) of freshly prepared termidomycin-enriched culture extracts and C) after storage for one day in NMR tube.

m/z= 1289.84-1299.84

m/z	Theo. Mass	Delta (mmu)	RDB equiv.	Composition
1294.8397	1294.8398	-0.10	11.5	$C_{70}H_{120}O_{20}N$
	1294.8425	-2.78	16.0	$C_{73}H_{118}O_{17}N_2$
	1294.8339	5.77	20.5	$C_{77}H_{116}O_{15}N$
	1294.8465	-6.80	20.0	$C_{78}H_{118}O_{15}$
	1294.8313	8.45	16.0	$C_{74}H_{118}O_{18}$
	1294.8272	12.47	12.0	$C_{69}H_{118}O_{20}N_2$
	1294.8551	-15.36	15.5	$C_{74}H_{120}O_{17}N$
	1294.8578	-18.04	20.0	$C_{77}H_{118}O_{14}N_2$
	1294.8187	21.03	16.5	$C_{73}H_{116}O_{18}N$
	1294.8160	23.71	12.0	$C_{70}H_{118}O_{21}$

A

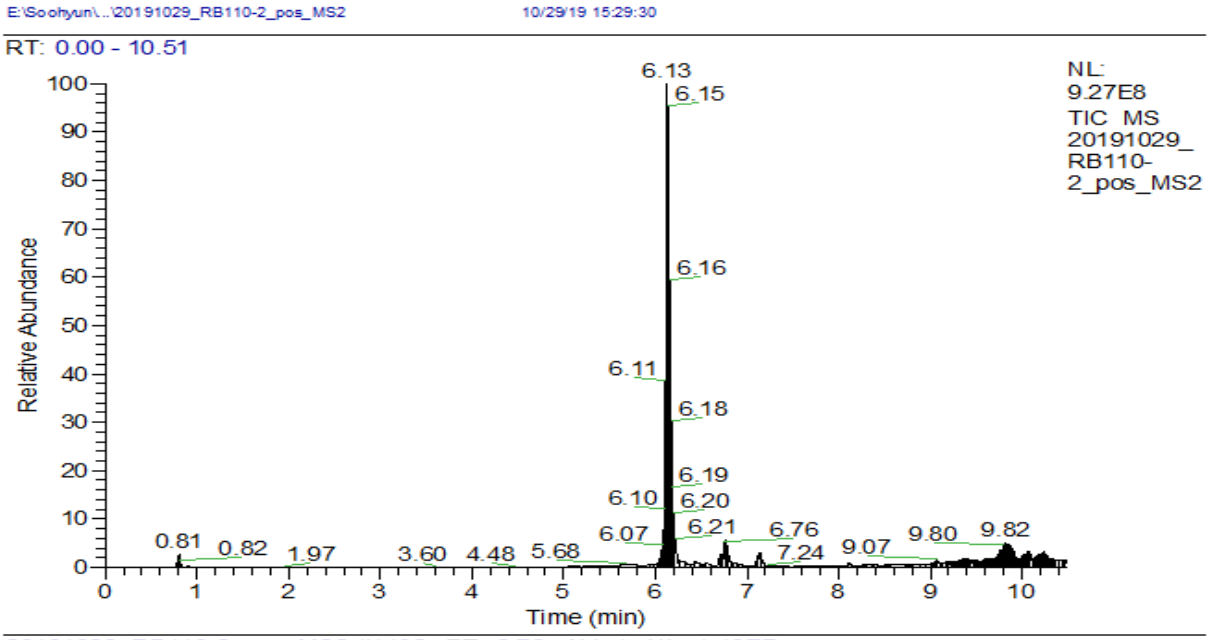

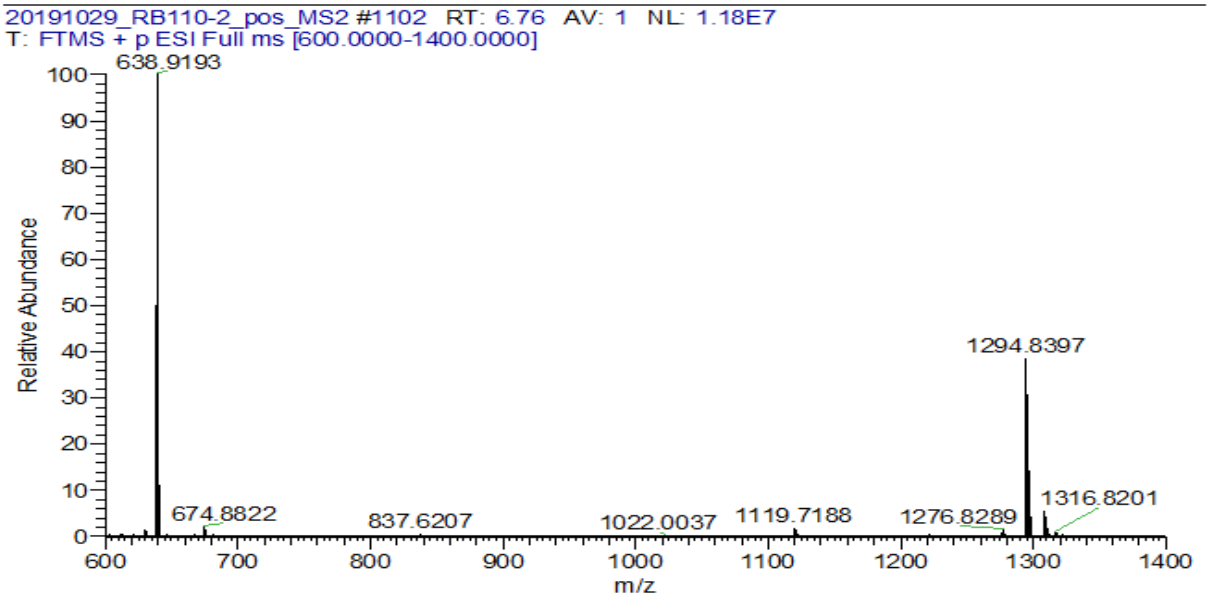

B

Figure S13.A) Elemental composition search on mass 1294.8397 for termidomycin A (**1**); B) ESI-HRMS spectra of termidomycin A (**1**)

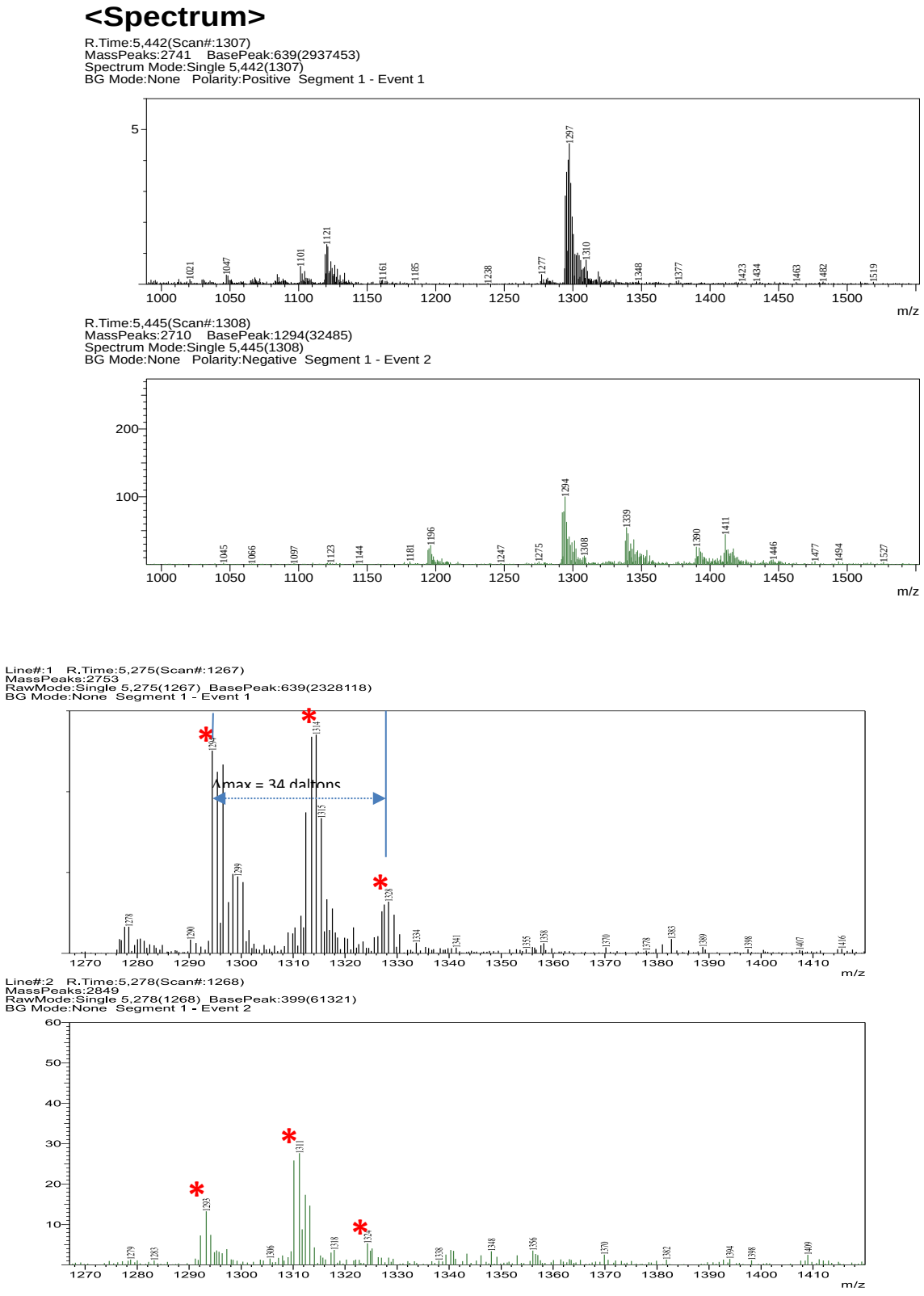

Figure S14. Positive (upper) and negative (bottom) modes of LC-MS spectra for ^{13}C acetate feeding study to increase ^{13}C carbon signal intensity of termidomycin A (**1**).

Table S2. NMR Data (pyridine-d_5, at 300 K) for termidomycin A (**1**).[a]

position	δ_C, type	δ_H, mult. (J in Hz)	COSY	HMBC	remark
1	177.8, C				
2	48.6, CH	2.95, qd (15.0, 7.5)	3, 4	1, 3, 4, 5	
3	15.2, CH_3	1.35. d (7.5)	4	1, 2, 4	
4	74.9, CH	4.53, dd (15.0, 7.0)	2, 5	1, 2, 3, 6	
5	133.0, CH	5.74, dd (15.0, 7.0)	4, 6	4, 6, 7	
6	133.9, CH	5.61, dd (15.0, 9.0)	5, 7	5, 7, 8, 10	
7	49.7, CH	2.45, m	6, 8, 10	6, 8, 9, 10	
8	25.0, CH_2	2.33, m	7, 9	6, 7, 9	
		1.50, m	7, 9	6, 7, 9	
9	12.2, CH_3	0.99, m	8	7, 8	
10	80.8, CH	4.15, d (8.5)	7	7, 11, 13	
11	143.1, C				
12	13.3, CH_3	2.03, s		10, 11, 13	
13	127.7, CH	6.24, d (13.0)	14	10, 11, 12, 14	
14	130.0, CH	6.72, dd (15.0, 13.0)	13, 15	13, 15	
15	134.2, CH	6.40,	14, 16	14, 16	
16	133.6, CH	6.63, m	15, 17	15, 17	
17	133.3, CH	6.48, m	16, 18	16, 18	
18	134.5-133.0, CH	6.63-6.45, m	17, 19	17, 19	overlapped
19	134.5-133.0, CH	6.63-6.45, m	18, 20	18, 20	overlapped
20	134.5-133.0, CH	6.63-6.45, m	19, 21	19, 21	overlapped
21	134.5-133.0, CH	6.63-6.45, m	20, 22	20, 22	overlapped
22	134.5-133.0, CH	6.63-6.45, m	21, 23	21, 23	overlapped
23	133.5, CH	6.72, m	22, 24	22, 24	
24	134.2, CH	6.42, dd (13.5, 6.5)	23, 25	23, 25, 26	
25	130.7, CH	5.98, ddd (13.5, 6.5, 6.5)	24, 26	24, 26, 27	
26	39.8, CH_2	2.49, m, 2.32, m	25, 27	24, 25, 27, 38	
27	70.5, CH	3.97, ddd (13.0, 7.0, 7.0)	26, 28	25, 26, 28, 31	
28	41.4, CH_2	1.49, dd (7.0, 3.0)	27, 29	24, 26, 27, 29	
29	63.9, CH	4.53, m	28, 30	28, 30	
30	45.2, CH_2	2.39, m, 2.08, m	29	28, 29, 31	
31	100.5, C				
32	41.1, CH_2	2.04, m	33	31, 33	
33	77.4, CH	4.08, m	32, 34	32, 34, 35	
34	45.4, CH_2	1.77, m	33, 35	32, 33, 35, 36	
35	74.7, CH	4.52, m	34, 36	33, 34, 36, 37	
36	45.9, CH_2	2.10, m	35, 37	34, 35, 37, 38	
37	70.8, CH	4.44, m	36, 38	35, 36, 38, 39	
38	40.4, CH_2	2.28, m	37, 39	36, 37, 39, 40	
39	77.5, CH	4.05, m	38, 40	37, 38, 40, 41	
40	45.8, CH_2	2.03, m	39, 41	38, 39, 41, 42	
41	72.3, CH	4.48, m	40, 42	39, 40, 42, 43	
42	48.9, CH_2	2.12, m	41, 43	40, 41, 43, 44	
43	69.2, CH	4.52, m	42, 44	41, 42, 44, 45	
44	44.5, CH_2	1.96, m	43, 45	42, 43, 45, 46	
45	74.3, CH	4.63, m	44, 46	43, 44, 46, 47, 49	
46	48.5, CH	2.14, m	45, 47, 49	45, 47, 49	
47	21.8, CH_2	1.80, m, 1.66, m	46, 48	45, 46, 49	
48	12.3, CH_3	1.03, d (7.5, 2.0)	47	46, 47	
49	77.8, CH	4.08, dd (12.0, 7.0)	46, 50	45, 46, 47, 50, 52	
50	36.8, CH	2.25, m	49, 51, 52	49, 51, 52	
51	11.1, CH_3	1.29, d (7.0)	50	49, 50, 52	
52	71.5, CH	4.49, m	50, 53	49, 50, 53, 55	
53	38.5, CH	1.54, m	54	52, 54, 55	
54	10.4, CH_3	1.09, d (6.5)	53	52, 53, 55	
55	75.7, CH	6.11, m	56	1, 52, 54, 56, 58	
56	41.5, CH	2.13, m	55, 57, 58	55, 57, 58	
57	10.3, CH_3	1.16, d (6.5)	56	55, 56, 58	
58	67.3, CH	4.31, dd (10.3, 3.0)	56, 59	55, 56, 57, 59, 60	
59	40.6, CH_2	2.29, m	58, 60	58, 60, 61	
60	78.2, CH	4.25, m	59, 61	59, 61, 62, 63	
61	28.0, CH_2	1.97, m, 1.80, m	60, 62	59, 60, 62	
62	10.4, CH_3	1.10, m	61	60, 61	
63	98.6, CH	4.82, m	64	60, 63	
64	42.5, CH_2	2.59, m, 2.03, m	63, 65	63, 65	
65	67.0, CH	4.05, m	64, 66	63, 64, 66	
66	73.2, CH	2.29, m	65, 69	65, 67, 68, 69, 70	
67	42.4, CH_3	2.52, s		66	
68	42.4, CH_3	2.52, s		66	
69	70.3, CH	3.42, qd (10.5, 6.5)	66, 70	63, 65, 66, 70	
70	20.3, CH_3	1.40, d (6.5)	69	66, 69	

[a]600 MHz for ^{1}H NMR and 150 MHz for ^{13}C NMR

7. *In silico* analysis of the PKS cluster *trm-1* and *trm-2* cluster

RB110-1: JAEKDS000000000.1: tig00000002_np1212 (Location: 783,249 - 959,410 nt) (total: 176,162 nt)

RB110-2: JAEKDR000000000.1: tig00000001_np1212 (Location: 88,477 - 262,099 nt) (total: 173,623 nt)

BGCs were first identified using antiSMASH 5.0.[13] Then, Basic Local Alignment Search Tool for proteins (BLASTp) (NCBI) was used to determine potential false positives or additional gene clusters. The PKS gene cluster was analysed by the BLAST server from the UniProt website using the UniProtKB/Swiss-Prot database with default settings. The first three hits were used for comparison and function prediction. Furthermore, the best three hits of the Minimum Information about a Biosynthetic Gene cluster (MIBiG) database embedded in antiSMASH 5.0 were taken into account when performing phylogenetic studies on the catalytic domains and comparison with other BGCs. Sequence similarities are defined as amino acid similarities based on BLASTp. Sequences were compared using the BLAST algorithm. Partial sequences were manually compiled, assembled and trimmed using BioEdit Version 7.2.0.[14] Initial tree(s) for the heuristic search were obtained automatically by applying Neighbour Joining method. The robustness of branches was assessed by bootstrap analysis with 1000 replicates. The trees are drawn to scale with branch lengths measured in the number of substitutions per site. Evolutionary analyses were conducted in MEGA7.8

Extender unit biosynthesis: The gene cluster encodes for the biosynthesis of additional PKS-extender units, such as the biosynthesis of ethyl malonate (EthMal). The biosynthesis of EthMal requires the action of CCR-homologues, which form phylogenetically distinct clades. The CCR encoded in the *trm* cluster form a clade within the typical ethylmalonyl incorporating CCR from other known natural product gene cluster and therefore the ethylmalonyl units incorporated in TrmI are provided by CCR.

AT Domains: Phylogenetic analysis of AT-domains suggests that ATs with the same substrate specify share a common evolutionary origin with malonyl- and methylmalonyl-speficifity clustering into distinct clades (Figure xx).[15,16]ATs accepting ethyl and/or propyl malonate as their extender units form a clade distinct from other ATs.

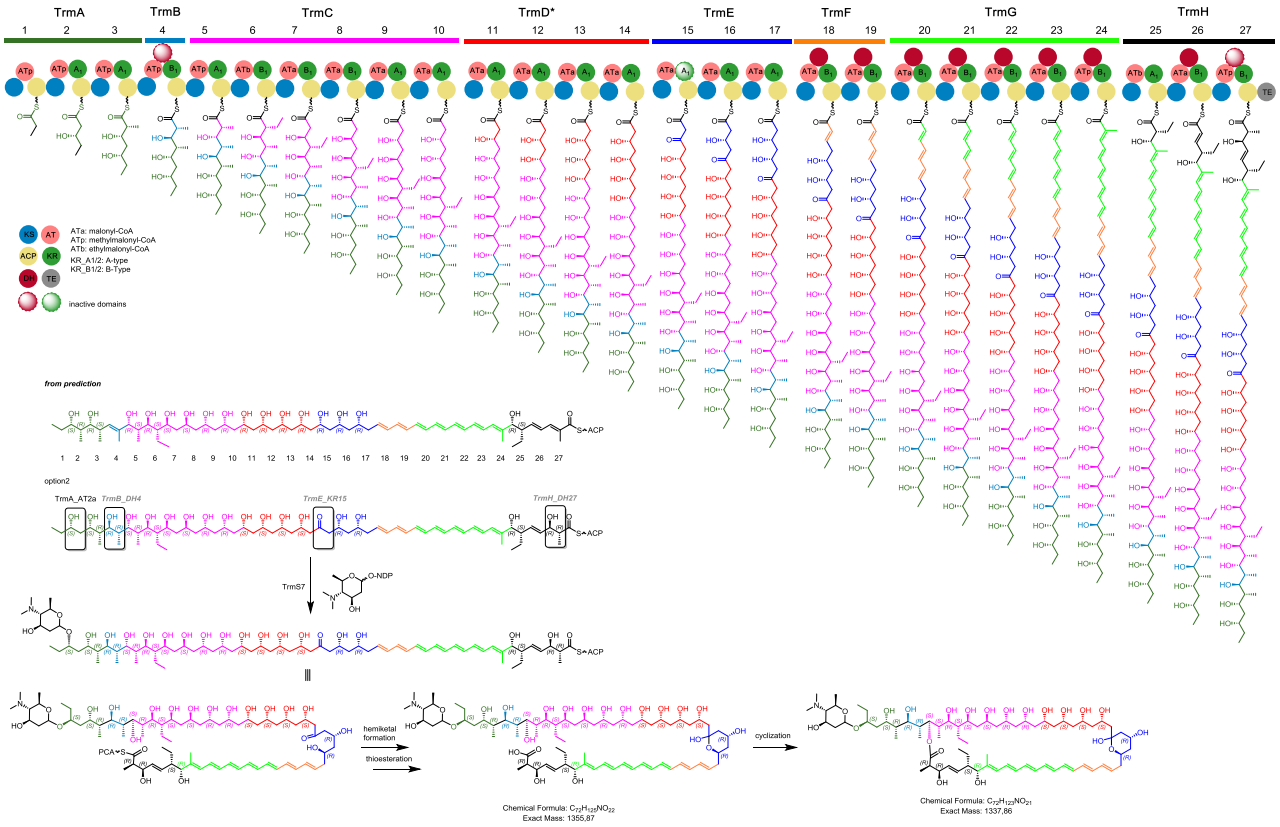

Figure S15. PKS-based biosynthetic assembly line of PKS encoded within *trm-1* and predicted absolute structure of termidomycin congeners.

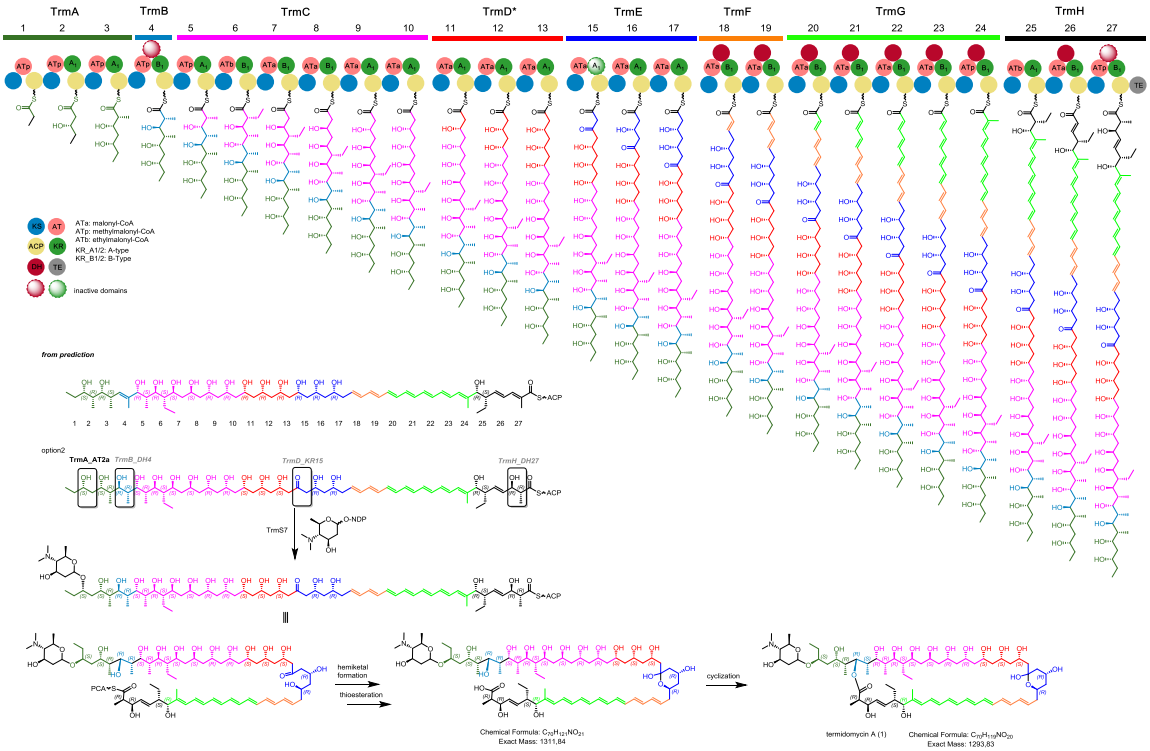

Figure S16. PKS-based biosynthetic assembly line of PKS encoded within *trm-2* and predicted absolute structure of termidomycin (**1**) and congeners**.**

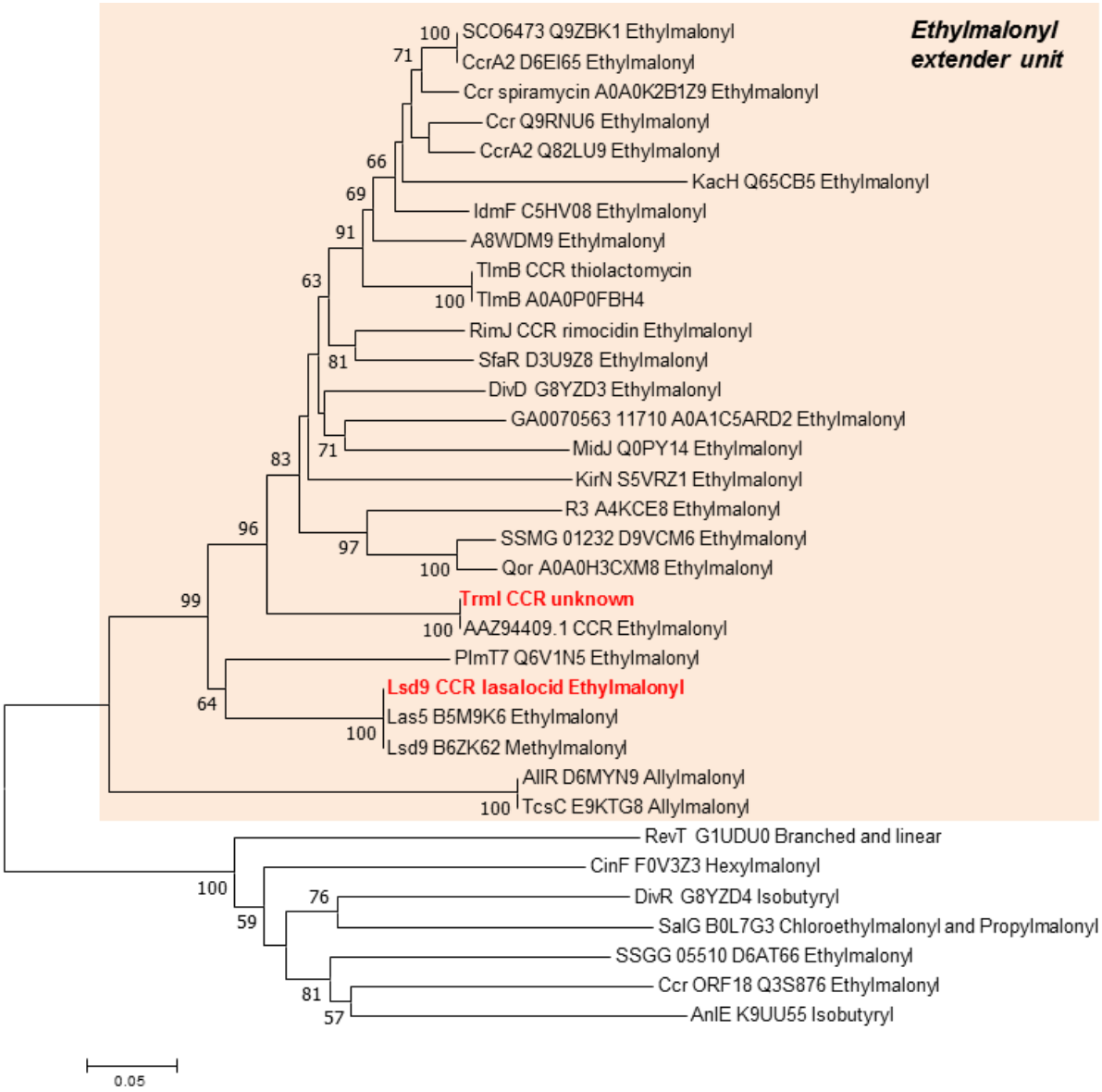

Figure S17. Phylogenetic analysis of CCR-domains using Neighbor-Joining method (Table S9). The optimal tree with the sum of branch length = 3.50006271 is shown. The percentage of replicate trees in which the associated taxa clustered together in the bootstrap test (1000 replicates) are shown next to the branches. The tree is drawn to scale, with branch lengths in the same units as those of the evolutionary distances used to infer the phylogenetic tree. The evolutionary distances were computed using the Poisson correction method and are in the units of the number of amino acid substitutions per site. The analysis involved 34 amino acid sequences. All positions with less than 95% site coverage were eliminated. That is, fewer than 5% alignment gaps, missing data, and ambiguous bases were allowed at any position. There were a total of 399 positions in the final dataset. Evolutionary analyses were conducted in MEGA7. [8]

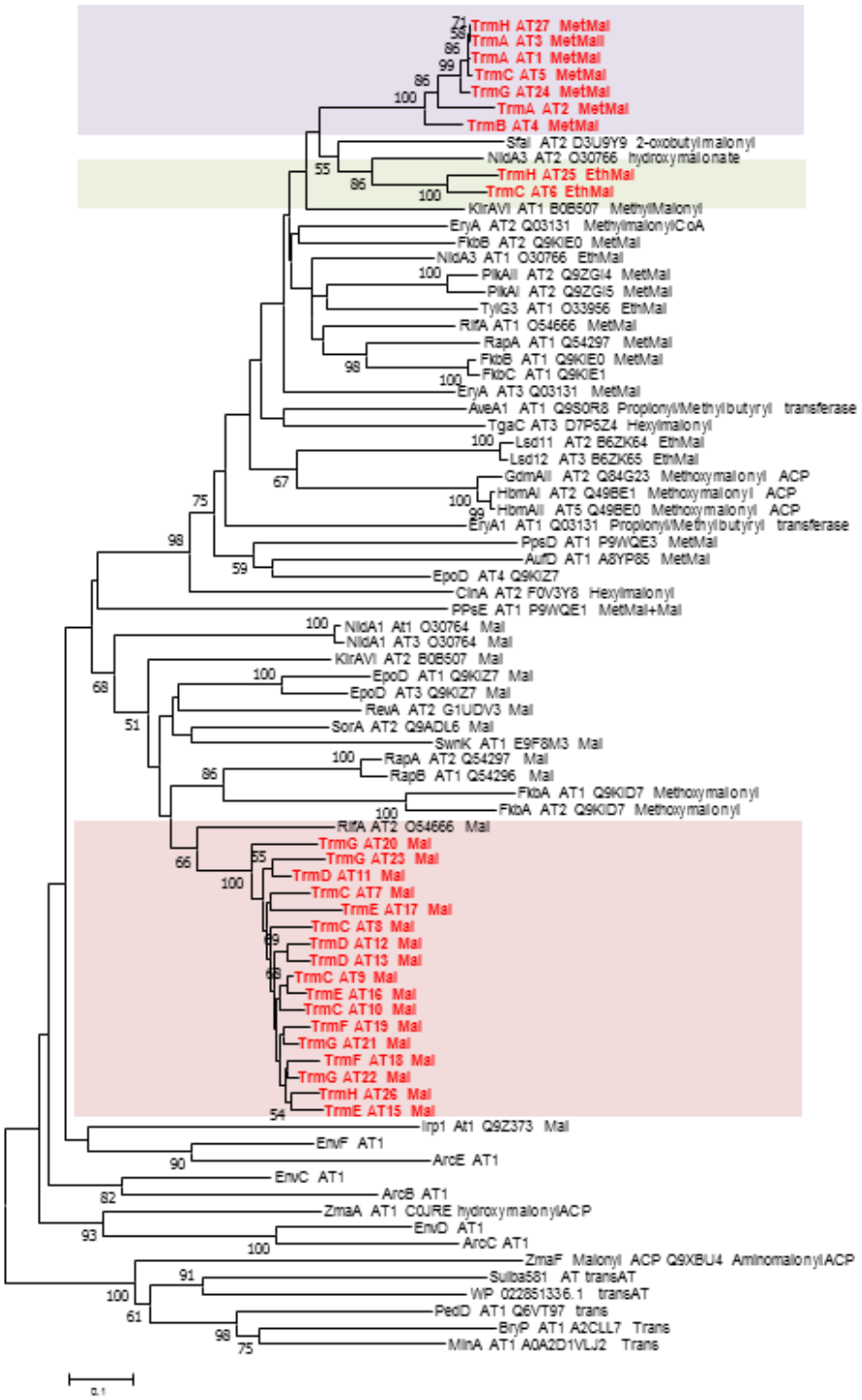

Figure S18. Phylogenetic analysis of AT-domains using Neighbor-Joining method (seeTable S12). The optimal tree with the sum of branch length = 18.80879066 is shown. The percentage of replicate trees in which the associated taxa clustered together in the bootstrap test (1000 replicates) is shown next to the branches. The tree is drawn to scale, with branch lengths in the same units as those of the evolutionary distances used to infer the phylogenetic tree. The evolutionary distances were computed using the Poisson correction method and are depicted in units of the number of amino acid substitutions per site. The analysis involved 80 amino acid sequences. All positions with less than 95% site coverage were eliminated. That is, fewer than 5% alignment gaps, missing data, and ambiguous bases were allowed at any position. There were a total of 232 positions in the final dataset. Evolutionary analyses were conducted in MEGA7.[8]

Table S3. Sequence alignments of KR-domains by CLUSTAL multiple sequence alignment by MUSCLE (3.8)

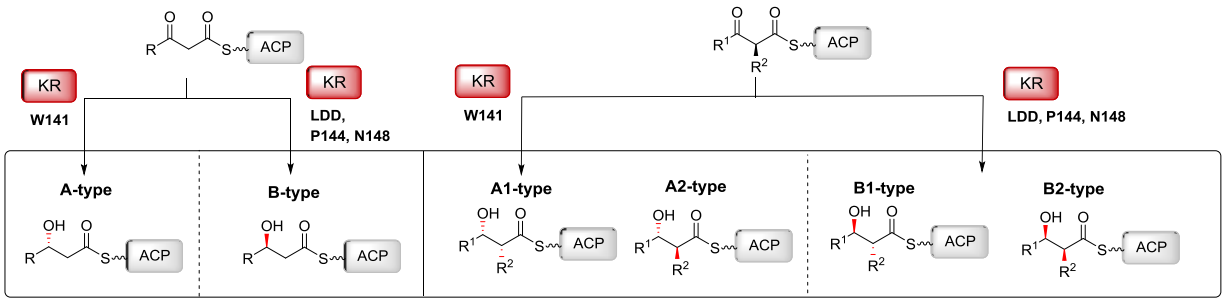

Module	Loop	Catalytic Region
Ery2_A1	HAAGLPQQVAI	SSGAGVWGSARQGAYAAANA
Tyl6_A1	HTAGTPHSAEF	SSGAAVWGSGGQTAYGAANA
Pik5_A1	HTAGAPGGDPL	SSNAGVWGSGWQGVYAAANA
Ole6_A1	HTAGVPDSRPL	SSNAGVWGSGGQAVYAAANA
Meg6_A1	HAAGVPQSTPL	SSGAGVWGSANLGAYAAANA
Sor6_A1	HAGGIEPHAPL	SSGAVVWGGGQQGGYAAANA
TrmA_KR2	HAAGISDTGPL	SSGAGVWGSGGQGAYGAANA
TrmA_KR3	HAAGTVQTAPV	SSGAGVWGSAGLAAYGPANA
TrmC_KR5	HAAGVAPSVPL	SSNAGVWGSGGQSAYAAANA
TrmC_KR9	HAAGAAATRPL	SSIAGVWGSGGQSAYAAANA
TrmC_KR10	HAAGAGQAAPL	SSIAGVWGSGGQSVYAAANA
TrmD_KR11	HAAGIGDAAPV	SSISGVWGSGGLAAYSAANA
TrmD_KR12	HAAGVSRDTLL	ASIAGVWGSGAGGAYSAANA
TrmD_KR13	HAAGVSRDTLL	ASIAGVWGSGAGGAYSAANA
TrmD_KR14	HAAGVSRSNVL	SSIAGVWGSGGGGSYAAANA
TrmE_KR15	HAAGASRSTLL	SSIAGVWGSGAGAAYSAANA
TrmE_KR16	HTAGLYDPAPL	SSIAATWGSLELGAYAAANT
TrmE_KR17	HTAGVPQTTAL	SSIAATWGSGNQAAYAAANA
TrmH_KR25	HAAGIAPLVPL	SSGAGVWGGGGQGAYAAANA
Nys1_A2	HAAAAIELSAL	SSTAGMWGSGVHAAYVAGNA
Pim7_A2	HTAVTIELAPL	SSTAGMWGSGAHAAYVAGNA
Can13_A2	HTAAVIELQSI	SSTAGMWGSGRHAAYVAANA
Amp1_A2	HTAAVIELAAL	SSTAGMWGSGVHAAYVAGNA
Ela4_A2	HIAGAGVLVPL	SSISAVWGSGEHGAYAAANA
Tyl1_B1	HTAGILDDAVI	SSAAATFGAPGQANYAAANA
Ave1_B1	HTAGILDDATL	SSVTGTWGNAGQGAYAAANA
Ave7_B1	HAAGVLDDATI	SSAAGILGSAGQANYAAANA
Ave9_B1	HAAGVLDDATI	SSAAGILGSAGQGNYAAANA
Asc8_B1	HTAATLDDGIL	SSAAAVLGSPGQGNYAAANA
Rap10_B1	HTAGVLDDGVV	SSAAGVLGSAGQGNYAVANA
TrmB_KR4	HTAAVLDDSVV	SSVAGRLSGVGQGSYTAANA
TrmC_KR6	HAAVVLDDGVF	SSLAGTMGNAGQGNYAAANA
TrmC_KR7	HTAGVLDDGVL	SSTAGFFGSSGQGNYAAANA
TrmC_KR8	HTAGVLDDGVL	SSTAGFFGSSGQGNYAAANA
TrmF_KR18	HTAGVLDDGVV	SSAASVFGNAGQASYSAANA
TrmF_KR19	HTAGVLDDGVF	SSVAATFGGAGQGNYAAANA
TrmG_KR20	HTAGVLDDGVV	SSAASVFGNAGQASYSAANA
TrmG_KR21	HTAGVLDDGVL	SSAAGVFGNAGQANYSAANA
TrmG_KR22	HTAGVLDDGVL	SSAAGVFGNAGQANYAAANS
TrmG_KR23	HTAGVLDDGVI	SSAAGVFGNAGQGNYAAANA
TrmG_KR24	HSAGVLDDGVL	SSAAATFGRPGQGNYAAANA
TrmH_KR26	HTAGVLDDGVL	SSAAGTVGSPGQANYAAANA
TrmH_KR27	HIAGALDDGVI	SSAAGTFGGPGQGNYAAANA
Lan1_B2	HTAATLDDGTL	SSFASAFGAPGLGCYAPGNA
Meg1_B2	HVAATLDDGTV	SSSTAAFGAPGLGGYVPGNA
Ery1_B2	HAAATLDDGTV	SSFASAFGAPGLGGYAPGNA
Pik1_B2	HTAGALDDGIV	SSVSSTLGIPGQGNYAPHNA
Oli14_C1	HTAGVAGHGPL	SSGAAVWGSGSNGANAAAGG
Meg3_C2	HAETLTNFAGV	SSVAGVWGGVGMAAYAAGSA
Ery3_C2	HAGTLTNFGSI	SSVAGIWGGAGMAAYAAGSA
Lan3_C2	HAATRTEFGPV	SSVAGVWGGAGMAGYAAGSA
Pik3_C2	HLPPTVDSEPL	SSVAAIWGGAGQGAYAAGTA
Nid4_C2	HAPPLVPLAPL	SSVSGVWGGAAQGAYAAATA
Tyl4_C2	VAPPVAPPTPL	SSVAGVWGGAGQGGYAAGTA

Table S1. Multiple sequence alignment of KR domains by CLUSTAL

```
TrmA_KR2        GTVLVTGGTGALGGHLARWLA-AEGAERIVLVGRRGADAP--------GAAEL-------  44
TrmA_KR3        GTVLITGGTGALGGRVARWLA-AEGAAHLVLTSRSGQAAP--------GADELAA-----  46
TrmB_KR4        GTVLVTGASGGLGMALARHLATAHDVRGLVLAARRGDAYA--------PLAALAD-----  47
TrmC_KR5        GTVLITGGTGALGGRVARRLA-AEGAEHLVLTSRRGPDAA--------GVTELAQ-----  46
TrmC_KR6        GTVLVTGGTGTVGARVGRWLA-ANGAAHVVLASRSGMTAP--------GAAELAA-----  46
TrmC_KR7        GTVLVTGGTGALGGHVARWLA-GAGAEHLVLAGRRGLEAP--------GAVELRE-----  46
TrmC_KR8        GTVLVTGGTGALGGHVARWLA-GAGAEHLVLAGRRGLEAP--------GAVELRE-----  46
TrmC_KR9        GTVLITGGTGALGLYVAHWLA-AAGAEHLVLASRSGGDAE----------AL-------  41
TrmC_KR10       GTVLVTGGTGALGSKVARWLI-EGGAEHVVLTSRRGADAP--------GAAEL-------  44
TrmD_KR11       GTVLVTGGTGALGTAVTRWLL-ESGAEHVVLLSRSGAGAE--------TPATSDRSTATE  51
TrmD_KR12       GTVLITGGTGALGVETARCLV-GAGAERVVLLSRSGVV----------------------  37
TrmD_KR13       GTVLITGGTGALGVETARCLV-GAGAERVVLLSRSGVV----------------------  37
TrmD_KR14       GTVLVTGGSGALGRVVTDWLV-AEGAERVVLVSRGGG----------------------  36
TrmE_KR15       GTVLVTGGTGALGREVARWLV-DTGAERVVLLGRRAVGQGSGGHTGGSGTGDLAGTSDPG  59
TrmE_KR16       ------------------------------------------------------------  0
TrmE_KR17       GTVLVTGGTGAIGTHVARWLA-KSGAARLVLTSRRGAAAP--------GAEELRE-----  46
TrmF_KR18       GTVLVTGASGGLGGLVARHLVVVHGVRDLLLVSRRGTVAD--------G---LEA-----  44
TrmF_KR19       --TLITGASGTLGGLFARHLVNRYDARDLVLVSRRGDTAP--------GMAELVA-----  45
TrmG_KR20       GTVLVTGASGGLGGLVARHLVVVHGVRDLLLVSRRGTVAD--------G---LEA-----  44
TrmG_KR21       -TVLVTGASGGLGSLVAVHLAAVHGVRRLVLASRRGTVS----------AELTG-----  43
TrmG_KR22       -VVLITGANGALGGAVARHLFFVHGVRTLVLASRRGEADP--------VAAGLRT-----  46
TrmG_KR23       -TVLLTGATGALGALIAEHLVTAHGVRRLVLTSRRGLDAP--------GAVELRD-----  46
TrmG_KR24       GAVLLTGASGALGGVVARHLVAGHGVRHLVLISRRGARAD--------GMAELEE-----  47
TrmH_KR25       GTVLVTGGVGGVGAHVARWLA-RRGADHLVLTSRRGEDSP--------GAARLAA-----  46
TrmH_KR26       GTVLVTGATGALGKLVATRLVTAHGVRSLVLVGRRGPAAE--------GADELVA-----  47
TrmH_KR27       GTVLVTGATGALGRLVARRLVTEHGARRLVLASRRGPDAD--------GAAELLA-----  47


TrmA_KR2        --AAELGDVVSFAACDTTDRDQLAALLDG------------IE-DLGAVVHAAGISDTGP  89
TrmA_KR3        -DLRDLGADVTIEACDAADREALGALLEK------------LP-DLTAVFHAAGTVQTAP  92
TrmB_KR4        -ELRVLGVEVRVPACDVSDPLQTRQLIDG------------IA-ELTAIVHTAAVLDDSV  93
TrmC_KR5        -ELQESGVRVTVAACDLADRDSVAALLESLRGPDG-------L-DIDAVVHAAGVAPSVP  97
TrmC_KR6        -DIRELGAQVTVAACDITDRDALSGLLDGLEGGR--------E-GLTAVVHAAVVLDDGV  96
TrmC_KR7        -ELAGSGVRVSVVACDVADRDALAALLEE------------HP--VDAVFHTAGVLDDGV  91
TrmC_KR8        -ELAGSGVRVSVVACDVADRDALAALLEE------------HP--VDAVFHTAGVLDDGV  91
TrmC_KR9        --AARLGTRVTVAVCDTADRDAMAGLLDA------------LP-ELTAVVHAAGAAATRP  86
TrmC_KR10       --LADLGPAATVAACDMADRDAVAALLDSLSATSGTPGASGLP-ALTAVVHAAGAGQAAP  101
TrmD_KR11       PHGTATDPRITALACDVADRDALAAALDG------------IT-GLTAVVHAAGIGDAAP  98
TrmD_KR12       ---SVADPRITAVAGDVTDRGFMAELVGS------------LP-ELTAVVHAAGVSRDTL  81
TrmD_KR13       ---SVADPRITAVAGDVTDRGFMAELVGS------------LP-ELTAVVHAAGVSRDTL  81
TrmD_KR14       -AVEGLGAGVESVACDVSDRQAVEELLGT------------LD-GLTAVVHAAGVSRSNV  82
TrmE_KR15       GHTPALGDRIVTIACDVTDRDALADVIAS------------LP-DLTAVVHAAGASRSTL  106
TrmE_KR16       -------------------SEQLEQLVLRLAAEG--------A-PVRSVIHTAGLYDPAP  32
TrmE_KR17       -ELTGLGADVLLEACDIADRASVAALLDRLEADG--------T-PVTSVFHTAGVPQTTA  96
TrmF_KR18       -ELAGLGARVRLAACDVADRGALAALLEG------------E--RLSGVVHTAGVLDDGV  89
TrmF_KR19       -ELTGLGATVTVRACDIADRQSVAALLEE------------LP--PTAVLHTAGVLDDGV  90
TrmG_KR20       -ELAGLGARVRLAACDVADRGALAALLEG------------E--RLSGVVHTAGVLDDGV  89
TrmG_KR21       -ELSALGVEFEAVACDVADRDAMAELLDR------------VP--FDSVVHTAGVLDDGV  88
TrmG_KR22       -ELTEVGADVTVVACDVADRAVLATVLND------------IE-GLTGIVHTAGVLDDGV  92
TrmG_KR23       -RLTALGADVRIPACDVSDRDAAAALLDS------------VP-DLTAVVHTAGVLDDGV  92
TrmG_KR24       -ELTSLGAEVTVAACDVADREALAELVDS------------IGAPVTGVVHSAGVLDDGV  94
TrmH_KR25       -ELRESGTEVTVAACDVADRAALAALVTSLAEAG--------T-PIRSVMHAAGIAPLVP  96
TrmH_KR26       -QLRELGADVRIEACDASDRQALAALLDT------------VP-GLTGVVHTAGVLDDGV  93
TrmH_KR27       -SLAELGAEATAVACDLADRDAAAALVAA------------HP-DLGAVVHIAGALDDGV  93
                                         :                  .:.* *


TrmA_KR2        LAGLTAERIDAVLAPKAKTAWDLHELTR----DRDLSAFVMFSSGAGVWGSGGQGAYGAA  145
TrmA_KR3        VAETGPADLAAAAHGKVQGAVNLDELLA----DRELDAFVLFSSGAGVWGSAGLAAYGPA  148
TrmB_KR4        VTGLTPDQLDRVLAPKADAARHLHELTR----DRDLSAFVLFSSVAGRLSGVGQGSYTAA  149
TrmC_KR5        LVDTTPADFAATLAVKAHGAHHLHDLLE----GTELDAFVLFSSNAGVWGSGGQSAYAAA  153
TrmC_KR6        FDALDPARFDRVLAPKVTAARHLHELTA----GLDLSAFILFSSAAGTIGSGGQANYAAS  152
TrmC_KR7        LEALTPERFETVFRAKVRSALNLHELVG------DVSAFVLFSSLAGTMGNAGQGNYAAA  145
TrmC_KR8        LEALTPERFETVFRAKVRSALNLHELVG------DVSAFVLFSSTAGFFGSSGQGNYAAA  145
TrmC_KR9        LADSDPDDLAAVMAAKVLGAAHLDELLG----DRELDAFVLFSSIAGVWGSGGQSAYAAA  142
```

```
TrmC_KR10      LDGLTPDETASVLAAKVLGAAHLDELLG----DRELDAFVLFSSIAGVWGSGGQSVYAAA 157
TrmD_KR11      VQDTDAAQAAAVFAAKVGGAAALHELLG----DRDLDAFVLFSSISGVWGSGGLAAYSAA 154
TrmD_KR12      LVDLSAGELAEITAAKMVGAAVLDEVLG----DRELDAFVLYASIAGVWGSGAGGAYSAA 137
TrmD_KR13      LVDLSAGELAEITAAKMVGAAVLDEVLG----DRELDAFVLYASIAGVWGSGAGGAYSAA 137
TrmD_KR14      LVDVEPDELAQVMAGKAVGAALLDELLG----ERELDAFVVFSSIAGVWGSGGGGSYAAA 138
TrmE_KR15      LADLGPAELAEVMAAKVTGAAHLDELLG----DRDLDAFVLFSSIAGVWGSGAGAAYSAA 162
TrmE_KR16      LTETTPERLAAVAAAKVAPLAALDALLD-----EPLDAFVLFSSIAATWGSLELGAYAAA 87
TrmE_KR17      LAEMSPGEYAATLAAKAEGARHLHELLS----STGLDAFVLFSSIAATWGSGNQAAYAAA 152
TrmF_KR18      VSSLTGERVGAVLRPKVDAAWHLHELTR----GHDLSAFVLFSSAASVFGNAGQASYSAA 145
TrmF_KR19      FTALTPERLDIVLRPKAEAATHLHELTR----GLDLTAFVLFSSVAATFGGAGQGNYAAA 146
TrmG_KR20      VSSLTGERVGAVLRPKVDAAWHLHELTR----GHDLSAFVLFSSAASVFGNAGQASYSAA 145
TrmG_KR21      LASLTPERISTVLRPKADAVWNLHELTA----DRALNRFVVFSSAAGVFGNAGQANYSAA 144
TrmG_KR22      LASLTPERISGVLRPKVDAAWHLHELTA----GLGLRHFVLFSSAAGVFGNAGQANYAAA 148
TrmG_KR23      ITSLTPERLDTVLRAKADAATHLHELTR----DRDLTAFVLFSSAAGVFGNAGQGNYAAA 148
TrmG_KR24      LSSLTPEKLDRVLRPKVHAAWNLHELTY----RHAPSAFVLFSSAAATFGRPGQGNYAAA 150
TrmH_KR25      LTETDAGVLADTLAAKVAGTAHLDALLDGAPGAEPLDAFVLFSSGAGVWGGGGQGAYAAA 156
TrmH_KR26      LSSLTAGQLSAVLRPKVDAAWYLHELTR----DRDLTAFVLFSSAAGTVGSPGQANYAAA 149
TrmH_KR27      ISSLTPRKLDRVLRPKVDAAWNLHELTR----GLALTAFVLFSSAAGTFGGPGQGNYAAA 149
               .              *      *. :            *::::* :.  .    . *  :

TrmA_KR2       NAVLDALAAHRRAAGLPATAVSWGAWQG        173
TrmA_KR3       NAHLEALALHRRARGLTATSVAWGTWD-        175
TrmB_KR4       NAAMEAVAAQRRSEGLPGTALAWGLWSE        177
TrmC_KR5       NAHLDAFAAWRRAQGLRATSVAWGAWA-        180
TrmC_KR6       NAHLDALAEQRRADGLPATSVAWGPWG-        179
TrmC_KR7       NAYLDALAQTRRAAGLPATSVAWGAWA-        172
TrmC_KR8       NAYLDALAQTRRAAGLPATSVAWGPWA-        172
TrmC_KR9       NAYLDGLAEQRRARGVTATSVAWGPWAE        170
TrmC_KR10      NAYLDALAQRRRTEGRPATAVAWGPWGE        185
TrmD_KR11      NAYLDGLAEHRRARGLAATSLSWGPWAE        182
TrmD_KR12      NAYLDGLAECRRARGLVATSIAWGPWA-        164
TrmD_KR13      NAYLDGLAECRRARGLVATSIAWGPWA-        164
TrmD_KR14      NAYVDGLVERRRARGLVGTSIAWGPWA-        165
TrmE_KR15      NAFLDGLAEQRRARGLKATAVAWGPWA-        189
TrmE_KR16      NTAAEAIVRNRRARGLNATSIAWAPWQ-        114
TrmE_KR17      NAYLDALAEHRRSRGLPATSVAWGAWA-        179
TrmF_KR18      NAFLDALARQRRAEGLPAHSLAWGLWE-        172
TrmF_KR19      NAHLDALAQRRRADGLPALSLAWGLWA-        173
TrmG_KR20      NAFLDALARQRRAEGLPAHSLAWGLWE-        172
TrmG_KR21      NAFLDALILHRRSLGLPGQSLAWGLWD-        171
TrmG_KR22      NSFLDALAEHRRAQGLPARSLAWGQWT-        175
TrmG_KR23      NAFLDALAVHRRSLGLPGQSLAWGAWA-        175
TrmG_KR24      NAFLDALAHHRRAAGLPAVAMAWGLWAE        178
TrmH_KR25      NAYQDAFAELRRARGLPATSVAWGGWSD        184
TrmH_KR26      NAFLDALAEQRAAEGLPATSLAWGMWE-        176
TrmH_KR27      NAFLDALAQHRRALGLPAASLAWGLWEE        177
               *:  :..   * : *  . :::*. *
```

Table S2. Multiple sequence alignment of DH domains (CLUSTAL, MUSCLE (3.8))

```
TrmB_DH4          HPLIGAAIAPADSDGVVLTGRLLPSAQPWLADHVVGGAALLPATALLDLALHAGAQVGCD
TrmF_DH18         HPLLGAAIGRADGEGSLLTGRLSLRTHPWLAEYAVGGRVVLPGAAMVELAIRAGDQVGCD
TrmF_DH19         HPLLGAAVPMADGEGHLFTGRLSLRTHPWLADHAVSDTVLLPGTAMLELALRAGEHLHCH
TrmG_DH20         HPLLGAAVGLADAEGSLLTGRLSLRTHPWLADHTVGGRVVLPGAAMVELAIRAGDQVGCD
TrmG_DH21         HPLLGAAVGLADG-GVVFTGRLSLESHPWLVGHVVSGAVLLPGAAMVELAVRAGDQVGCD
TrmG_DH22         HPLLGAAVGLADG-GVVFTGRLSLESHPWLVGHVVSGAVLLPGAAMVELAVRAGDQVGCD
TrmG_DH23         HPLLGAGVATADHDGYLFTGRLSVETHPWLADHVVAGAVLVPGAALLELAVRAGDQVDCD
TrmG_DH24         HPLLGAAVTLADAQTTLLTGRVSLRTHPWLADHAVADVILLPGAALLELAIRAGDQVGCG
TrmH_DH26         HPLLGAAVFLAGERGLVLTGRLSLRTHPWLADHTVAGVALLAGTAFVDLAVHAGDHIGRD
TrmH_DH27         HPLLGAAVTLADTEGALFTGRLSTESHPWLADYSVLDTALVPGTALVEIALHAGRSLDCD
                  ***:**.:  *.    ::***:   ::***. : * .  ::..:*::::*:.**  :

TrmB_DH4          LVEELTLESPLVLHEHSGVLIQVTVGAPDPSGSRPLAVYSRG-----DDDPDWVRRCGGT
TrmF_DH18         AVEELTLEAPLVLPGAGAVVVQLAVGAADGAGRRTLNLYSRAE----DAEDTWVRHATGV
TrmF_DH19         RVEELTLEAPLVLPDQGGVAIQVTVGAA-VDGRRTLALHSRSDA---DRDEEWTRNAAGF
TrmG_DH20         AVEELTLEAPLVLPGAGAVVVQLAVGAADGAGRRTLNLYSRAE----DAEDTWVRHATGV
TrmG_DH21         LVEELTLEAPLVLPERGGVAVQLTVSAAGADGRRGVELHS-------SVGEVWTRHASGV
TrmG_DH22         LVEELTLEAPLVLPERGGVAVQLTVSAAGADGRRGVELHS-------SVGEVWTRHASGV
TrmG_DH23         RVAELTIEAPLVLPERGGVAVQLWVSSADGTGARNLALYSRAD----GADSVWTRHAGGL
TrmG_DH24         RVDELTLEAPLVVPETGSIALQVSVTAPDEEGRRALTVHSS------GDEGRWTRHASGL
TrmH_DH26         RLEELTIEAPLVVPERGGVLLQIAVDAPDGFGRCPVAVHSRAED--AAPDALWTRHATGY
TrmH_DH27         LATELLLEAPLVLPAAGGVAVQVTVTAPDDTGLRTVTLHSRPDARPDGDDLPWVRHLTGT
                     ** :*:***:   ..: :*: * :.   *   : ::*           *.*.  *

TrmB_DH4          L-----AIGGPEPV-T-ELVVWPPSAAEPLSVDGLYDRLAAQGAEYGPAFQGL
TrmF_DH18         L-----GTAVAGAG-E-GLAEWPPAGAQAVEVEGLYEGLAEAGLAHGPVFRGL
TrmF_DH19         L-----TAGDPGVPFN-DIDTWPPAQAEAVDVAGLYPGLAAAGFGYGPVFQGL
TrmG_DH20         L-----GTAVAGAG-E-GLAEWPPAGAEPVETEGYYEGLAEAGFDYGPAFRGL
TrmG_DH21         L-----GSG-APVG-E-GLVEWPPAGAEAVDLAGFYEGLE-----YGPEFQGL
TrmG_DH22         L-----GSG-APVG-E-GLVEWPPAGAETVDLAGFYEGLE-----YGPEFQGL
TrmG_DH23         LERTDGTDGTRGSA-A-DLSVWPPQDATETDVAALYDGLASAGLEYGTAFRGL
TrmG_DH24         L-----SVRADAAG-F-DLAQWPPSDAVRIDTDDLYDRLAVAGFQYGPLFQGL
TrmH_DH26         L-----GAAPAAPEVTPDSGPWPPQGATALPVEGLYEALGQHGFSYGPAFQGL
TrmH_DH27         L-----GASEASPS-G-ELSVWPPADAVEIPVDDLYSRLMAAGFAHGPAFQGV
                  *                    ***  *        *  *      :*. *.*:
```

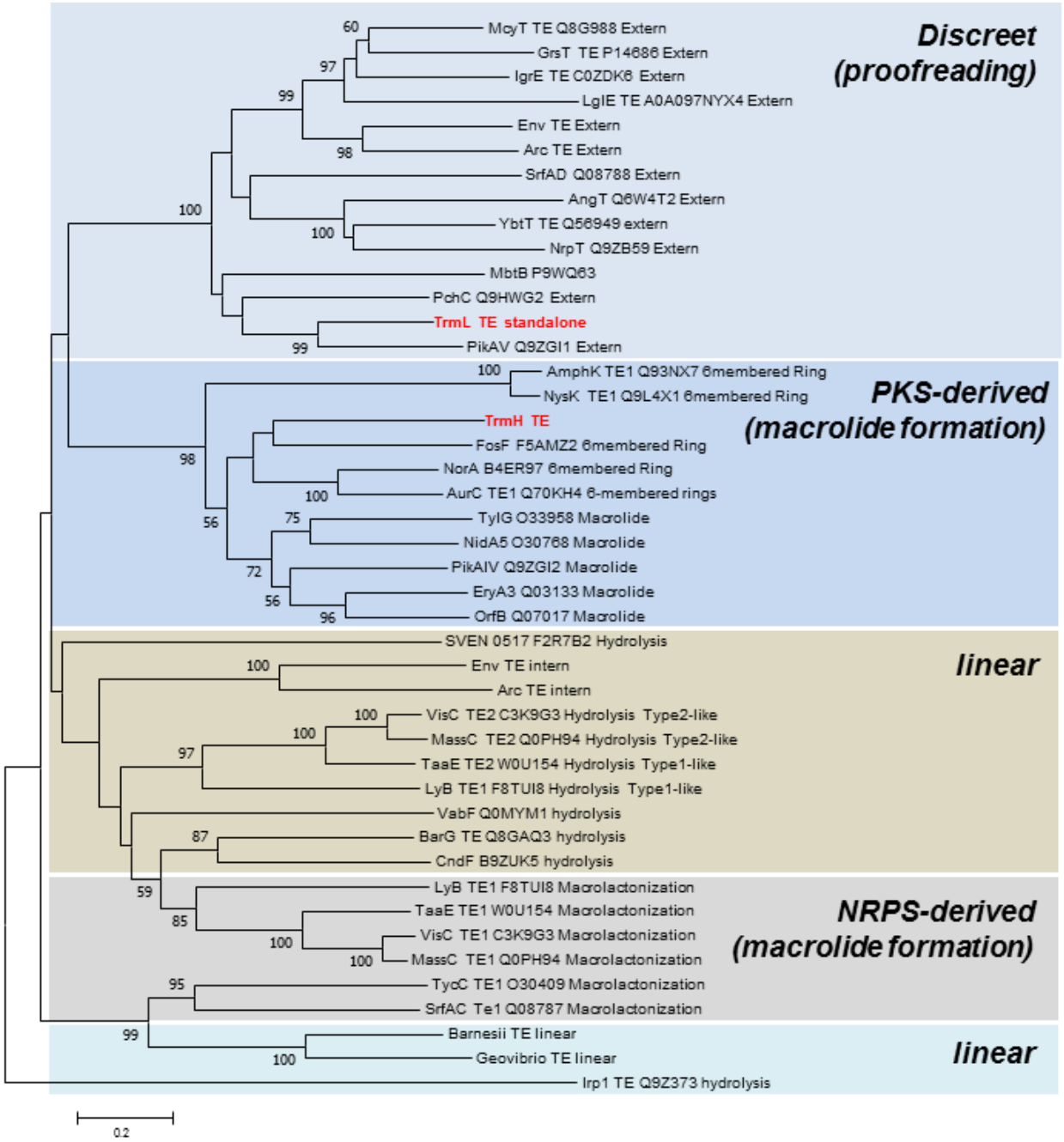

Figure S19. Phylogenetic analysis of TE-domains using Neighbor-Joining method (see **Table S11**). The optimal tree with the sum of branch length = 21.11922060 is shown. The percentage of replicate trees in which the associated taxa clustered together in the bootstrap test (1000 replicates) are shown next to the branches. The tree is drawn to scale, with branch lengths in the same units as those of the evolutionary distances used to infer the phylogenetic tree. The evolutionary distances were computed using the Poisson correction method and are in the units of the number of amino acid substitutions per site. The analysis involved 44 amino acid sequences. All positions with less than 95% site coverage were eliminated. That is, fewer than 5% alignment gaps, missing data, and ambiguous bases were allowed at any position. There were a total of 173 positions in the final dataset. Evolutionary analyses were conducted in MEGA7.[8]

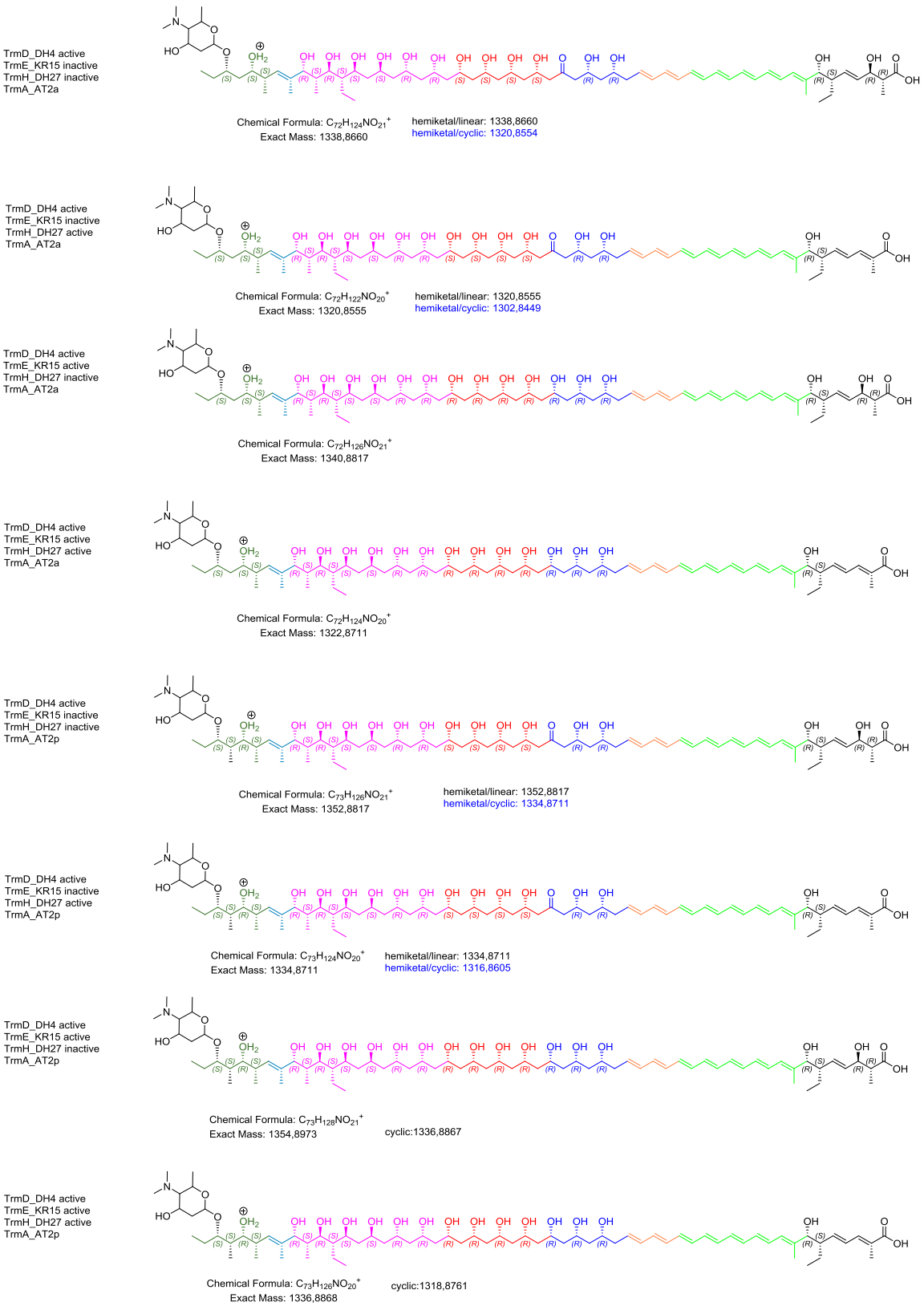

Figure S20. Chemical structures of putative linear termidomycin congeners derived from *trm-1*.

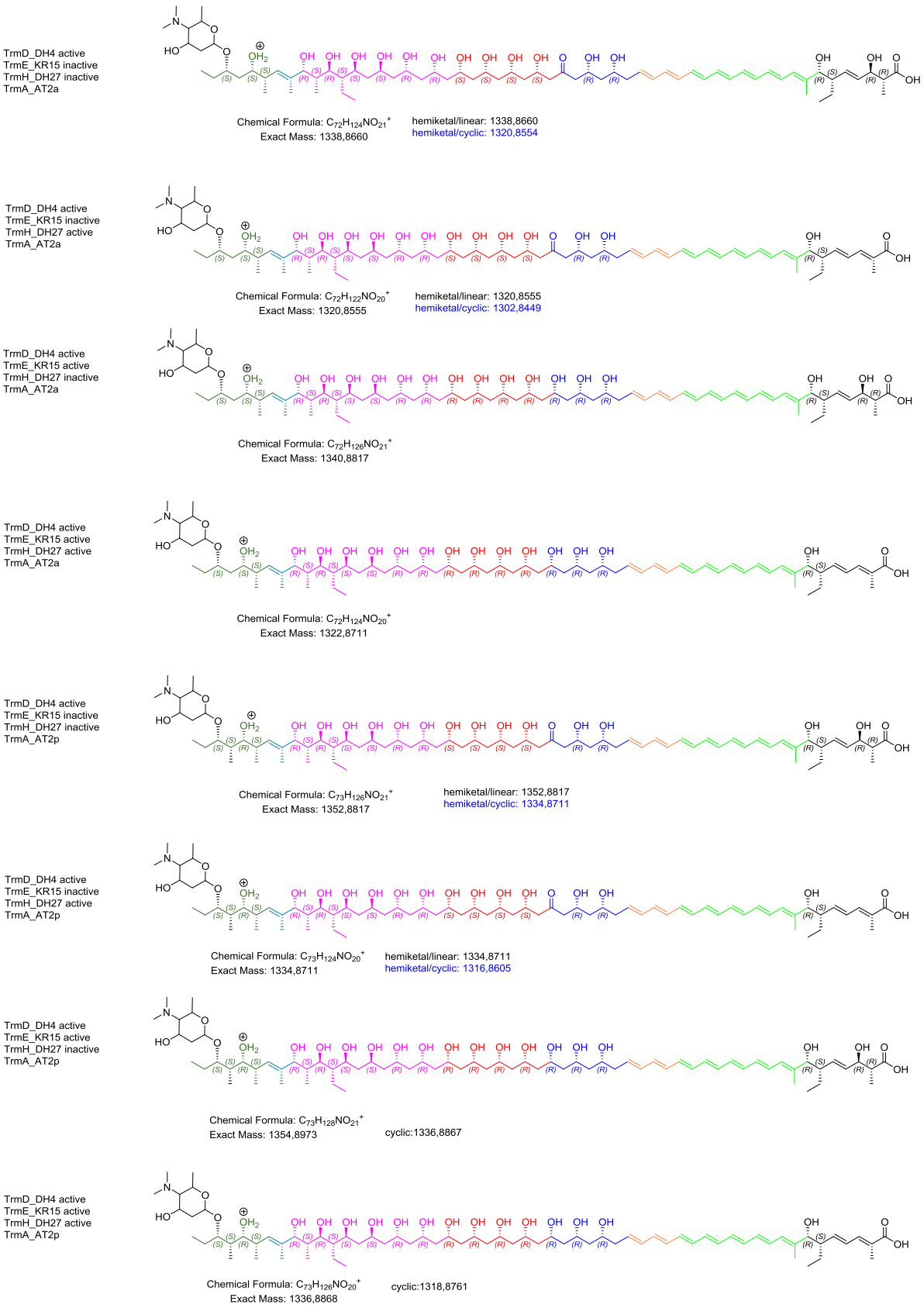

Figure S21. Chemical structures of putative cyclic termidomycin congeners derived from *trm-1*.

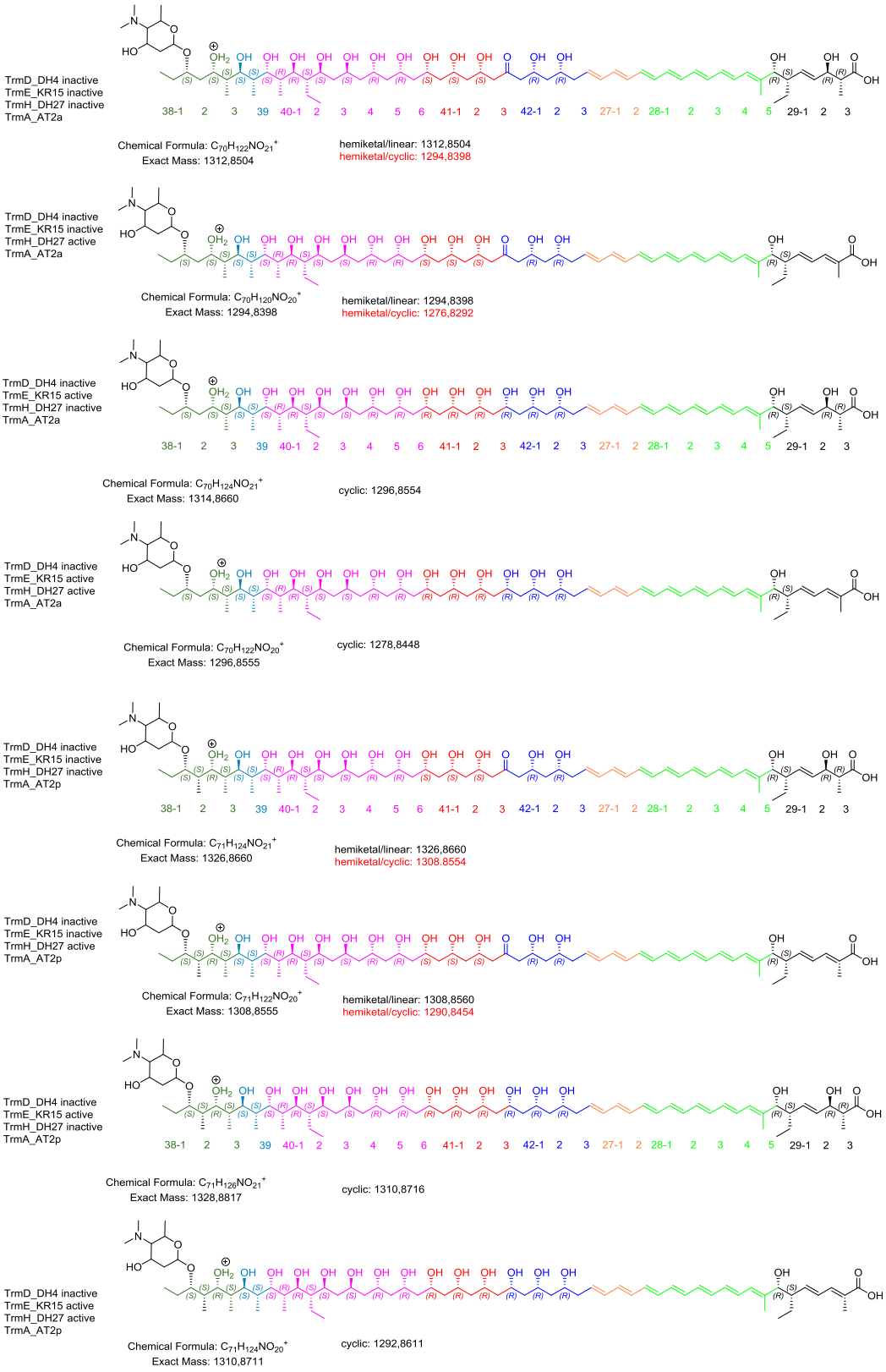

Figure S22. Chemical structures of putative open-chain termidomycin congeners derived from *trm-2*.

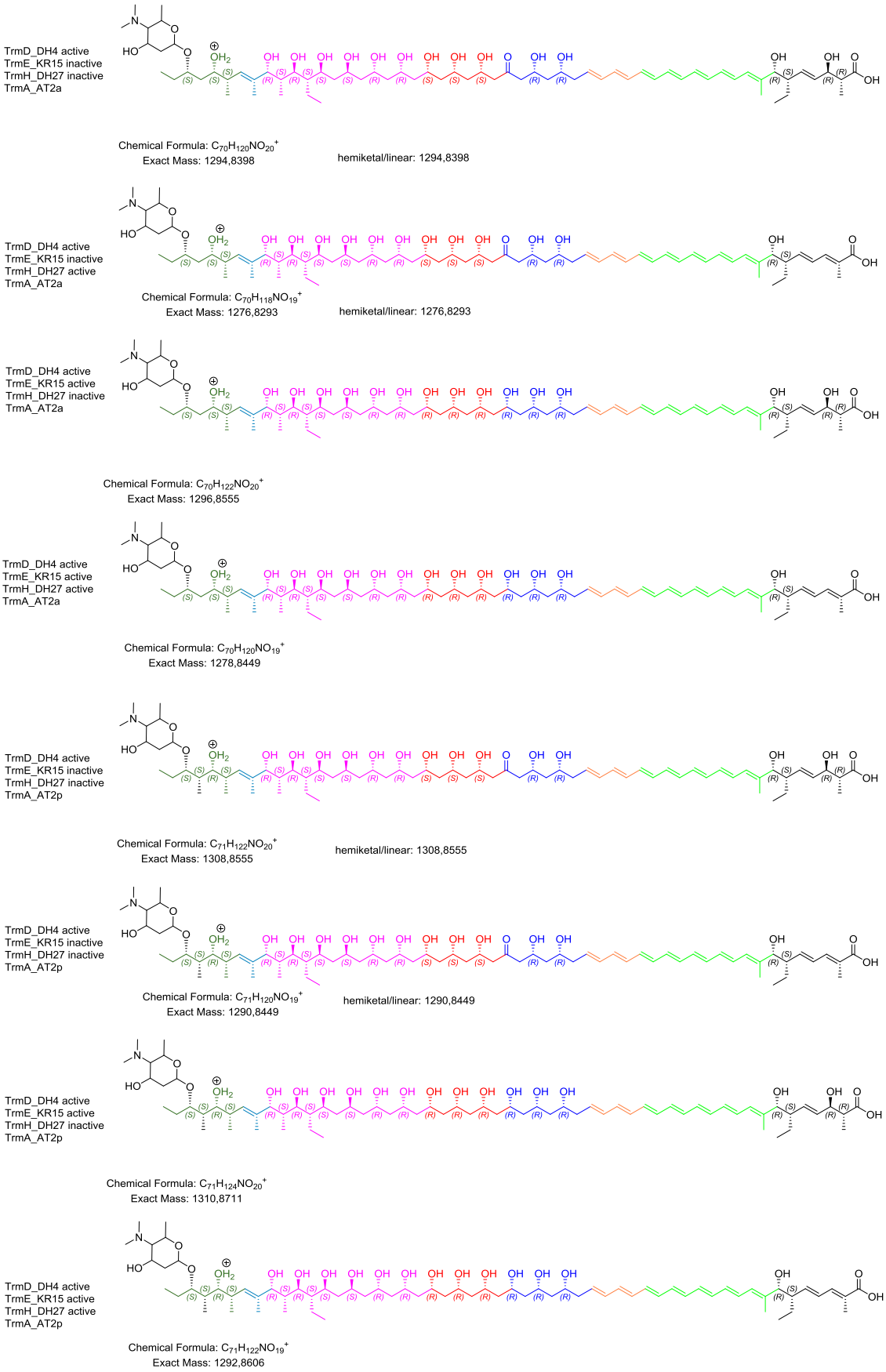

Figure S23. Chemical structures of putative cyclic termidomycin congeners. derived from *trm-2*.

8. Biological Activities

Antimicrobial activity: The activity assay was done by the broth dilution method according to National Committee for Clinical Laboratory Standards. Bacterial and fungal strains including *Bacillus subtilis* 6633, *Staphylococcus aureus* SG511, *Escherichia coli* SG458, *Pseudomonas aeruginosa* K799/61, *Mycobacterium vaccae* 10670, *Sporobolomyces salmonicolor* 549, *Candida albicans*, *Penicillium notatum* JP36 were used as indicator strains. Antimicrobial activity was determined by measuring the inhibition zone in mm (**Table S5**).[17]

Table S4. Antimicrobial activity of crude extracts of RB 110-1 (alias RB1) and RB110-2 (alias RB2) (grey areas represent not tested conditions).

Crude extracts	Inhibition zone (mm) (Mean ±SD)							
	Bacteria					Fungi		
	Gram positive		Gram negative		Acid-fast	Yeast-like molds	Yeasts	Molds
	B. subtilis	*S. aureus*	*E. coli*	*P. aeruginosa*	*M. vaccae*	*Sporobolomyces salmonic*	*Candida albican*	*Penicillium notatum*
Streptomyces sp. RB1	20,33 ±0,58	18,33 ±0,58	0	0	24,67 ±2,08	0	0	0
Streptomyces sp. RB2	21,33 ±0,58	24,33 ±1,53	0	0	30,33 ±3,79	0	12	14,33 ±0,58
MS media Ctrl.	11	10,67 ±0,58	0	0	17,67 ±1,52	0	0	0
MeOH	0	0	0	11	0	10	0	10
Ciprofloxacin (5 µg/ml)	29	18	33	36	22			
Amphotericin (10 µg/ml)						19	21	18

Table S5. Antimicrobial activity of termidomycin A (**1**) (1 mg/mL in DMSO), ciprofloxacin (cip.) and amphotericin B (amp.) against Gram positive, negative bacterial and fungal strains.[a]

compd.	*B. subtilis 6633*	*S. aureus SG511*	*E.coli SG458*	*P. aeruginosa 137*	*VRSA E. faecalis*	*M.vaccae 10670*	*S. salmonic. 549*	*C. albicans*	*P. notatum JP36*
1	12P	0	15P	13p/18P	11	10/20p	12p/20P	0	15p
cip.	28	18	24/31p	23	16F	22p			
amp.							20p	20	18p

[a]: The value indicated the diameter of inhibition zone (in mm).

Anti-proliferative and cytotoxic activity: Termidomycin (**1**) was assayed by using human umbilical vein endothelial cells HUVEC (ATCC CRL-1730, human umbilical vein endothelial cell line), human chronic myeloid leukemia cells K-562 (DSM ACC-10, human immortalized myelogenous leukaemia line) for their anti-proliferative effects (GI_{50}) as well as using human cervix carcinoma cells HeLa (DSM ACC-57, human cervical cancer cell line) for their cytotoxic effects (CC_{50}).

Table S6. Antiproliferative and cytotoxicity activity of termidomycin A (**1**).

	antiproliferative effect GI_{50} [µg/mL]		Cytotoxicity CC_{50} [µg/mL]
compd.	**HUVEC**	**K-562**	**HeLa**
termidomycin A (**1**)	> 5	> 5	> 5

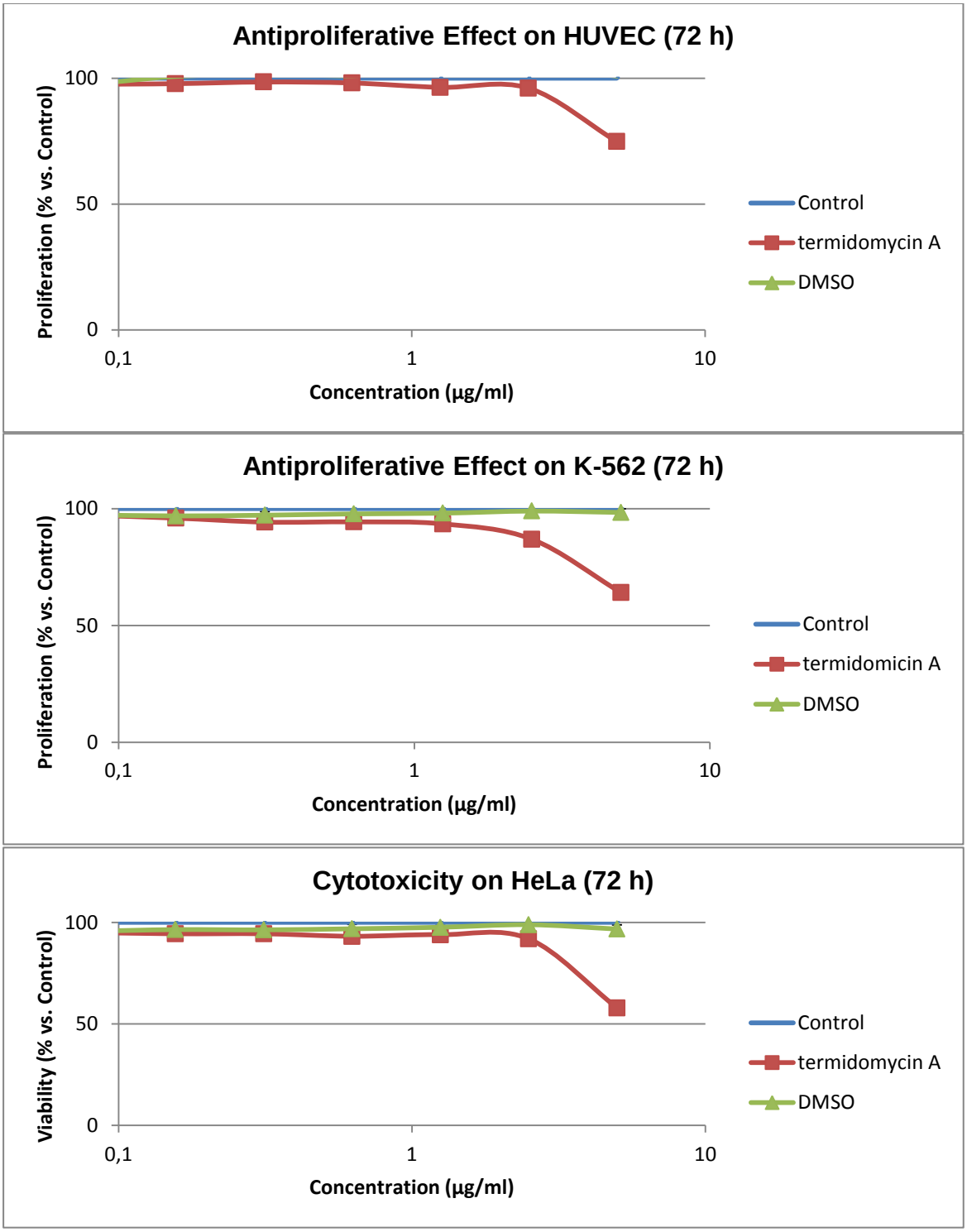

Figure S24. Antiproliferative effect and cytotoxicity of termidomycin A (**1**).

9. Appendix

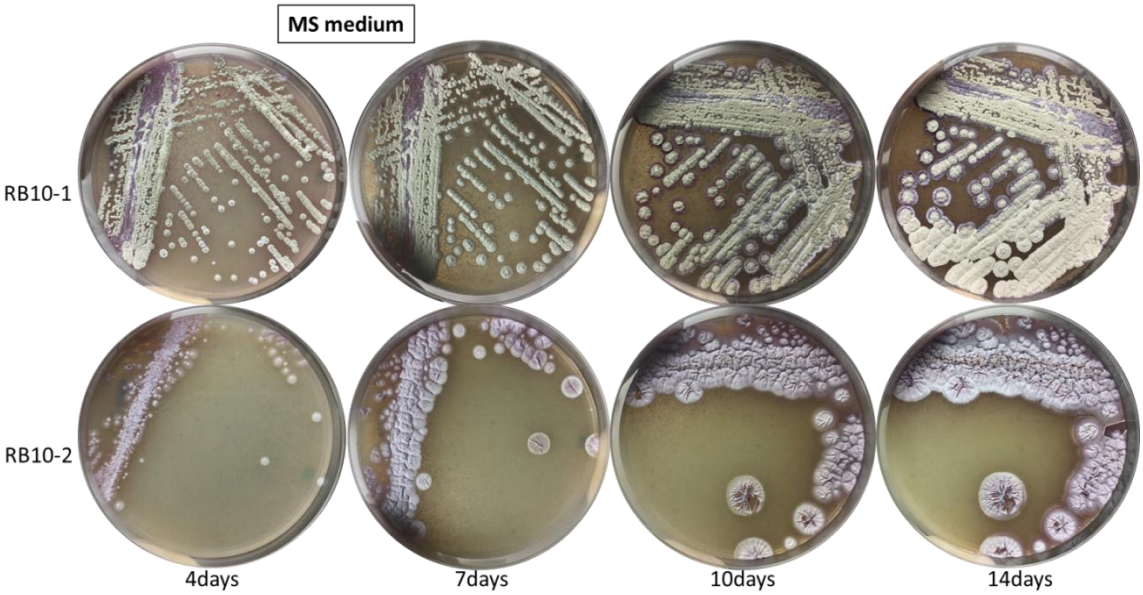

Figure S25. Cultivation of RB110-1 and RB110-2 on MS medium for up to 14 days.

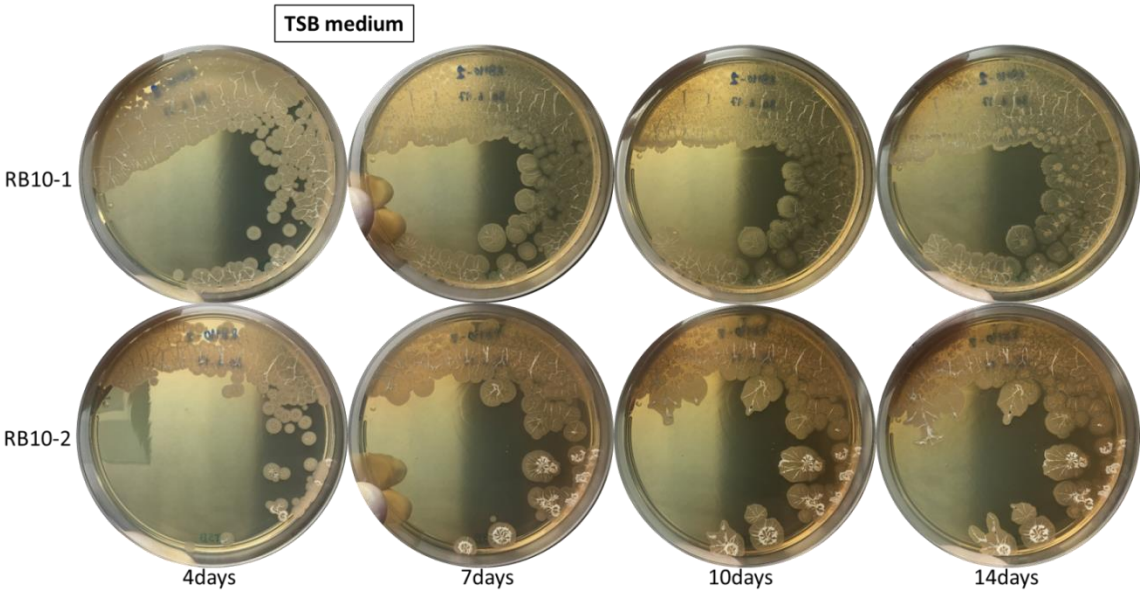

Figure S26. Cultivation of RB110-1 and RB110-2 on TSB medium for up to 14 days.

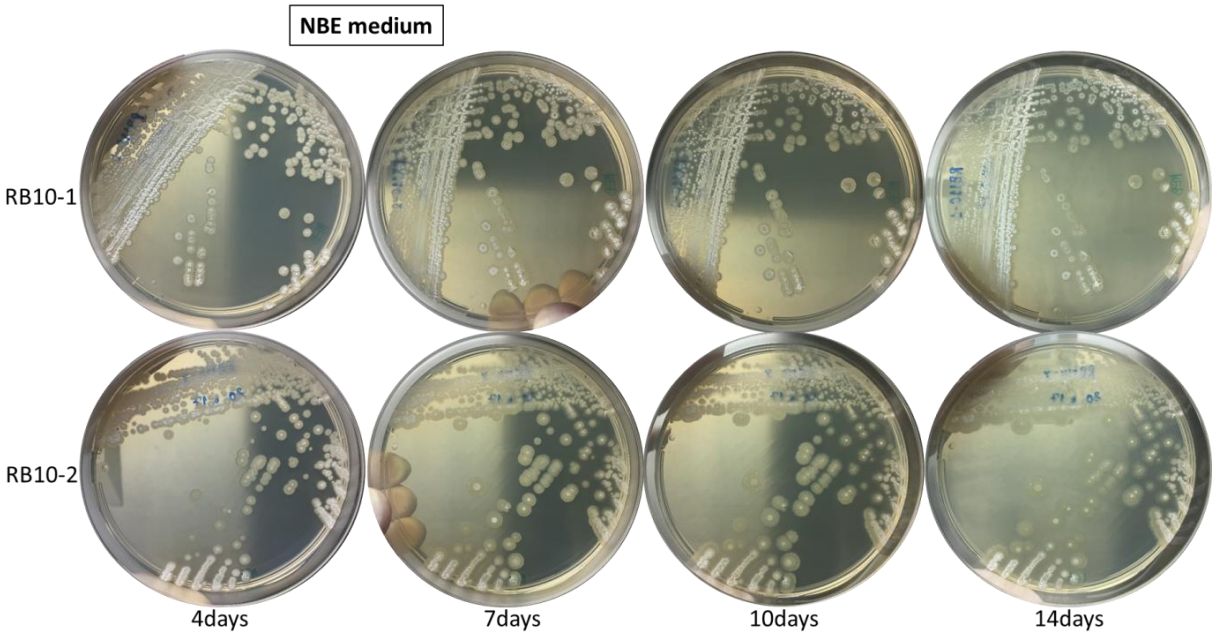

Figure S27. Cultivation of RB110-1 and RB110-2 on NBE medium for up to 14 days.

Table S7. Closest type strains of *Streptomyces* sp. RB110 (both morphotypes, RB110-1, RB110-2) according to BLASTn searches against the NCBI database (https://blast.ncbi.nlm.nih.gov/Blast.cgi, last visit 7.11.2018, 17:12 PM) using 16S rRNA gene. Both morphotypes have the same closest relative type strains.

Closest type strain	**Sequence Similarity**[a]	**Accession Number**
Streptomyces californicus NBRC12750	100%	NR112257
Streptomyces puniceus NBRC12811	99.93%	AB184163
Streptomyces badius NRRLB-2567	99.87%	AY999783
Streptomyces pluricolorescens NRRLB-2121	99.86%	DQ442540
Streptomyces rubiginosohelvolus NBRC 2912	99.86%	AB184240.2
Streptomyces griseinus NBRC12869	99.80%	AB184205
Streptomyces fulvissimus DSM40593	99.80%	NR103947
Streptomyces caviscabies ATCC51928	99.80%	AF112160
Streptomyces globisporus NRRLB-2872	99.80%	EF178686
Streptomyces fimicarius CSSP537	99.80%	NR043351
Streptomyces anulatus NRRLB-2000	99.80%	DQ026637
Streptomyces microflavus NRRLB-2156	99.80%	DQ445795
Streptomyces parvus NRRLB-1455	99.80%	DQ442537
Streptomyces albovinaceus NBRC12739	99.80%	AB249958
Streptomyces luridiscabiei S63	99.74%	AF361784
Streptomyces flavofuscus NRRLB-2594	99.73%	EF178690
Streptomyces baarnensis NRRLB-1902	99.67%	EF178688
Streptomyces finlayi CSSP541	99.60%	NR043354
Streptomyces clavifer NRRLB-2557	99.40%	DQ026670

Table S8. Annotation of biosynthetic proteins (Trm) based on sequence homology.

protein name	Locus tag (RB110-1) GFOCLIGC	Locus tag (RB110-2) FOIKDEDA	size (aa)	annotation	closest homolog(s)	iden(%)/ cover(%)	access.Nr.
TrmU1	01320	00169	903	rifamycin-inactivating phosphotransferase Rph	putative phosphor-enolpyruvate synthase	73/82	ADX66475
TrmU2	01321	00168	147	Cyclase/dehydrase; putatively involved in polyketide (linear poly-beta-ketones)	Polyketide cyclase / dehydrase and lipid transport	35/95	CAQ71823
TrmU3	01322	00167	202	glyoxalase	glyoxalase	74/98 34/127	ABQ42336 ARD70887
TrmU4	01323	00166	165	Guanine deaminase	deaminase	29/89 33/57	AEA30246 KKZ73238
TrmU5	01324	00165	156	Cyanate hydratase	Cyanate hydratase	83/100	BAI70372
TrmU6	01325	00164	210	Carbonic anhydrase 1	Carbonic anhydrase	98/91	WP_098008836
TrmR	01326	00163	302	HTH-type transcriptional regulator CynR	FunR2	34/69	AXI91536
TrmU7	01328	00161	285	hypothetical protein	FunA14	70/94	AXI91562
TrmK	01329	00160	224	4'-phosphopantetheinyl transferase Npt	scaPT	56/97	QBF51747
TrmS1	01330	00159	475	NDP-hexose-2,3-dehydratase	KedS2 LanS AurS8 SipS10	60/93 67/95 66/93 65/93	AFV52155 AAD13549 AWR88417 WP_107413708
TrmS2	01331	00158	326	NDP-hexose-3-ketoreductase	KedS3 KijD10 AurS14 SipS11	57/98 53/97 53/90 53/90	AFV52211 ACB46498 AWR88423 PSK68975
TrmS3	01332	00157	346	NAD-dependent epimerase/4,6-dehydratase	KedS5 SgcA AurS7 SipS6	28/45 63/94 76/91 76/91	AFV52185 AAL06671 AWR88416 WP_107413707
TrmL	01333	00156	255	Thioesterase PikA5	pteH scaT	64/98 58/97	BAC68117 QBF51790
TrmS4	01334	00155	260	N-Methyltransferase	KedS8 KedS9 SgcA5 AurS9 SipS8	43/90 41/91 39/81 82/92 81/92	AFV52159 AFV52160 AAL06660 AWR88418 WP_100562862
TrmS5	01335	00154	364	Adenylyl/thymidylyltransferase	AurS6 SipS7	69/97 69/97	AWR88415 WP_107413706
TrmF	01336	00153	3472	PKS6	cle6 cle5	59/104 58/104	AWC08660 AWC08659
TrmG	01337	00152	8441	PKS7	fscC nysC	53/107 51/112	AAQ82564 AAF71776
TrmH	01338	00151	5297	PKS8	cle5 cle6	53/97 51/101	AWC08659 AWC08660
TrmS6	01339	00150	395	Aminotransferase	KedS7 MdpA5 AurS15 SipS13	28/93 29/92 71/99 74/99	AFV52158 ABY66023 AWR88424 WP_107413714
TrmS7	01340	00149	422	Glycosyltransferase	KedS10 SgcA6 AurS13 SipS9	43/100 35/99 42/100 30/99	AFV52161 AAL06670 AWR88422 WP_107413709

TrmT1	01341	00148	276	Daunorubicin/doxorubicin resistance ABC transporter permease protein DrrB	cmiR4	48/94	BAO66522
TrmT2	01342	00147	336	Daunorubicin/doxorubicin resistance ATP-binding protein DrrA	cmiR3	61/93	BAO66521
TrmI	01343	00146	445/ 441	Crotonyl-CoA reductase	lsd9 idmF	82/91 76/100	BAG85024 ACN69982
TrmJ	01344	00145	604	3-hydroxybutyryl-CoA dehydrogenase	lsd10 idmE	47/93 51/92	BAG85025 ACN69981
TrmU7	01345	00144	535	hypothetical protein	FunO2	41/92	AXI91555
TrmU8	01346	00143	183	hypothetical protein	FunO3	59/91	AXI91556
TrmA	01347	00142	3951	PKS1	scaP1 aalA1 gfsA	54/107 56/99 52/103	QBF51754 BBA66511 BAJ16467
TrmB	01348	00141	1812	PKS2	apoS7	55/97	AEP40934
TrmC	01349	00140	8985	PKS3	FunP1 SgnS2	52/104 49/107	AXI91552 AQT01393
TrmD	01350	00139	5869/ 4441	PKS4	pteA4 cle1	55/106 53/111	BAC68126 AWC08655
TrmE	01351	00138	4529	PKS5	npmE pteA4 cle1	54/107 55/105 53/110	AUO16400 BAC68126 AWC08655
TrmU9	01352	00137	200	hypothetical protein	DUF1707 and DUF2154 domain-containing protein	100/100	WP_098012688
TrmM	01353	00136	312	D-3-phosphoglycerate dehydrogenase	putative dehydrogenase	48/100	AAX31571

Ked = kedarcidin BGC (*Streptoalloteichus* sp. ATCC 53650); *Lan* = landomycin BGC (*Streptomyces cyanogenus*); *Kij* = kijanimicin BGC (*Actinomadura kijaniata* ATCC 31588)[18]; *Aur* = auroramycin BGC (*S. roseosporus NRRL 15998 ; S. filamentosus*)[19]; *Sip* = sipanmycin BGC (*Streptomyces* sp. strain CS149)[20]; *Sca*: = caniferolide BGC (*S. caniferus* CA-271066)[21]; *Aal* = actinoallolide A BGC (*Actinoallomurus fulvus)*[22]; *Gfs* = FD-891 BGC (*S. graminofaciens*)[23]; *Apo* = apoptolidin BGC (*Nocardiopsis* sp. *FU 40*)[24]; *Fun* = funisamine BGC (*Streptosporangium sp.*)[25]; *Sgn* = natamycin BGC (*S. gilvosporeus*)[26]; *Pte* = filipin BGC (*S. avermitilis MA-4680*)[27]; *Cle* = mediomiycin A BGC (*Kitasatospora mediocidica*)[28]; *Npm* = niphimycins C-E BGC (*Streptomyces* sp. IMB7-145)[29]; *Fsc* = levorin A3 BGC (*Streptomyces* sp. FR-008)[30]; *Nys* = nystatin A1 BGC (*S. noursei* ATCC 11455)[31]; *Lsd* = lasalocid BGC (*S. lasaliensis*)[32]; *Idm* = X-14547 BGC (*S. antibioticus*); *Cmi* = cremimycin BGC (*Streptomyces* sp. *MJ635-86F5*)[33]

Table S9. List of reference protein sequences of the crotonyl reductase (CRR)-domain, the producing organisms, corresponding natural products and identifier used in phylogenetic analysis.

Protein	Organism	Product of BGC	Acc. No.
AllR	*Streptomyces tsukubensis* DSM 42081	FK506	D6MYN9
AnlE	*Streptomyces* sp. CNH189	Ansalactam A	K9UU55
Ccr	*Streptomyces cinnamonensis* ATCC 12308	n.d.	Q9RNU6
Ccr	*Streptomyces neyagawaensis* ATCC 27449	Concanamycin	Q3S876
Ccr	*Streptomyces ambofaciens* ATCC 23877	Spiramycin	A0A0K2B1Z9
Ccr	*Micromonospora carbonacea* ATCC 27114	Rosaramicin	A0A1C5ARD2
CcrA2	*Streptomyces lividans* TK24	n.d.	D6EI65
CcrA2	*Streptomyces avermitilis* ATCC 31267	Oligomycin	Q82LU9
CinF	*Streptomyces cinnabarigriseus* DSM 101724	Cinnabaramide	F0V3Z3
Crr	*Streptomyces eurythermus* ATCC 14975	Angolamycin	A8WDM9
Crr	*Streptomyces eurythermus* ATCC 14975	n.d.	A8WDM9
DivD	*Streptomyces* sp. HKI0576	Divergolide	G8YZD3
DivR	*Streptomyces* sp. HKI0576	Divergolide	G8YZD4
FkbS	*Streptomyces hygroscopicus* subsp. *Ascomyceticus*	FK520	Q9KID2
IdmF	*Streptomyces antibioticus* ATCC 23879	Idanomycin	C5HV08
KacH	*Streptomyces kanamyceticus* ATCC 12853	Kanamycin	Q65CB5
KirN	*Streptomyces collinus* DSM 40733	Kirromycin	S5VRZ1
Las5	*Streptomyces lasaliensis* ATCC 31180	Lasalocid	B5M9K6
Lsd9	*Streptomyces lasaliensis* ATCC 31180	Lasalocid	B6ZK62
MidJ	*Streptomyces mycarofaciens* ATCC 21454	Mycaminose	Q0PY14
PlmT7	*Streptomyces* sp. HK803	Phoslactomycin	Q6V1N5
Qor	*Amycolatopsis mediterranei* U-32	n.d.	A0A0H3CXM8
R3	*Streptomyces* sp. CK4412	Tautomycetin	A4KCE8
RimJ	-	Rimocidin	
RevT	*Streptomyces* sp. SN-593	Reveromycin	G1UDU0
SalG	*Salinispora tropica* ATCC BAA-916	Salinosporamide A	B0L7G3
SCO6473	*Streptomyces coelicolor* A3(2)	n.d.	Q9ZBK1
SfaR	*Streptomyces flaveolus* ATCC 19754	Sanglifehrin	D3U9Z8
SSGG_05510	*Streptomyces filamentosus* NRRL 15998	n.d.	D6AT66
TcsC	*Streptomyces* sp. KCTC 11604BP	FK506	E9KTG8
SSMG	-		D9VCM6
SSGG	-		D6AT66
TlmB	*Salinispora pacifica DSM 45543*	Thiolactomycin	A0A0P0FBH4

Table S10. List of reference protein sequences of KR domains, the producing organisms, corresponding natural products and identifier used for alignment.

Protein	Organism	Product of BGC	Acc. No.
AmphB	*Streptomyces nodosus* ATCC 14899	Amphotericin	Q93NW7
AmphJ	*Streptomyces nodosus* ATCC 14899	Amphotericin	Q93NX8
AveA1	*Streptomyces avermitilis* ATCC 31267	Avermectin	Q9S0R8
AveA2	*Streptomyces avermitilis* ATCC 31267	Avermectin	Q9S0R7
BrnF	*S. barnesii* SES-3	Barnesin A	(Rischer *et al.*, 2018)
EpoC	*Sorangium cellulosum* SMP44	Epothilone	Q9KIZ8
EpoD	*Sorangium cellulosum* SMP44	Epothilone	Q9KIZ7
EpoE	*Sorangium cellulosum* SMP44	Epothilone	Q9KIZ6
EryA1	*Saccharopolyspora erythraea* ATCC 11635	Erythromycin	Q03131
FkbA	*Streptomyces* sp. MA6548	FK506	Q9ZGA3
FkbB	*Streptomyces* sp. MA6548	FK506	Q9ZGA4
Irp1	*Yersinia pestis* ATCC 19428	Yersiniabactin	Q9Z373
MtaE	*Stigmatella aurantiaca* ATCC 25190	Myxohiazol	Q9RFK7
MteQ_STRM39_07778_1	*Amycolatopsis* sp. M39	Macrotermycin	(Beemelmanns *et al.*, 2017)
MteR_STRM39_07779	*Amycolatopsis* sp. M39	Macrotermycin	(Beemelmanns *et al.*, 2017)
MxaC	*Stigmatella aurantiaca* ATCC 25190	Myxalamid	Q93TW7
MxaD	*Stigmatella aurantiaca* ATCC 25190	Myxalamid	Q93TW8
MxaE	*Stigmatella aurantiaca ATCC 25190*	Myxalamid	Q93TW7
MxaF	*Stigmatella aurantiaca* ATCC 25190	Myxalamid	Q93TW6
NidA1	*Streptomyces caelestis* ATCC 14924	Niddamycin	O30764
NidA3	*Streptomyces caelestis* ATCC 14924	Niddamycin	O30766
NidA2	*Streptomyces caelestis* ATCC 14924	Niddamycin	O30765
NysB	*Streptomyces noursei* ATCC 11455	Nystatin	Q9L4W4
NysI	*Streptomyces noursei* ATCC 11455	Nystatin	Q9L4X3
OleA1	*Streptomyces antibioticus* JCM 4620	Deoxyoleandolide	Q9KIV4
PikA1	*Streptomyces venezuelae* ATCC 10712	Pikromycin	Q9ZGI5
PikA2	*Streptomyces venezuelae* ATCC 10712	Pikromycin	Q9ZGI4
RapB	*Streptomyces hygroscopicus* ATCC 27438	Rapamycin	Q54296
RifA	*Amycolatopsis mediterranei* ATCC 13685	Rifamycin	O54666
RifD	*Amycolatopsis mediterranei* ATCC 13685	Rifamycin	O54591
SorA	*Sorangium cellulosum* SMP44	Soraphen	Q9ADL6
SorB	*Sorangium cellulosum* SMP44	Soraphen	Q53840
TylG1	*Streptomyces fradiae* ATCC 10745	Tylosin	O33954

Table S11. List of proteins, their producing organisms and corresponding natural products used as reference in the TE-domain phylogenetic analysis.

Protein	Organism	Product of BGC	Acc. No.
AmphK	*Streptomyces nodosus* ATCC 14899	Amphotericin	Q93NX7
AngT	*Vibrio anguillarum* ATCC 68554	Anguibactin	Q6W4T2
ArcE	*Arcobacter nitrofigilis* DSM 7299	n. d.	D5V0Q3
ArcF	*Arcobacter nitrofigilis* DSM 7299	n. d.	D5V0Q4
AurC	*Streptomyces thioluteus* ATCC 12310	Aureothin	Q70KH4
BarG	*Lyngbya 46ajuscule* CCAP 1446/4	Barbamide	Q8GAQ3
BrnF	*S. barnesii* SES-3	Barnesin A	(Rischer *et al.*, 2018)
CndF	*Chondromyces crocatus* DSM 14714	Chondrochlorens	B9ZUK5
EnvF	*Enterovibrio pacificus* CAIM 1920	n. d.	A0A1C3EMC5
EnvG	*Enterovibrio pacificus* CAIM 1920	n. d.	A0A1C3EMD6
EryA3	*Saccharopolyspora erythraea* ATCC 11635	Erythromycin	Q03133
FosF	*Streptomyces pulveraceus* ATCC 13875	Fostriecin	F5AMZ2
GrsT	*Aneurinibacillus migulanus* ATCC 9999	Gramicidin	P14686
IgrE	*Brevibacillus brevis* 47	Planktothrix	C0ZDK6
Irp1	*Yersinia pestis* ATCC 19428	Yersiniabactin	Q9Z373
LglE	*Legionella parisiensis* ATCC 35299	Legioliulin	A0A097NYX4
LybB	*Lysobacter* sp. ATCC 53042	Lysobactin	F8TUI8
MassC	*Pseudomonas fluorescens* ATCC 13525	Massetolide	Q0PH94
MbtB	*Mycobacterium tuberculosis* ATCC 25618	Phenyloxazoline	P9WQ63
McyT	*Planktothrix agardhii* CCAP 1460/5	Mycrocystin	Q8G988
NidA5	*Streptomyces caelestis* ATCC 14924	Niddamycin	O30768
NorA	*Streptomyces orinoci* ATCC 23202	Neoaureothin	B4ER97
NrpT	*Proteus mirabilis* ATCC 29906	Proteobactin	Q9ZB59
NysK	*Streptomyces noursei* ATCC 11455	Nystatin	Q9L4X1
OrfB	*Streptomyces antibioticus* ATCC 23879	Oleandomycin	Q07017
PchC	*Pseudomonas aeruginosa* ATCC 15692	Pyochelin	Q9HWG2
PikAIV	*Streptomyces venezuelae* ATCC 10712	Pikromycin	Q9ZGI2
PikAV	*Streptomyces venezuelae* ATCC 10712	Pikromycin	Q9ZGI1
SrfAC	*Bacillus subtilis* 168	Surfactin A	Q08787
SrfAD	*Bacillus subtilis* 168	Surfactin	Q08788
SVEN_0517	*Streptomyces venezuelae ATCC 10712*	Pyochelin	F2R7B2
TaaE	*Pseudomonas costantinii* PS 3a	Tolaasin	W0U154
TycC	*Brevibacillus parabrevis* ATCC 10027	Tyrocidine	O30409
TylG7	*Streptomyces fradiae* (*Streptomyces roseoflavus*)	Tylosin	O33958
VabF	*Vibrio anguillarum* 96F	Anguibactin	Q0MYM1
ViscC	*Pseudomonas fluorescens* SBW25	Viscosin	C3K9G3
WP_022851249	*Geovibrio* sp. L21-Ace-BES	n. d.	(Rischer *et al.*, 2018)
YbtT (irp4)	*Yersinia pestis* ATCC 19428	Yersiniabactin	Q56949

Table S12. List of reference protein sequences of AT-domains, the producing organisms, corresponding natural products and identifier used for phylogenetic analysis.

Protein	Organism	Product of BGC	Acc. No.
AufD	*Stigmatella aurantiaca* ATCC 25190	Aurafuron	A8YP85
AveA1	*Streptomyces avermitilis* ATCC 31267	Avermectin	Q9S0R8
BryP	Bacterial symbiont from bryozoan *Burgula neritina*	Bryostatin	A2CLL7
CyrB	*Aphanizomenon* sp. 10E9	Cylindrospermopsin	D6MS41
CynA	*Streptomyces cinnabarigriseus* DSM 101724	n. d.	F0V3Y8
EpoD	*Sorangium cellulosum* Thaxter 1904	Epothilone	Q9KIZ7
EryA	*Saccharopolyspora erythraea* ATCC 11635	Erythromycin	Q03131
EryA	*Saccharopolyspora erythraea* ATCC 11635	Erythromycin	Q03131
FkbA	*Streptomyces hygroscopicus var. ascomyceticus* ATCC 14891	FK520	Q9KID7
FkbB	*Streptomyces* sp. KCTC 11604BP	FK506	E9KTI2
FkbC	*Streptomyces sp.* KCTC 11604BP	FK506	Q9KIE1
GdmAII	*Streptomyces hygroscopicus* ATCC 27438	Hygrocin	Q84G23
HbmAI	*Streptomyces hygroscopicus* ATCC 27438	Herbimycin	Q49BE1
HbmAII	*Streptomyces hygroscopicus* ATCC 27438	Herbimycin	Q49BE0
Irp1	*Yersinia pestis* ATCC 19428	Yersiniabactin	Q9Z373
KirAVI	*Streptomyces collinus* ATCC 19743	Kirromycin	B0B507
Lsd11	*Streptomyces lasaliensis* ATCC 31180	Lasalocid	B6ZK64
Lsd12	*Streptomyces lasaliensis* ATCC 31180	Lasalocid	B6ZK65
MlnA	*Bacillus amyloliquefaciens* ATCC 23350	Macrolactin	A0A2D1VLJ2
NidA1	*Streptomyces caelestis* ATCC 14924	Niddamycin	O30764
NidA3	*Streptomyces caelestis* ATCC 14924	Niddamycin	O30766
PedD	Symbiont bacterium of *Paederus fuscipes*	Pederin	Q6VT97
PikAI	*Streptomyces venezuelae* ATCC 10712	Narbonolide	Q9ZGI5
PikAII	*Streptomyces venezuelae* ATCC 10712	Narbonolide	Q9ZGI4
PpsD	*Mycobacterium tuberculosis* ATCC 25618	Phthiocerol	P9WQE3
PpsE	*Mycobacterium tuberculosis* ATCC 25618	Phthiocerol	P9WQE1
RapA	*Streptomyces hygroscopicus* ATCC 27438	Rapamycin	Q54297
RapB	*Streptomyces hygroscopicus* ATCC 27438	Rapamycin	Q54296
RevA	*Streptomyces* sp. SN-593	Reveromycin	G1UDV3
RifA	*Amycolatopsis mediterranei* ATCC 13685	Rifamycin	O54666
SfaI	*Streptomyces flaveolus* ATCC 19754	Sanglifehrin A	D3U9Y9
SwnK	*Metarhizium robertsii* ARSEF 23	Swainsonine	E9F8M3
SorA	*Sorangium cellulosum* SMP44	Soraphen	Q9ADL6
Sulba581	*S. barnesii* SES-3	Barnesin A	(Rischer *et al.*, 2018)
TgaC	*Sorangium cellulosum (Polyangium cellulosum)*	Thuggacin	D7P5Z5
TylG3	*Streptomyces fradiae* ATCC 10745	Tylosin	O33956
WP_022851336	*Geovibrio* sp. L21-Ace-BES	n. d.	(Rischer *et al.*, 2018)
ZmaA	*Bacillus cereus* UW85	Zwittermicin	C0JRE5
ZmaF	*Bacillus cereus* UW85	Zwittermicin	Q9XBU4

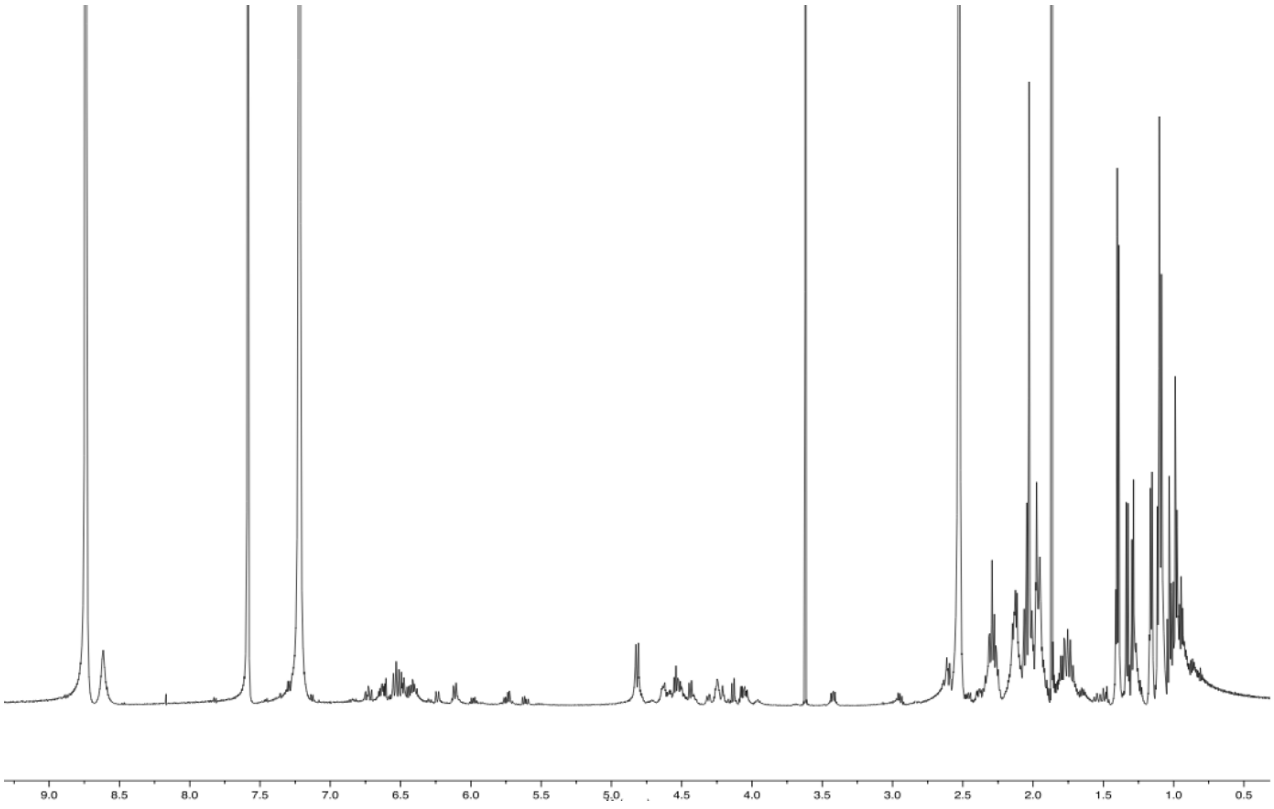

Figure S28. ^{1}H NMR spectrum of termidomycin A (**1**) in pyridine-d_5 at 600 MHz.

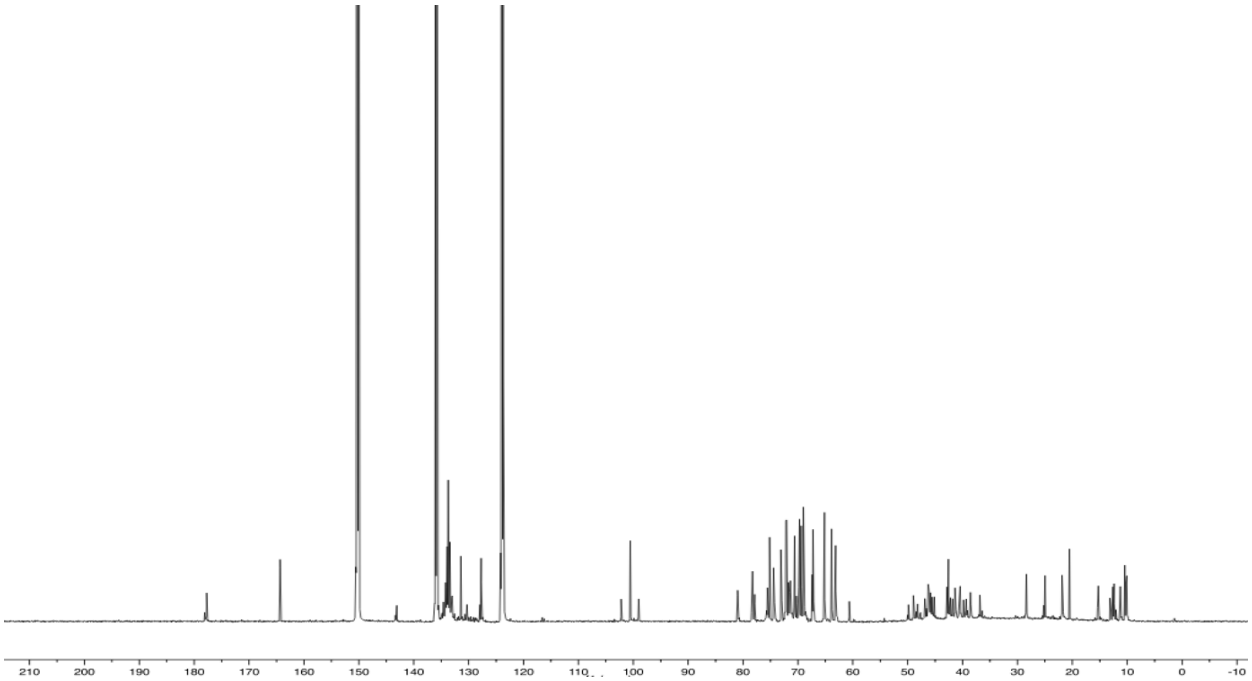

Figure S29. ^{13}C NMR spectrum of termidomycin A (**1**) in pyridine-d_5 at 150 MHz.

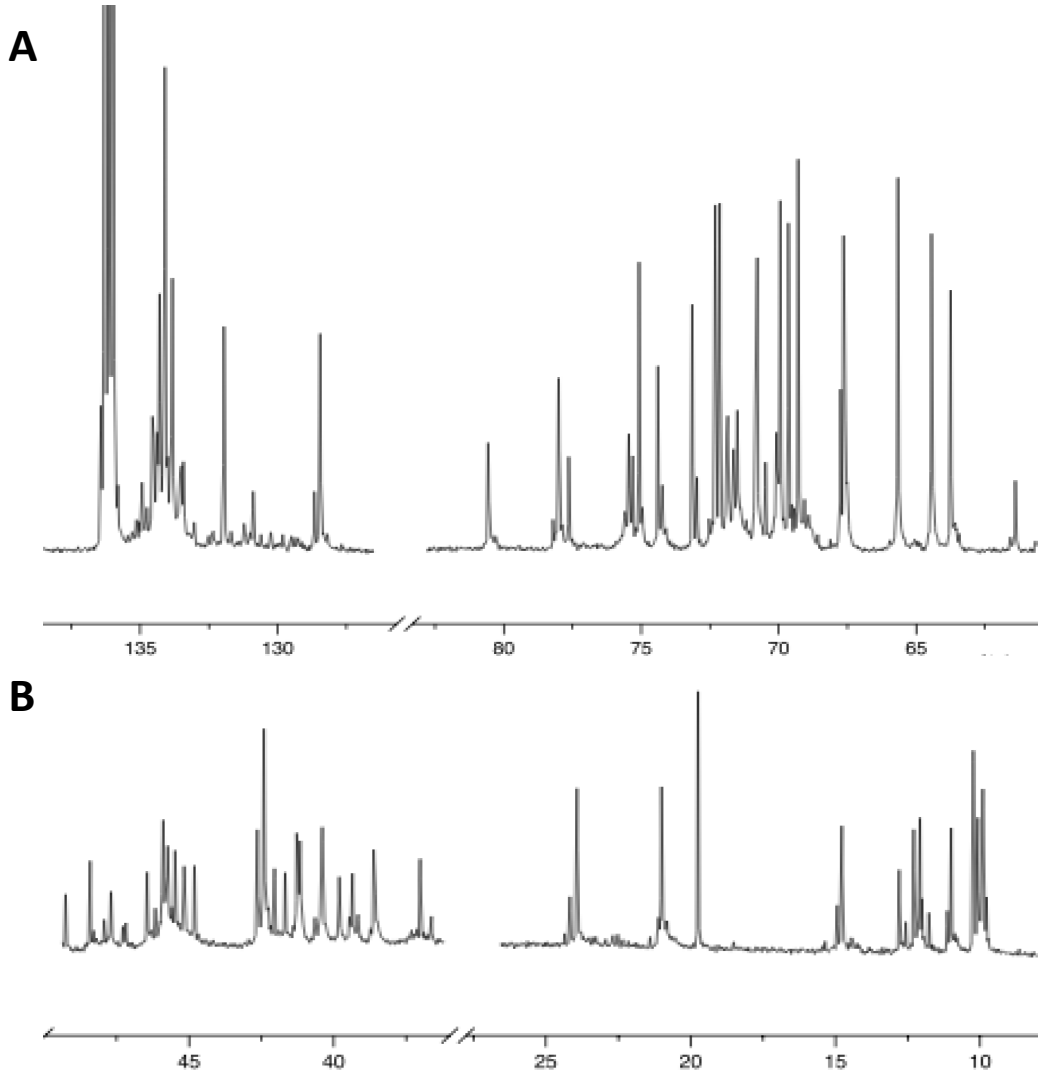

Figure S30. Zoom-in ^{13}C NMR spectra of termidomycin A (**1**). **A**) olefin carbons [d_C 140.0 – 124.0] and methine carbons [d_C 83.0 – 60.0], **B**) methylene carbons [d_C 50.0 – 35.0] and methyl carbons [d_C 25.0 – 8.0].

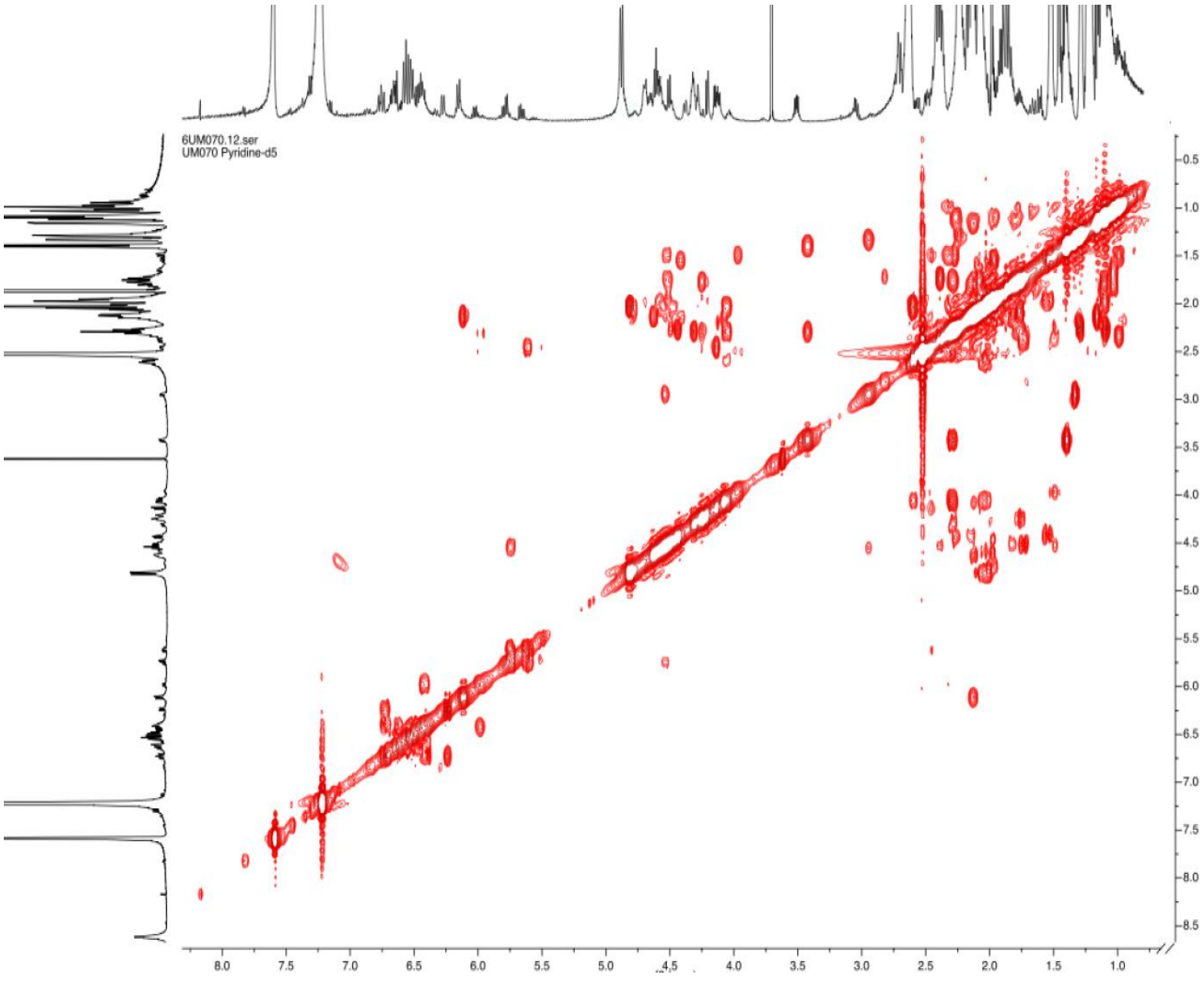

Figure S31. ^{1}H-^{1}H COSY NMR spectrum of termidomycin A (**1**) in pyridine-d_5 at 600 MHz.

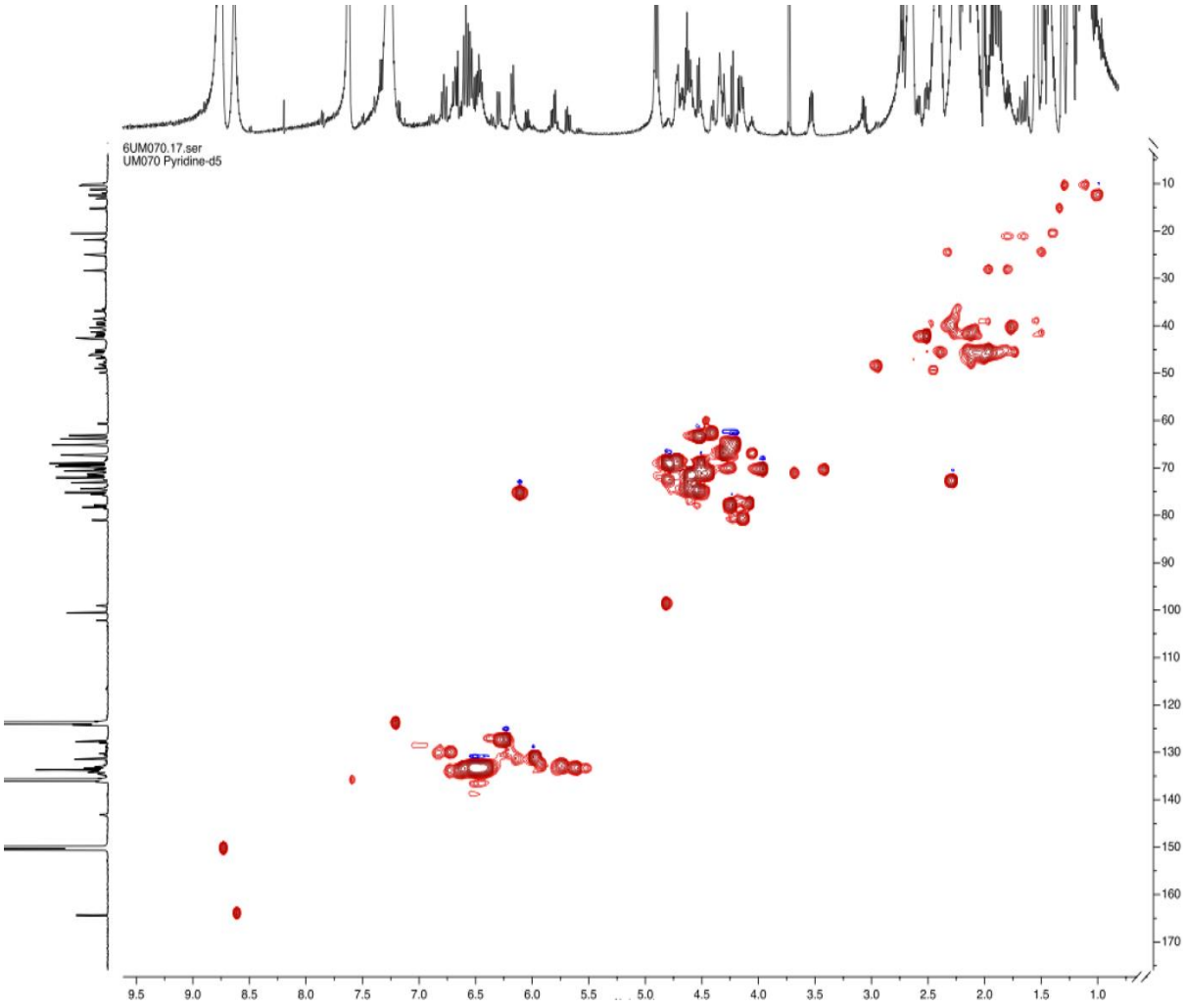

Figure S32. HSQC NMR spectrum of termidomycin A (**1**) in pyridine-d_5 at 600 MHz.

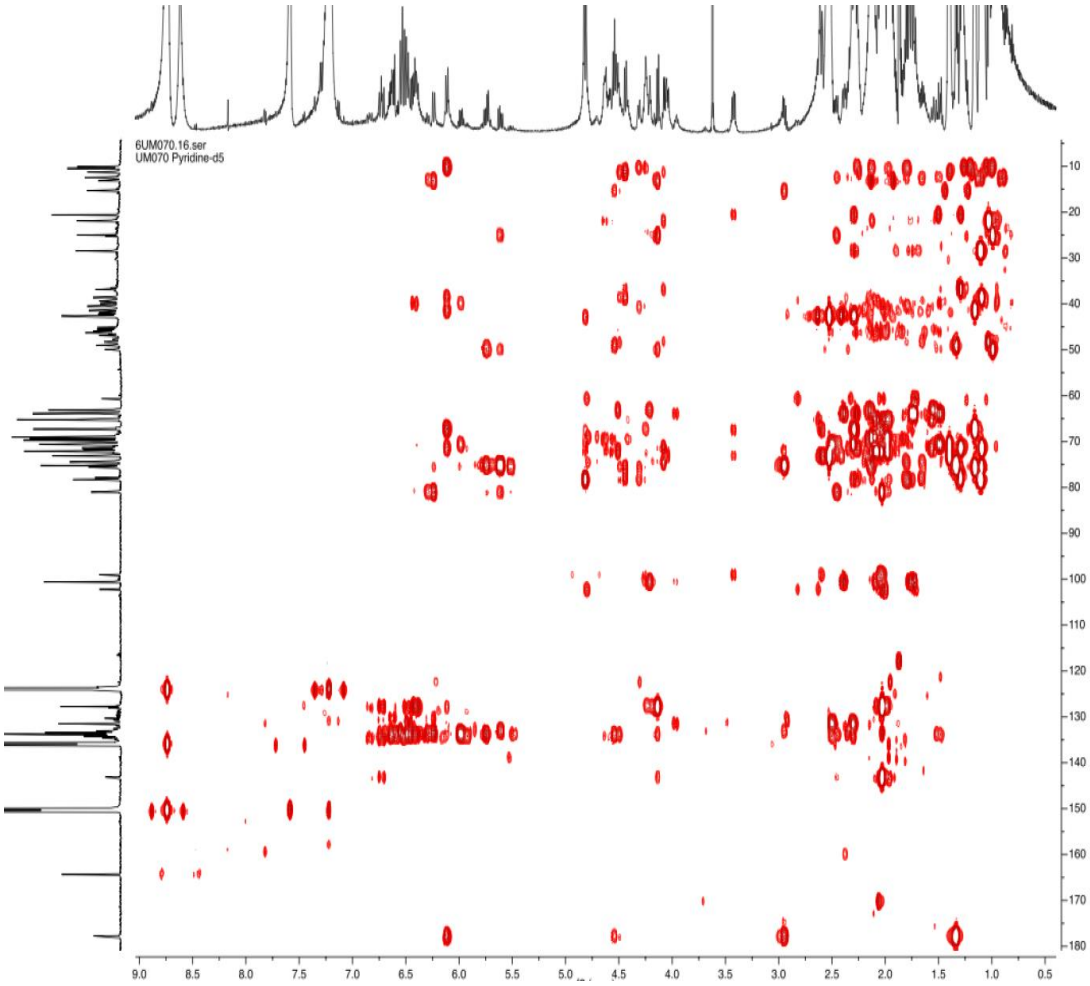

Figure S33. HMBC NMR spectrum of termidomycin A (**1**) in pyridine-d_5 at 600 MHz.

10. References

[1] Murphy, R., Benndorf, R., de Beer, Z. W., Vollmers, J., Kaster, A. K., Beemelmanns, C., and Poulsen, M. (2021) Comparative genomics reveals prophylactic and catabolic capabilities of *Actinobacteria* within the fungus-farming termite symbiosis, *mSphere 6*, e01233-20.

[2] Meier-Kolthoff, J. P., Auch, A. F., Klenk, H. P., and Goker, M. (2013) Genome sequence-based species delimitation with confidence intervals and improved distance functions. *BMC Bioinformatics 14*, 60.

[3] Kurtz, S., Phillippy, A., Delcher, A. L., Smoot, M., Shumway, M., Antonescu, C., and Salzberg, S. L. (2004) Versatile and open software for comparing large genomes. *Genome Biol*. *5*, R12.

[4] Benndorf, R., Guo, H., Sommerwerk, E., Weigel, C., Garcia-Altares, M., Martin, K., Hu, H., Kuefner, M., de Beer, Z. W., Poulsen, M., and Beemelmanns, C. (2018) Natural products from Actinobacteria associated with fungus-growing termites, *Antibiotics 7*, E83.

[5] Pruesse, E., Peplies, J., and Glöckner, F. O. (2012) SINA: Accurate high-throughput multiple sequence alignment of ribosomal RNA genes, Bioinformatics *28*, 1823-1829.

[6] Felsenstein J. (1981) Evolutionary trees from DNA sequences: A maximum likelihood approach. *J. Mol. Evol*. *17*, 368-376.

[7] Saitou, N., and Nei, M. (1987) The neighbor-joining method: a new method for reconstructing phylogenetic trees. *Mol. Biol. Evol*. *4*, 406-425.

[8] Kumar, S., Tamura, K., and Nei, M. (2004) MEGA3: Integrated software for Molecular Evolutionary Genetics Analysis and sequence alignment. *Brief Bioinform*. *5*, 150-163.

[9] Tamura, K., and Nei, M. (1993) Estimation of the number of nucleotide substitutions in the control region of mitochondrial DNA in humans and chimpanzees. *Mol. Biol. Evol*. *10*, 512-526.

[10] Felsenstein J., (1985) Confidence limits on phylogenies: an approach using the bootstrap. *Evolution 39*, 783-791

[11] Wang, M., Carver, J. J., Phelan, V. V., Sanchez, L. M., Garg, N., Peng, Y., Nguyen, D. D., Watrous, J., Kapono, C. A., Luzzatto-Knaan, T., Porto, C., Bouslimani, A., Melnik, A. V., Meehan, M. J., Liu, W. T., Crüsemann, M., Boudreau, P. D., Esquenazi, E., Sandoval-Calderón, M., Kersten, R. D., Pace, L. A., Quinn, R. A., Duncan, K. R, Hsu, C. C., Floros, D. J., Gavilan, R. G., Kleigrewe, K., Northen, T., Dutton, R. J., Parrot, D., Carlson, E. E., Aigle, B., Michelsen, C. F., Jelsbak, L., Sohlenkamp, C., Pevzner, P., Edlund, A., McLean, J., Piel, J., Murphy, B. T., Gerwick, L., Liaw, C. C., Yang, Y. L., Humpf, H. U., Maansson, M., Keyzers, R. A., Sims, A. C., Johnson, A. R., Sidebottom, A. M., Sedio, B. E., Klitgaard, A., Larson, C. B., Boya P, C. A., Torres-Mendoza,

D., Gonzalez, D. J., Silva, D. B., Marques, L. M., Demarque, D. P., Pociute, E., O'Neill, E. C., Briand, E., Helfrich, E. J. N., Granatosky, E. A., Glukhov, E., Ryffel, F., Houson, H., Mohimani, H., Kharbush, J. J., Zeng, Y., Vorholt, J. A., Kurita, K. L., Charusanti, P., McPhail, K. L., Nielsen, K. F., Vuong, L., Elfeki, M., Traxler, M. F., Engene, N., Koyama, N., Vining, O. B., Baric, R., Silva, R. R., Mascuch, S. J., Tomasi, S., Jenkins, S., Macherla, V., Hoffman, T., Agarwal, V., Williams, P. G., Dai, J., Neupane, R., Gurr, J., Rodríguez, A. M. C., Lamsa, A., Zhang, C., Dorrestein, K., Duggan, B. M., Almaliti, J., Allard, P. M., Phapale, P., Nothias, L. F., Alexandrov, T., Litaudon, M., Wolfender, J. L., Kyle, J. E., Metz, T. O., Peryea, T., Nguyen, D. T., VanLeer, D., Shinn, P., Jadhav, A., Müller, R., Waters, K. M., Shi, W., Liu, X., Zhang, L., Knight, R., Jensen, P. R., Palsson, B. O., Pogliano, K., Linington, R. G., Gutiérrez, M., Lopes, N. P., Gerwick, W. H., Moore, B. S., Dorrestein, P. C., and Bandeira, N. (2016) Sharing and community curation of mass spectrometry data with Global Natural Products Social Molecular Networking, *Nat*. *Biotechnol*. *34*, 828-837.

[12] Shannon, P., Markiel, A., Ozier, O., Baliga, N. S., Wang, J. T., Ramage, D., Amin, N., Schwikowski, B., and Ideker, T. (2003) Cytoscape: A software environment for integrated models of biomolecular interaction networks, *Genome Res*. *13*, 2498-2504.

[13] Blin, K., Shaw, S., Steinke, K., Villebro, R., Ziemert, N., Lee, S. Y., Medema, M. H., and Weber, T. (2019) antiSMASH 5.0: updates to the secondary metabolite genome mining pipeline, *Nucleic Acids Res*. *47*, W81–W87.

[14] Hall, T. A. (1999) BioEdit: A user-friendly biological sequence alignment editor and analysis program for Windows 95/98/NT, *Nucl. Acids Symp*. *41*, 95-98.

[15] Jenke-Kodama, H., Sandmann, A., Müller, R., and Dittmann, E. (2005) Evolutionary implications of bacterial polyketide synthases, *Mol Biol Evol. 22*, 2027-2039.

[16] Wilson M. C., and Moore, B. S. (2012) Beyond ethylmalonyl-CoA: The functional role of crotonyl-CoA carboxylase/reductase homologs in expanding polyketide diversity, *Nat. Prod. Rep*. *29*, 72-86.

[17] Methods for dilution antimicrobial susceptibility tests for bacteria that grow aerobically, Approved Standard, 4th ed.; Clinical and Laboratory Standards Institute: Wayne, PA, 2006; Vol. 26.

[18] Zhang, H., White-Phillip, J. A., Melançon, III C. E., Kwon, H.-j., Yu, W.-l., and Liu, H.-w., (2007) Elucidation of the Kijanimicin Gene Cluster: Insights into the Biosynthesis of Spirotetronate Antibiotics and Nitrosugars, *J. Am. Chem. Soc*. *129*, 14670–14683.

[19] Yeo, W. L., Heng, E., Tan, L. L., Lim, Y. W., Ching, K. C., Tsai, D. J., Jhang, Y. W., Lauderdale, T .L., Shia, K. S., Zhao, H., Ang, E. L., Zhang, M. M., Limm Y.H., and Wong, F.T. (2020) Biosynthetic engineering of the antifungal, anti-MRSA auroramycin, *Microb Cell Fact*. *19*, 3.

[20] Malmierca, M. G., Pérez-Victoria, I. Martín, J., Reyes, F., Méndez, C., Olano, C., and Salas, J. A. (2018) Cooperative Involvement of Glycosyltransferases in the Transfer of Amino Sugars during the Biosynthesis of the Macrolactam Sipanmycin by *Streptomyces* sp. Strain CS149, *Appl. Env. Microbiol. 84*, e01462-18;

[21] Pérez-Victoria, I., Oves-Costales, D., Lacret, R., Martín, J., Sánchez-Hidalgo, M., Díaz, C., Cautain, B., Vicente, F., Genilloud, O., and Reyes, F. (2019) Structure elucidation and biosynthetic gene cluster analysis of caniferolides A–D, new bioactive 36-membered macrolides from the marine-derived *Streptomyces caniferus* CA-271066, *Org. Biomol. Chem*. *17*, 2954-2971.

[22] Inahashi, Y., Shiraishi, T., Také, A., Matsumoto, A., Takahashi, Y., Ōmura, S., Kuzuyama, T., and Nakashima, T. (2018) Identification and heterologous expression of the actinoallolide biosynthetic gene cluster. *J Antibiot (Tokyo) 71*, 749-752.

[23] Kudo, F., Motegi, A., Mizoue, K., and Eguchi, T. (2010) Cloning and characterization of the biosynthetic gene cluster of 16-membered macrolide antibiotic FD-891: involvement of a dual functional cytochrome P450 monooxygenase catalyzing epoxidation and hydroxylation. *Chembiochem.* 11, 1574-82. Erratum in: *Chembiochem. 11*, 1798.

[24] Du, Y., Derewacz, D.K., Deguire, S.M., Teske, J., Ravel, J., Sulikowski, G.A., and Bachmann, B.O. (2011) Biosynthesis of the Apoptolidins in *Nocardiopsis* sp. FU 40. *Tetrahedron 67*, 6568-6575.

[25] Covington, B.C., Spraggins, J.M., Ynigez-Gutierrez, A.E., Hylton, Z.B., and Bachmann, B.O. (2018) Response of Secondary Metabolism of Hypogean Actinobacterial Genera to Chemical and Biological Stimuli. *Appl Environ Microbiol*. *84*, e01125-18.

[26] Wang, Y., Tao, Z., Zheng, H., Zhang, F., Long, Q., Dengm Z., and Tao, M. (2016) Iteratively improving natamycin production in *Streptomyces gilvosporeus* by a large operon-reporter based strategy. *Metab Eng. 38*, 418-426.

[27] Ikeda, H., Kazuo, S.Y., and Omura, S. (2014) Genome mining of the *Streptomyces avermitilis* genome and development of genome-minimized hosts for heterologous expressionn of biosynthetic gene clusters, *J. Ind. Microbiol. Biotechnol. 41*, 233-250.

[28] Sun, F., Xu, S., Jiang, F., and Liu, W. (2018) Genomic-driven discovery of an amidinohydrolase involved in the biosynthesis of mediomycin A, *Appl. Microbiol. Biotechnol*. *102*, 2225-2234.

[29] Hu, Y., Wang, M., Wu, C., Tan, Y., Li, J., Hao, X., Duan, Y., Guan, Y., Shang, X., Wang, Y., Xiao, C., and Gan, M. (2018) Identification and Proposed Relative and Absolute Configurations of Niphimycins C-E from the Marine-Derived *Streptomyces* sp. IMB7-145 by Genomic Analysis, *J. Nat. Prod. 81*, 178-187

[30] Chen, S., Huang, X., Zhou, X., Bai, L., He, J., Jeong, K. J., Lee, S. Y., and Deng, Z. (2003) Organizational and mutational analysis of a complete FR-008/candicidin gene cluster encoding a structurally related polyene complex, *Chem. Biol*. *10*, 1065-1076.

[31] Brautaset, T., Sekurova, O. N., Sletta, H., Ellingsen, T.E., StrŁm, A.R., Valla, S., and Zotchev, S.B. (2000) Biosynthesis of the polyene antifungal antibiotic nystatin in *Streptomyces noursei* ATCC 11455: analysis of the gene cluster and deduction of the biosynthetic pathway, *Chem. Biol*. *7*, 395-403.

[32] Migita, A., Watanabe, M., Hirose, Y., Watanabe, K., Tokiwano, T., Kinashi, H., and Oikawa H., (2009) Identification of a gene cluster of polyether antibiotic lasalocid from *Streptomyces lasaliensis*, *Biosci. Biotechnol. Biochem. 73*, 169-176.

[33] Amagai, K., Takaku, R., Kudo, F., and Eguchi, T. A. (2013) A unique amino transfer mechanism for constructing the β-amino fatty acid starter unit in the biosynthesis of the macrolactam antibiotic cremimycin, *Chembiochem 14*, 1998-2006.